NEUROLOGIA I NEUROCHIRURGIA POLSKA

POLISH JOURNAL OF NEUROLOGY AND NEUROSURGERY

The Official Journal of Polish Neurological Society

2019, vol. 53, no. 3

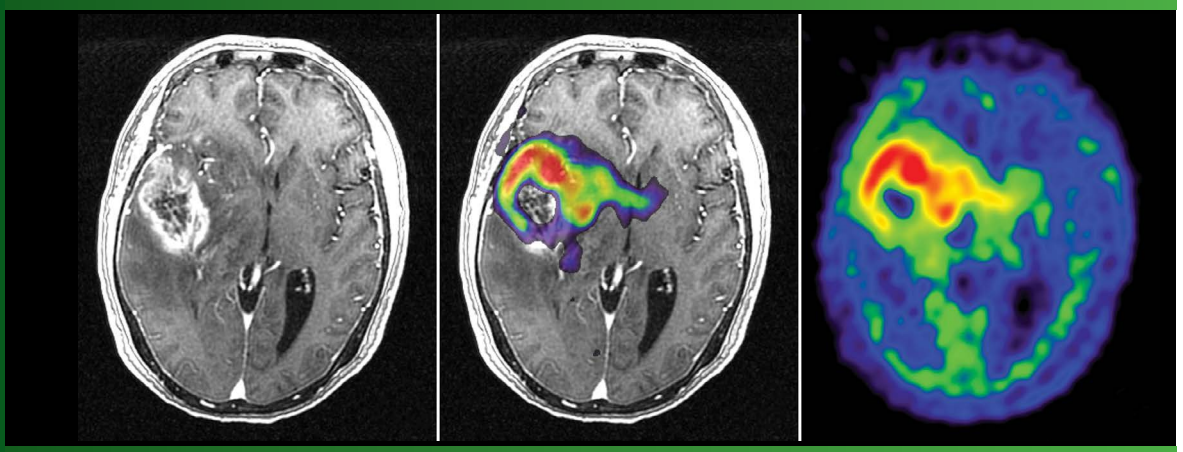

Established: 1938

VIA MEDICA

ISSN 0028-3843

www.journals.viamedica.pl/neurologia_neurochirurgia_polska

NEUROLOGIA I NEUROCHIRURGIA POLSKA

POLISH JOURNAL OF NEUROLOGY AND NEUROSURGERY

The Official Journal of Polish Neurological Society
www.journals.viamedica.pl/neurologia_neurochirurgia_polska

VIA MEDICA

NEUROLOGIA I NEUROCHIRURGIA POLSKA

POLISH JOURNAL OF NEUROLOGY AND NEUROSURGERY

The Official Journal of Polish Neurological Society
www.journals.viamedica.pl/neurologia_neurochirurgia_polska

Neurologia i Neurochirurgia Polska also known under the name of *Polish Journal of Neurology and Neurosurgery (PJNNS)* is a premier research and educational platform of the Polish Neurological Society and Polish Society of Neurosurgeons. It has a long and accomplished history dating back to earlier days of the XX Century. The journal publishes the results of basic and clinical research contributing to the understanding, diagnosis, and treatment of neurological and neurosurgical disorders.

Neurologia i Neurochirurgia Polska (ISSN: 0028-3843) is published 6 times a year by VM Media sp. z o.o. VM Group sp.k.

Editorial Address: VM Media sp. z o.o. VM Group sp.k.
ul. Swietokrzyska 73, 80–180 Gdansk,
tel: (+48 58) 320 94 94, fax: (+48 58) 320 94 60
www.journals.viamedica.pl/neurologia_neurochirurgia_polska,
e-mail: editorialoffice@pjnns.viamedica.pl

Journal has an international indexation in Directory of Open Access Journals (DOAJ); Chemical Abstracts; EMBASE; Index Copernicus; MEDLINE; OpenMED; MEDLINE; Polish Scientific Bibliography / Pol-index; Polish Medical Bibliography (GBL); Science Citation Index Expanded

Current Impact Factor of Neurologia i Neurochirurgia Polska (2018) is 1.006

Editorial policies and author guidelines are published on journal website:
www.journals.viamedica.pl/neurologia_neurochirurgia_polska

Cover photo: Jingwang Zhao et al., Visual comparison of enhanced MRI with MET PET of primary GBM, see figure on page 201.

18-0354.002.001

NEUROLOGIA I NEUROCHIRURGIA POLSKA

POLISH JOURNAL OF
NEUROLOGY
AND NEUROSURGERY

The Official Journal of Polish Neurological Society

2019, vol. 53, no. 3

Table of Contents

EDITORIAL NOTE

Neurologia i Neurochirurgia Polska
Polish Journal of Neurology and Neurosurgery
2019, Volume 53, no. 3

ISSN 0028–3843

Current Status of the Polish Journal of Neurology & Neurosurgery (Neurologia i Neurochirurgia Polska)

Recently, Clarivate Analytics released its 2018 InCites Journal Citation Reports™, and Elsevier's Scopus its 2018 CiteScore™ reports. We are very pleased to share with you our ranking status. The 2018 Impact Factor (IF) for the Polish Journal of Neurology and Neurosurgery (Neurologia i Neurochirurgia Polska) is 1.006, and the 2018 CiteScore (CS) is 0.99. Our 2017 IF was 0.817, and our 2017 CS was 0.96; therefore, both publication metrics have improved for 2018.

For the calculation period for the IF, 175 manuscripts have been citied. Our 5 most citied articles (1–5) deal with different aspects of neurology, including epilepsy, stroke, migraine, and others.

The majority of our articles included in the calculation scores were submitted by Polish authors. Authors from 4 other countries, Turkey, Italy, USA, and China, were listed in the first five positions.

Polish institutions with which the authors of the most cited papers are associated include the Medical University of Warsaw (Warsaw, Poland), Medical University of Silesia (Katowice, Poland), Jagiellonian University (Krakow, Poland), Institute of Psychiatry and Neurology (Warsaw, Poland), and Medical University of Lodz (Lodz, Poland). From outside of Poland, we have received articles from Mayo Clinic (Jacksonville, FL, USA), Rudolfstiftung Hospital (Vienna, Austria), Capital Medical University (Beijing, Peoples Republic of China), Kobe University, Grad. Sch. Med. (Kobe, Japan), and many others.

Clarivate Analytics IF is a result of mathematical calculations taking into consideration number of published articles in previous 2 years (2016 and 2017) and number of cited articles in the last year (2018): IF = Citations in 2018 to items published in 2016 + 2017 divided by number of citable items in 2016 + 2017.

Elsevier's CS is calculated for three years according to the following formula: CS = Citation Count 2018 divided by Documents 2015–2017. CS includes all available document types.

We very much thank our Readers, Authors, and Reviewers for their support of our Journal. We are grateful to our Readers sharing with us their comments regarding further improvements to the journal activities and status. We are extremely grateful to our Authors for submitting to us their best manuscripts. We are also very much grateful and indebted to our Journal Reviewers for their work and expertise. We appreciate the guidance that we have received from our Editorial Board members. We hope to improve the administrative operations of our Journal further, including reducing the time required to review and publish the papers submitted to us.

The Journal's success is your success!

Zbigniew K. Wszolek, M.D.
Co-Editor-in-Chief
Jaroslaw Slawek, M.D., Ph.D.
Co-Editor-in-Chief
Mariusz Sieminski, M.D., Ph.D.
Managing editor

References

1. Harat M, Rudaś M, Zieliński P, et al. Nucleus accumbens stimulation in pathological obesity. Neurol Neurochir Pol. 2016; 50(3): 207–210, doi: 10.1016/j.pjnns.2016.01.014, indexed in Pubmed: 27154450.
2. Stöllberger C, Finsterer J. Recurrent venous thrombosis under rivaroxaban and carbamazepine for symptomatic epilepsy. Neurol Neurochir Pol. 2017; 51(2): 194–196, doi: 10.1016/j.pjnns.2017.01.010, indexed in Pubmed: 28215696.
3. Siuda J, Patalong-Ogiewa M, Żmuda W, et al. Cognitive impairment and BDNF serum levels. Neurol Neurochir Pol. 2017; 51(1): 24–32, doi: 10.1016/j.pjnns.2016.10.001, indexed in Pubmed: 28341039.
4. Kotlęga D, Peda B, Zembroń-Łacny A, et al. The role of brain-derived neurotrophic factor and its single nucleotide polymorphisms in stroke patients. Neurol Neurochir Pol. 2017; 51(3): 240–246, doi: 10.1016/j.pjnns.2017.02.008, indexed in Pubmed: 28291539.
5. Kuzawińska O, Lis K, Cessak G, et al. Targeting of calcitonin gene-related peptide action as a new strategy for migraine treatment. Neurol Neurochir Pol. 2016; 50(6): 463–467, doi: 10.1016/j.pjnns.2016.07.012, indexed in Pubmed: 27553188.

INVITED REVIEW ARTICLE

Neurologia i Neurochirurgia Polska
Polish Journal of Neurology and Neurosurgery
2019, Volume 53, no. 3, pages: 173–180
DOI: 10.5603/PJNNS.a2019.0023

ISSN 0028–3843

Molecular biomarkers for neuromuscular disorders – challenges and future perspectives

Magdalena Mroczek[1], Liliana Machoń[2], Izabela Filipczyńska[3]

[1]The John Walton Muscular Dystrophy Research Centre, Institute of Genetic Medicine, The International Centre for Life, Newcastle University, Newcastle upon Tyne, United Kingdom

[2]Department of Neurology, Czerniakowski Hospital in Warsaw, Warsaw, Poland

[3]Academy of Physical Education, Department of Rehabilitation; Cathedral of Psychosocial Foundations of Health and Rehabilitation; Part of Bioethics and Social Problems of Medicine, Warsaw, Poland

Abstract

There is an ever-growing need for molecular biomarkers in assessing clinical course and diagnosing neuromuscular disorders, as well as in monitoring drug therapy. With the development of high throughput techniques, there has been an acceleration in the discovery of potential biomarkers. It is quite easy to find potential candidates, but difficult to validate them and translate into a clinical setting. Neuromuscular diseases (NMD) are a major challenge in terms of finding potential molecular biomarkers, mainly because of their heterogeneous aetiology and variability in phenotype, their as yet incompletely understood pathophysiology, and their slow clinical progression. Furthermore, it is challenging to assemble a large cohort of patients, as many NMDs are rare diseases.

In this literature review, we provide an update on the latest discoveries in DNA, RNA, miRNA, epigenetic, protein, metabolic and cellular biomarkers for NMD. The advantages and potential difficulties of clinical application and the role of identification of biomarker panels are discussed. We have especially sought to highlight translational biomarkers which can be easily transferred to the clinic, where they may eventually present possible future therapies related to molecular biomarker discoveries.

Key words: translational biomarkers, neuromuscular diseases, NMD, biomarkers

(*Neurol Neurochir Pol 2019; 53 (3): 173–180*)

Introduction

In the field of NMD (neuromuscular disorders) there is an ever-increasing need for new molecular biomarkers. The discovery of new biomarkers is essential, not only for diagnostic purposes, but also to help monitor disease course in clinical trials and changes in treatment. This type of biomarker, known as a pharmacodynamic biomarker, can indicate e.g. if a protein is restored in the course of treatment. Innovative therapeutic trials, which tend to be shorter and not always impact phenotype, require efficient biomarkers. Some molecular biomarkers can even replace functional outcome measures in clinical trials and therapy, i.e. surrogate biomarkers.

A good example of such a surrogate biomarker is dystrophin increase in skeletal muscle during therapy with eteplirsen [1]. In this case, an effective biomarker enabled accelerated approval by the United States FDA (Food and Drug Administration). However, despite much effort and countless developments in this field, finding a biomarker suitable for clinical use remains a challenge. The development of high throughput technologies such as NGS (next generation sequencing) and omic technologies for proteins have significantly speeded up

Address for correspondence: Magdalena Mroczek, The John Walton Muscular Dystrophy Research Centre, Institute of Genetic Medicine, The International Centre for Life, Newcastle University, Central Parkway, Newcastle upon Tyne, United Kingdom, e-mail: magdalena.mroczek@newcastle.ac.uk

the process of screening for molecular biomarkers, but have also at the same time created problems related to the interpretation of large amounts of data. As screening usually reveals multiple potential candidates, it is likely that only a few will prove to be effective in the course of clinical validation, which is demanding, time-consuming, and expensive. The application of a panel of molecular biomarkers may also be recommended in some cases. Furthermore, large clinical studies led by international consortia allow for surveys to be carried out on a large cohort of patients, something of great importance when dealing with rare diseases. In this article, we discuss recent advances in the field of molecular biomarkers for NMDs, analyse approaches to testing, and review the possible development directions and clinical applications in this field.

Criteria for useful biomarkers in NMD

According to the NIH (National Institutes of Health), a biomarker is defined as a "characteristic that is objectively measured and evaluated as an indicator of normal biological processes, pathogenic processes, or pharmacologic response to a therapeutic intervention" [2]. The most important characteristics of biomarkers for NMD are:

- analytical validity (the ability to accurately distinguish between normal and altered status as well as treatment response/non-response),
- clinical validity (the ability to reflect the features of the disease),
- non-invasiveness,
- feasibility (how simple it is to measure),
- cost-effectiveness (being quick and easy to use) [3].

According to the FDA, an ideal biomarker must be specifically associated with a particular disease or disease state, and be able to differentiate between similar physiological conditions [4–5]. Biomarkers should also correlate with clinical outcomes and radiological measures. In terms of accessibility, an ideal biomarker would be easily accessible e.g. from plasma [6]. However, due to the tissue-specific expression of a number of proteins, biomarkers from muscle and skin biopsies still play an important role. CK is still widely used as a biomarker in NMD despite its limitations (it is neither a specific nor a sensitive marker for neuromuscular disease). Reliable biomarkers for NMD in urine or saliva have yet to be identified. In this article, we will differentiate between seven types of biomarkers:

- diagnostic – to detect or confirm the presence of a disease or condition of interest, or identify an individual with a subtype of the disease,
- monitoring – to assess the status of a disease or to detect the effect of a medical product or biological agent,
- pharmacodynamic response - changes in response to exposure to a medical product,
- predictive – its presence or change predicts whether an individual will experience an effect from the exposure to a medical product,
- prognostic - identifies the likelihood of a clinical event in an individual,
- safety - indicates the likelihood, presence, or extent of a toxicity
- susceptibility/risk biomarkers – indicates potential for developing a disease in a healthy individual [7].

A surrogate biomarker is defined as 'a biomarker intended to substitute for a clinical endpoint'. Biomarkers used as an endpoint are often easier to assess and more cost efficient than clinical biomarkers. Translational biomarkers can be easily transferred between pre-clinical and clinical research.

Neuromuscular disorders

NMDs are heterogeneous groups of neurological diseases, including both myopathies as well as neuropathies. The term encompasses various conditions with a different pathophysiological and genetic aetiology, distinct pathophysiological pattern, and heterogeneous phenotypes, even within one disease [8]. There are 955 neuromuscular diseases associated with 535 different genes [9]. They affect directly, by causing pathology in a muscle, or indirectly, by affecting a neuromuscular junction or nerves. The onset varies from infancy to late adulthood. The most common symptoms include muscle weakness that can lead to twitching, cramps and pains, muscle atrophy and hypertrophy, ptosis, swallowing problems, skeletal deformities, fatigability, a waddling gait, and respiratory and cardiac dysfunction. In this article we will concentrate on muscular dystrophy (DMD, BMD), limb girdle muscular dystrophy (LGMD), amyotrophic lateral sclerosis (ALS), facioscapulohumeral muscular dystrophy (FSHD), Charcot-Marie-Tooth disease (CMT), spinal muscle atrophy (SMA), dystrophic myotonias (DM1 and DM2) and Pompe disease (MP). As some of these neuromuscular diseases are very rare, one of the main obstacles to discovering potential molecular biomarkers is the scarcity of samples. Rare neuromuscular conditions can often remain undiagnosed, which significantly impacts upon care.

Molecular biomarkers

We classified the biomarkers based on their chemical structure into:

- DNA
- RNA (including miRNA)
- proteins and peptides
- others (metabolic, cellular) [10].

The main advantages and disadvantages of each class of biomarker are set out in Table 1.

Genomic biomarkers

RNA, and DNA and DNA epigenetic modifications encompass a larger class of genomic biomarkers.

Table 1. Advantages and disadvantages of DNA, RNA and protein biomarkers

Type of biomarker	Advantages	Disadvantages
DNA	High stability High specificity Good accessibility	Demanding validation and discovery process Difficulties with data interpretation
RNA	Tissue specificity	Low stability Low accessibility
Protein	Good accessibility High specificity	Low stability

DNA

DNA biomarkers include SNP (single polymorphism variant) and CNV (copy number variant) as well as insertions, deletions and translocations. DNA biomarkers are easily accessible and repeatable, but their functional meaning is often difficult to assess. Next generation sequencing (NGS) has enabled the rapid discovery of new genes in one-gene disorders and genetic modifiers due to the possibility of finding statistical correlations between phenotypes and genetic variants.

SNP

A single-nucleotide polymorphism (SNP), which is a variation in a single nucleotide that occurs at a specific position in the genome, is a promising alternative biomarker. DMD is one of the neuromuscular conditions most often screened for SNP biomarkers, mainly because of the range of phenotypes among individuals who carry the same mutation. Several independent studies have identified genetic diagnostic and prognostic biomarkers belonging to pathways involved in inflammation, muscle regeneration and contraction (TGF-β), calcium homeostasis, fibrosis and macrophage infiltration (*Cd68)* and genetic modifiers (SPP1) [11]. Large studies, with more than 200 DMD patients enrolled, have shown that the following variants: V194I, T787A, T820A, and T1140M, form the VTTT and IAAM in LTBP4 haplotypes. LTBP4 encoding TGF-beta-binding protein acts as a genetic modifier. Steroid-treated DMD patients homozygous for IAAM remained ambulatory significantly longer (up to 12.5 ± 3.3 years) than similarly treated individuals heterozygotes or homozygotes for VTTT (ambulatory up to 10.7 ± 2.1 years under treatment) [12–13].

Another candidate biomarker for DMD is osteopontin (SPP1). SPP1 expression has been found to be downregulated approximately three-fold in DMD patients with a mild phenotype compared to those who are severely affected. SNP –66T>G in the promoter region of *SPP1* correlates with greater DMD phenotype severity [14]. *SMN2*, *PLS3* and *ZPR1* were rated as modifiers for SMN2 and *EPHA4* and *SMN* for ALS. The modifier effect is not yet fully understood, and further studies are needed [15]. Four single nucleotide SNPs in *SIPA1L2* were recently proved to correlate with foot dorsiflexion strength in Charcot-Marie-Tooth patients. This study was performed on more than 300 patients using genome-wide methods [16].

CNV

Another very promising alternative biomarker is a copy number variation (CNV). This refers to the structural variations – individually variable repeats in the genome. They have already found their diagnostic application in diseases such as CMT1A with *PMP22* duplication and SMA with *SMN1* duplication [17]. Some smaller studies regarding CMT showed that neuropathy-associated CNVs outside of the *PMP22* locus are rare [18]. In ALS, *EPHA3* deletion was defined as a potential protective factor (prognostic and monitoring biomarker), but here again the data was gathered only in a small study [19]. There are ongoing works for validating potential modifying CNVs in the SD region of *TTN* and the TRI region of *NEB* [20]. One big biomarker study failed to identify CNV biomarkers in DMD and COL6 myopathies [21].

Epigenetic biomarkers

Epigenetics is a heritable and acquired alteration in gene activity and expression via chromatin reorganisation without changes in DNA sequence. Epigenetic alterations can occur even in the differentiated cells in response to external factors. Examples of epigenetic changes are DNA methylation and histone modifications. FSHD is a neuromuscular disease associated with an impaired methylation pattern. FSHD is caused by a reduction in the number of 3.3 kb *D4Z4* units arrayed on chromosome 4 to fewer than 11 units. This epigenetic pattern results in transcription of the *DUX4*, which is normally repressed, but only in patients with permissive *D4Z4* haplotypes. The latest research indicates that other factors may be involved in *DUX4* repression and may therefore act as biomarkers [22]. These are *PRC2* as the complex primarily responsible for *DUX4* repression in FSHD, and H3K9 acetylation along with loss of H3K27me3 as key epigenetic events that result in *DUX4* expression [23]. Other examples of the NMD with impaired epigenetics pattern are Emery-Dreifuss muscular dystrophy (EDMD) and progeria. It is still not fully understood how the disease can manifest with two extremely diverse phenotypes. A decrease of the heterochromatin mark H3K9me3 in pericentric regions and a downregulation of the *PRC2* may act as a modifier and may be regarded as a prognostic biomarker in assessing the course of the disease [24].

RNA

RNA, and particularly miRNA, has been investigated as a biomarker in multiple recent studies. Measuring RNA as biomarkers is effective, as RNA provides the most direct route for biomarker validation and assay development. A significant bottleneck in advancing RNA biomarker discoveries to the clinic is the lack of standardised and robust technologies for

measuring RNA biomarkers *in situ* in clinical specimens, not to mention the fact that RNA is unstable and not easily accessible.

mRNA

The possibility of whole transcriptome analysis has contributed greatly to the diagnosis and discovery of RNA expression patterns in numerous NMDs. The limitation is the tissue-specificity of RNA.

In DM, aberrant alternative splicing plays a key role in the pathogenesis. The timing of the appearance of certain miss--spliced events correlates well with disease severity [25]. However, there is not always a direct link between phenotype and RNA level. An SMA study (copy variant dependent disease) surprisingly did not show a clear correlation between SMN RNA expression and motor function [26]. In hereditary neuropathies, recent studies have proved a correlation with several RNA biomarkers from skin biopsies (which can be regarded as prognostic and monitoring biomarkers): *PARG, GSTT2, CTSA, CDA, ENPP1* and *NRG1* in different metabolic pathways with disease progression over time [27]. One analysis addressing whole transcriptome in ALS detected more than 2,000 differentially expressed transcripts in whole blood transcriptome among nearly 400 ALS patients and a large group of healthy individuals. Nevertheless, data interpretation is challenging [28]. Whole transcriptome analysis of a DMD animal model showed different expression patterns in a substantial number of genes. A major obstacle to this study is data interpretation [29].

Non-coding RNA

In recent years, high throughput technologies have enabled an outline of how non- coding RNAs play a regulatory role, providing a potential biomarker for NMD.

miRNAs are non-coding nucleic acids which target mRNA. They are relatively stable and have high concentrations in the blood and the cerebrospinal fluid (CSF). MiRNAs are especially attractive as biomarkers because of their potential utility in experimental therapy, as some of them correlate with therapeutic outcomes. Several microRNAs showed dysregulated expression levels in NMD [30]. miR-1, miR-133a, and miR-206 can be used as powerful prognostic serum biomarkers, not only in DMD but also in myotonic dystrophy 1 (DM1), limb-girdle muscular dystrophy (LGMD), facioscapulohumeral muscular dystrophy (FSHD), Becker muscular dystrophy (BMD), and distal myopathy with rimmed vacuoles (DMRV). DMD is probably the most-investigated NMD in terms of miRNA. Not only three different miRNAs, also known as myomiRs (miR-1, miR-133a/b, and miR-206), showed increased expression in DMD, but also others, such as: miR-208b, miR-499 and miR-31, were overexpressed in DMD patients [31–32]. Studies with phosphorodiamidate morpholino oligonucleotide (PMO)-mediated dystrophin restoration therapy in mdx mice (animal model of DMD) showed the ability of the therapy to correct the dysregulation of the myomiRs (miR-1, -133a/b, -206) to normal wild type levels in serum [33]. These are especially attractive as potential surrogate biomarkers. Serum levels of miRNAs: miR-206, 143-3p and 374b-5p could differentiate a patient with ALS from healthy controls and from patients with other, similar, neuromuscular diseases [34]. MiR-9, miR-132, miR-206, miR-183 and miR-375 were identified as prospective biomarkers for SMA [35]. miR-133a was increased in patients with Pompe disease in a study of 52 patients, while in three newborns miR-133a decreased after starting a replacement therapy [36].

Piwi-interacting RNAs have only recently been linked to human diseases. piRNAs are of interest because they have established gene regulatory functions. Specific serum piRNAs also responded to exon skipping therapy. The role of Piwi--interacting RNAs needs further investigation [37].

Proteins and peptides

Proteomic biomarkers have rapidly developed in recent years, mainly because of the introduction of new discovery techniques. Thanks to mass spectrometry (MS)-based proteome profiling and affinity multiplexing assays, candidate proteins and peptide biomarkers can be identified faster and more effectively [38]. Protein and peptide biomarkers are easily accessible and relatively cost effective to test. Their limitations are instability and problems with repeatability.

CK

A protein diagnostic biomarker still widely used in clinical practice is creatinine kinase-M (CK-M). This is a diagnostic biomarker of muscle (sarcolemma) damage. CK can be applied as a screening parameter for NMD, but it does not correlate well with disease progression and treatment, and shows variability among individuals.

NfL as marker of nerve damage

Neurofilament is a major cytoskeletal protein, expressed in both CNS and PNS, which increases during neuronal damage both in the blood and in the CSF. It is composed of neurofilament light (NFL), medium (NFM), and heavy (NFH) chains. NfL is elevated in multiple neurodegenerative disorders, including Alzheimer's disease, multiple sclerosis, and frontotemporal dementia. A 20-year study revealed that NfL can be a reliable biomarker for ALS, particularly when measured in CSF [39]. Some recent studies have shown that NfL may find its application as a prognostic biomarker for CMT. NfL tested in the blood of patients with CMT was increased compared to healthy controls. This biomarker correlated with clinical disease severity assessed with Rasch modified CMT examination and neuropathy scores [40].

Candidate protein biomarkers

Recent studies, based on multi omics techniques, have identified multiple potential protein biomarkers, but very few of them have found an application in clinics. DMD is of great

interest regarding serum protein biomarkers. As potential candidates, the following proteins have been identified: carbonic anhydrase III (CA-III), MMP9, TIMP1, osteopontin, amyoglobin, myosin light chain-3 (MYL3), troponin T, fast skeletal muscle (TNNT3), plastin-2 (LCP1), protein phosphatase 1F (PPM1F) and electron transfer flavoprotein A (ETFA) [41–43]. They are tied to different pathobiochemical pathways indicative of muscle fibre leakage, inflammation, fibrosis and muscle degeneration/regeneration. MMP-9, a serum marker of degradation and remodelling of the extracellular matrix, was identified a few years ago as one of the most suitable serum biomarkers to monitor disease progression and therapy in DMD [44]. MMP-9 is not specific for DMD and is also elevated in patients with Bethlem and Ullrich myopathy compared to controls. The rise in MMP-9 levels in COL6-related myopathies was less pronounced than in DMD and BMD. Recent studies have revealed that MMP-9 is not a reliable marker to monitor disease course in antisense therapy of DMD [45]. High throughput technologies have highlighted myomesin 3 (MYOM3) as a potential proteomic biomarker, which correlates well with clinical course of both LGMD and DMD. MYOM3 is a myofibrillar structural protein, present in the sera of DMD and LGMD2D patients, as well as in their respective animal models [46]. No powerful candidate biomarker has been identified in the sera of patients with SMA: there was a trend correlation with clinical symptoms for a few candidates, but statistical significance was not reached [47, 48]. Some recent studies have indicated exosome-derived SMN protein as a promising biomarker for SMA [48]. For LGMD, troponin I (sTnI), myosin light chain 3 (Myl3) and fatty acid binding protein 3 (FABP3) have been proposed as potential protein serum biomarkers. These proteins reached statistical significance with some clinical endpoints [49]. In CMT patients, a decrease of some mitochondrial proteins in skin biopsies was noticed [50]. In a small study of CMT patients, several biomarkers were identified, including alterations to serum amyloid protein specific for CMT1 patients and serum transferrin. These results should be verified on a larger cohort of patients [52]. In ALS patients, the most promising protein biomarkers are p75 neurotrophin domain and neurofilaments subunit proteins (NfH and NfL). All these markers are released by neuron or Schwann cell injury and they are not specific for ALS only. p75, which regulates growth and cell differentiation, is high after birth, then decreases in later life and is released to the CSF by Schwann cell or axonal damage. p75 is also elevated in the urine of affected individuals and model animals, and increases with disease progression [53]. Another discussed candidate is one of the growth factors - progranulin (PGRN), which rises in CSF as ALS progresses (monitoring biomarker) [54].

Other biomarkers

Metabolites – These are the intermediate end product of metabolism and are usually various types of small molecules. A new metabolomics technology to study data from a large number of metabolites at the same time is called metabolomics [55]. For NMD there are only a few known metabolic biomarkers, as they are not always useful in this application. Prostaglandin D2 metabolite is increased in DMD patients compared to healthy controls [56]. Other studies have shown increased lipid profile and L-arginine/nitric oxide pathway imbalance in DMD patients [57, 58]. In omni metabolomics analysis, IBM (inclusion body miosities) and mitochondrial neuromuscular diseases clustered differently from other NMDs. Sorbitol, alanine, myoinositol, and cystathionine have been proposed as candidate metabolite biomarkers for mitochondrial myopathies [59].

Cellular biomarkers – for collagen disease in Bethlem myopathy and Ullrich myopathy, the infiltration of macrophages can serve as a biomarker. A difference between DMD

Table 2. Promising biomarkers for NMD in terms of possible clinical application

Biomarker	Disease	Chemical class	Comment
CK	NMD	protein	Not useful in monitoring disease course; great inter-individual variability
LTBP4	DMD	SNP	Haplotypes well characterised in a relatively large cohort of DMD patients
SPP1	DMD	SNP	Correlates well with time of ambulation loss
miR-1, -133a/b, -206	DMD	miRNA	Correlates with treatment outcomes
miR-133a	Pompe disease	miRNA	Assessed in a large cohort of patients afflicted with Pompe disease
NfL	ALS, CMT	protein	Large and long term studies on ALS patients; correlates well with ALS course especially when measured in CSF
PGRN	ALS	protein	
MMM-9	DMD	protein	Not suitable for monitor splicing therapy
Troponin I (sTnI), myosin light chain 3 (Myl3) and fatty acid binding protein 3 (FABP3)	LGMD	protein	Apart from LGMD expressed also in DMD, BMD, but presents a different pattern
Serum amyloid protein and serum transferrin	CMT	protein	Serum amyloid protein is specific to CMT genetic type

and healthy controls can be tested with a flow cytometer. In the case of SMA, the expression of SMN protein in CD3+, CD19+, and CD33++ cells from SMA patients was significantly reduced compared to that in cells from control subjects [60].

Conclusion

Future directions and clinical implications. High-throughput technologies have enabled fast screening for candidate biomarkers, but clinical validation remains a challenge. The integration of molecular biomarkers with clinical endpoints and MRI biomarkers is needed. In some cases, a panel of biomarkers can be much more sensitive than one. Because many NMDs are rare, the omics databases should be available for the researcher community. Another challenge is the interpretation of big data produced in high-throughput technologies and establishing a reliable pattern of biomarkers expression in healthy and affected individuals. Novel biomarkers such as miRNA and protein biomarkers open new therapy perspectives as they can correlate with disease course. A few attractive potential biomarkers have already been outlined, and their advantages and limitations are set out in Table 2. Many of them were investigated only in small studies, and validation on a larger cohort of patients is required. Due to the discovery of candidate biomarkers, molecular pathogenesis of NMDs is better understood and potential targets for future therapies can be identified. Some candidates are attractive options for surrogate biomarkers in future clinical trials. This could significantly speed up trials, thus making them more affordable. The efforts to deliver reliable and sensitive biomarkers have intensified in recent years. We hope that some of the achievements from basic science and pre-clinical trials can be successfully translated into clinical practice.

Funding: *None*

Conflict of interest: *The authors report no conflicts of interest in this work*

Ethical approval *was not necessary for preparation of this article*

References

1. Lim KR, Maruyama R, Yokota T. Eteplirsen in the treatment of Duchenne muscular dystrophy. Drug Des Devel Ther. 2017; 11: 533–545, doi: 10.2147/DDDT.S97635, indexed in Pubmed: 28280301.
2. Strimbu K, Tavel JA. What are biomarkers? Curr Opin HIV AIDS. 2010; 5(6): 463–466, doi: 10.1097/COH.0b013e32833ed177, indexed in Pubmed: 20978388.
3. Scotton C, Ferlini A. Biomarkers in Rare Genetic Diseases. Role of Biomarkers in Medicine. 2016, doi: 10.5772/63354.
4. Jain K. The Handbook of Biomarkers. 2017, doi: 10.1007/978-1-4939-7431-3.
5. Mayeux R. Biomarkers: potential uses and limitations. NeuroRx. 2004; 1(2): 182–188, doi: 10.1602/neurorx.1.2.182, indexed in Pubmed: 15717018.
6. Fleming TR, Powers JH. Biomarkers and surrogate endpoints in clinical trials. Stat Med. 2012; 31(25): 2973–2984, doi: 10.1002/sim.5403, indexed in Pubmed: 22711298.
7. Califf RM. Biomarker definitions and their applications. Exp Biol Med (Maywood). 2018; 243(3): 213–221, doi: 10.1177/1535370217750088, indexed in Pubmed: 29405771.
8. Tasker R, Darras B. Neuromuscular disorders. Current Opinion in Pediatrics. 2013; 25(6): 674–675, doi: 10.1097/mop.0b013e328365de49.
9. Bonne G., Rivier F. Gene Table of Neuromuscular Disorders. http://www.musclegenetable.fr.
10. Scotton C, Passarelli C, Neri M, et al. Biomarkers in rare neuromuscular diseases. Exp Cell Res. 2014; 325(1): 44–49, doi: 10.1016/j.yexcr.2013.12.020, indexed in Pubmed: 24389168.
11. Aartsma-Rus A, Spitali P. Circulating Biomarkers for Duchenne Muscular Dystrophy. J Neuromuscul Dis. 2015; 2(s2): S49–S58, doi: 10.3233/JND-150102, indexed in Pubmed: 27858763.
12. Flanigan KM, Ceco E, Lamar KM, et al. United Dystrophinopathy Project. LTBP4 genotype predicts age of ambulatory loss in Duchenne muscular dystrophy. Ann Neurol. 2013; 73(4): 481–488, doi: 10.1002/ana.23819, indexed in Pubmed: 23440719.
13. Szigyarto CAK, Spitali P. Biomarkers of Duchenne muscular dystrophy: current findings. Degener Neurol Neuromuscul Dis. 2018; 8: 1–13, doi: 10.2147/DNND.S121099, indexed in Pubmed: 30050384.
14. Vianello S, Pantic B, Fusto A, et al. SPP1 genotype and glucocorticoid treatment modify osteopontin expression in Duchenne muscular dystrophy cells. Hum Mol Genet. 2017; 26(17): 3342–3351, doi: 10.1093/hmg/ddx218, indexed in Pubmed: 28595270.
15. Lamar KM, McNally EM. Genetic Modifiers for Neuromuscular Diseases. J Neuromuscul Dis. 2014; 1(1): 3–13, doi: 10.3233/JND-140023, indexed in Pubmed: 25729645.
16. Tao F, Beecham GW, Rebelo AP, et al. Inherited Neuropathy Consortium. Variation in SIPA1L2 is correlated with phenotype modification in Charcot- Marie- Tooth disease type 1A. Ann Neurol. 2019; 85(3): 316–330, doi: 10.1002/ana.25426, indexed in Pubmed: 30706531.
17. Novelli G, Ciccacci C, Borgiani P, et al. Genetic tests and genomic biomarkers: regulation, qualification and validation. Clin Cases Miner Bone Metab. 2008; 5(2): 149–154, indexed in Pubmed: 22460999.
18. Høyer H, Braathen GJ, Eek AK, et al. Copy number variations in a population-based study of Charcot-Marie-Tooth disease. Biomed Res Int. 2015; 2015: 960404, doi: 10.1155/2015/960404, indexed in Pubmed: 25648254.
19. Uyan Ö, Ömür Ö, Ağım ZS, et al. Genome-wide copy number variation in sporadic amyotrophic lateral sclerosis in the Turkish population: deletion of EPHA3 is a possible protective factor. PLoS One. 2013; 8(8): e72381, doi: 10.1371/journal.pone.0072381, indexed in Pubmed: 23991104.
20. Sagath L, Lehtokari VL, Välipakka S, et al. An Extended Targeted Copy Number Variation Detection Array Including 187 Genes for the Diagnostics of Neuromuscular Disorders. J Neuromuscul Dis. 2018; 5(3): 307–314, doi: 10.3233/JND-170298, indexed in Pubmed: 30040739.
21. Final Report Summary - BIO-NMD (Identifying and validating preclinical biomarkers for diagnostics and therapeutics of Neuromuscular Disorders). https://cordis.europa.eu/project/rcn/93293/reporting/en.
22. Lanzuolo C. Epigenetic alterations in muscular disorders. Comp Funct Genomics. 2012; 2012: 256892, doi: 10.1155/2012/256892, indexed in Pubmed: 22761545.

23. Haynes P, Bomsztyk K, Miller DG. Sporadic DUX4 expression in FSHD myocytes is associated with incomplete repression by the PRC2 complex and gain of H3K9 acetylation on the contracted D4Z4 allele. Epigenetics Chromatin. 2018; 11(1): 47, doi: 10.1186/s13072-018-0215-z, indexed in Pubmed: 30122154.
24. Collins CM, Ellis JA, Holaska JM. MAPK signaling pathways and HDAC3 activity are disrupted during differentiation of emerin-null myogenic progenitor cells. Dis Model Mech. 2017; 10(4): 385–397, doi: 10.1242/dmm.028787, indexed in Pubmed: 28188262.
25. Nakamori M, Sobczak K, Puwanant A, et al. Splicing biomarkers of disease severity in myotonic dystrophy. Ann Neurol. 2013; 74(6): 862–872, doi: 10.1002/ana.23992, indexed in Pubmed: 23929620.
26. Crawford TO, Paushkin SV, Kobayashi DT, et al. Pilot Study of Biomarkers for Spinal Muscular Atrophy Trial Group. Evaluation of SMN protein, transcript, and copy number in the biomarkers for spinal muscular atrophy (BforSMA) clinical study. PLoS One. 2012; 7(4): e33572, doi: 10.1371/journal.pone.0033572, indexed in Pubmed: 22558076.
27. Fledrich R, Mannil M, Leha A, et al. Biomarkers predict outcome in Charcot-Marie-Tooth disease 1A. J Neurol Neurosurg Psychiatry. 2017; 88(11): 941–952, doi: 10.1136/jnnp-2017-315721, indexed in Pubmed: 28860329.
28. van Rheenen W, Diekstra FP, Harschnitz O, et al. Whole blood transcriptome analysis in amyotrophic lateral sclerosis: A biomarker study. PLoS One. 2018; 13(6): e0198874, doi: 10.1371/journal.pone.0198874, indexed in Pubmed: 29939990.
29. Almeida CF, Martins PCm, Vainzof M. Comparative transcriptome analysis of muscular dystrophy models Large(myd), Dmd(mdx)/Large(myd) and Dmd(mdx): what makes them different? Eur J Hum Genet. 2016; 24(9): 1301–1309, doi: 10.1038/ejhg.2016.16, indexed in Pubmed: 26932192.
30. Eisenberg I, Alexander MS, Kunkel LM. miRNAS in normal and diseased skeletal muscle. J Cell Mol Med. 2009; 13(1): 2–11, doi: 10.1111/j.1582-4934.2008.00524.x, indexed in Pubmed: 19175696.
31. Zaharieva IT, Calissano M, Scoto M, et al. Dystromirs as serum biomarkers for monitoring the disease severity in Duchenne muscular Dystrophy. PLoS One. 2013; 8(11): e80263, doi: 10.1371/journal.pone.0080263, indexed in Pubmed: 24282529.
32. Matsuzaka Y, Kishi S, Aoki Y, et al. Three novel serum biomarkers, miR-1, miR-133a, and miR-206 for Limb-girdle muscular dystrophy, Facioscapulohumeral muscular dystrophy, and Becker muscular dystrophy. Environ Health Prev Med. 2014; 19(6): 452–458, doi: 10.1007/s12199-014-0405-7, indexed in Pubmed: 25150707.
33. Roberts TC, Blomberg KE, McClorey G, et al. Expression analysis in multiple muscle groups and serum reveals complexity in the microRNA transcriptome of the mdx mouse with implications for therapy. Mol Ther Nucleic Acids. 2012; 1: e39, doi: 10.1038/mtna.2012.26, indexed in Pubmed: 23344181.
34. Waller R, Goodall EF, Milo M, et al. Serum miRNAs miR-206, 143-3p and 374b-5p as potential biomarkers for amyotrophic lateral sclerosis (ALS). Neurobiol Aging. 2017; 55: 123–131, doi: 10.1016/j.neurobiolaging.2017.03.027, indexed in Pubmed: 28454844.
35. Magri F, Vanoli F, Corti S. miRNA in spinal muscular atrophy pathogenesis and therapy. J Cell Mol Med. 2018; 22(2): 755–767, doi: 10.1111/jcmm.13450, indexed in Pubmed: 29160009.
36. Tarallo A, Carissimo A, Gatto F, et al. microRNAs as biomarkers in Pompe disease. Genet Med. 2019; 21(3): 591–600, doi: 10.1038/s41436-018-0103-8, indexed in Pubmed: 29997386.
37. Coenen-Stass AML, Sork H, Gatto S, et al. Comprehensive RNA-Sequencing Analysis in Serum and Muscle Reveals Novel Small RNA Signatures with Biomarker Potential for DMD. Mol Ther Nucleic Acids. 2018; 13: 1–15, doi: 10.1016/j.omtn.2018.08.005, indexed in Pubmed: 30219269.
38. Hathout Y. Proteomic methods for biomarker discovery and validation. Are we there yet? Expert Rev Proteomics. 2015; 12(4): 329–331, doi: 10.1586/14789450.2015.1064771, indexed in Pubmed: 26186709.
39. Weydt P, Oeckl P, Huss A, et al. Neurofilament levels as biomarkers in asymptomatic and symptomatic familial amyotrophic lateral sclerosis. Ann Neurol. 2016; 79(1): 152–158, doi: 10.1002/ana.24552, indexed in Pubmed: 26528863.
40. Sandelius Å, Zetterberg H, Blennow K, et al. Plasma neurofilament light chain concentration in the inherited peripheral neuropathies. Neurology. 2018; 90(6): e518–e524, doi: 10.1212/WNL.0000000000004932, indexed in Pubmed: 29321234.
41. Nicholson LV, Walls TJ, Nicholson LV. Serum myoglobin in muscular dystrophy and carrier detection. J Neurol Sci. 1981; 51(3): 411–426, indexed in Pubmed: 7276986.
42. Ohta M, Itagaki Y, Itoh N, et al. Carbonic anhydrase III in serum in muscular dystrophy and other neurological disorders: relationship with creatine kinase. Clin Chem. 1991; 37(1): 36–39, indexed in Pubmed: 1899062.
43. Ayoglu B, Chaouch A, Lochmüller H, et al. Affinity proteomics within rare diseases: a BIO-NMD study for blood biomarkers of muscular dystrophies. EMBO Mol Med. 2014; 6(7): 918–936, doi: 10.15252/emmm.201303724, indexed in Pubmed: 24920607.
44. Nadarajah VD, van Putten M, Chaouch A, et al. Serum matrix metalloproteinase-9 (MMP-9) as a biomarker for monitoring disease progression in Duchenne muscular dystrophy (DMD). Neuromuscul Disord. 2011; 21(8): 569–578, doi: 10.1016/j.nmd.2011.05.011, indexed in Pubmed: 21724396.
45. Lourbakos A, Yau N, de Bruijn P, et al. Evaluation of serum MMP-9 as predictive biomarker for antisense therapy in Duchenne. Sci Rep. 2017; 7(1): 17888, doi: 10.1038/s41598-017-17982-y, indexed in Pubmed: 29263366.
46. Rouillon J, Poupiot J, Zocevic A, et al. Serum proteomic profiling reveals fragments of MYOM3 as potential biomarkers for monitoring the outcome of therapeutic interventions in muscular dystrophies. Hum Mol Genet. 2015; 24(17): 4916–4932, doi: 10.1093/hmg/ddv214, indexed in Pubmed: 26060189.
47. Sumner CJ, Kolb SJ, Harmison GG, et al. SMN mRNA and protein levels in peripheral blood: biomarkers for SMA clinical trials. Neurology. 2006; 66(7): 1067–1073, doi: 10.1212/01.wnl.0000201929.56928.13, indexed in Pubmed: 16481599.
48. Crawford TO, Paushkin SV, Kobayashi DT, et al. Pilot Study of Biomarkers for Spinal Muscular Atrophy Trial Group. Evaluation of SMN protein, transcript, and copy number in the biomarkers for spinal muscular atrophy (BforSMA) clinical study. PLoS One. 2012; 7(4): e33572, doi: 10.1371/journal.pone.0033572, indexed in Pubmed: 22558076.
49. Nash LA, McFall ER, Perozzo AM, et al. Survival Motor Neuron Protein is Released from Cells in Exosomes: A Potential Biomarker for Spinal Muscular Atrophy. Sci Rep. 2017; 7(1): 13859, doi: 10.1038/s41598-017-14313-z, indexed in Pubmed: 29066780.
50. Burch PM, Pogoryelova O, Goldstein R, et al. Muscle-Derived Proteins as Serum Biomarkers for Monitoring Disease Progression in Three Forms of Muscular Dystrophy. J Neuromuscul Dis. 2015; 2(3): 241–255, doi: 10.3233/JND-140066, indexed in Pubmed: 26870665.

51. Soldevilla B, Cuevas-Martín C, Ibáñez C, et al. Plasma metabolome and skin proteins in Charcot-Marie-Tooth 1A patients. PLoS One. 2017; 12(6): e0178376, doi: 10.1371/journal.pone.0178376, indexed in Pubmed: 28575008.
52. Jennings MJ, Roos A, Horvath R. Serum biomarker discovery for Charcot-Marie-Tooth disease. Neuromuscular Disorders. 2018; 28: S21, doi: 10.1016/s0960-8966(18)30351-1.
53. Katyal N, Govindarajan R. Shortcomings in the Current Amyotrophic Lateral Sclerosis Trials and Potential Solutions for Improvement. Front Neurol. 2017; 8: 521, doi: 10.3389/fneur.2017.00521, indexed in Pubmed: 29033893.
54. Benatar M, Boylan K, Jeromin A, et al. ALS biomarkers for therapy development: State of the field and future directions. Muscle Nerve. 2016; 53(2): 169–182, doi: 10.1002/mus.24979, indexed in Pubmed: 26574709.
55. Kim SuJ, Kim SuH, Kim JiH, et al. Understanding Metabolomics in Biomedical Research. Endocrinol Metab (Seoul). 2016; 31(1): 7–16, doi: 10.3803/EnM.2016.31.1.7, indexed in Pubmed: 26676338.
56. Nakagawa T, Takeuchi A, Kakiuchi R, et al. A prostaglandin D2 metabolite is elevated in the urine of Duchenne muscular dystrophy patients and increases further from 8 years old. Clin Chim Acta. 2013; 423: 10–14, doi: 10.1016/j.cca.2013.03.031, indexed in Pubmed: 23603101.
57. Srivastava NK, Pradhan S, Mittal B, et al. High resolution NMR based analysis of serum lipids in Duchenne muscular dystrophy patients and its possible diagnostic significance. NMR Biomed. 2010; 23(1): 13–22, doi: 10.1002/nbm.1419, indexed in Pubmed: 19787747.
58. Hörster I, Weigt-Usinger K, Carmann C, et al. The L-arginine/NO pathway and homoarginine are altered in Duchenne muscular dystrophy and improved by glucocorticoids. Amino Acids. 2015; 47(9): 1853–1863, doi: 10.1007/s00726-015-2018-x, indexed in Pubmed: 26066683.
59. Buzkova J, Nikkanen J, Ahola S, et al. Metabolomes of mitochondrial diseases and inclusion body myositis patients: treatment targets and biomarkers. EMBO Mol Med. 2018; 10(12), doi: 10.15252/emmm.201809091, indexed in Pubmed: 30373890.
60. Otsuki N, Arakawa R, Kaneko K, et al. A new biomarker candidate for spinal muscular atrophy: Identification of a peripheral blood cell population capable of monitoring the level of survival motor neuron protein. PLoS One. 2018; 13(8): e0201764, doi: 10.1371/journal.pone.0201764, indexed in Pubmed: 30102724.

REVIEW ARTICLE

Neurologia i Neurochirurgia Polska
Polish Journal of Neurology and Neurosurgery
2019, Volume 53, no. 3, pages: 181–189
DOI: 10.5603/PJNNS.a2019.0018

ISSN 0028–3843

Statement by a Working Group conceived by the Polish National Consultants in Cardiology and Neurology addressing the use of implantable cardiac monitors in patients after ischaemic embolic stroke of undetermined source

Michał M. Farkowski[1], Michał A. Karlinski[2], Jarosław Kaźmierczak[3], Piotr Kułakowski[4], Przemysław Mitkowski[5], Paweł Ptaszyński[6], Danuta Ryglewicz[2], Jarosław Sławek[7], Agnieszka Słowik[8], Maciej Sterliński[1]

[1]Institute of Cardiology, Warsaw, Poland
[2]Institute of Psychiatry and Neurology, Warsaw, Poland
[3]Pomeranian Medical University, Szczecin, Poland
[4]Postgraduate Medical Education Center, Warsaw, Poland
[5]Poznan University of Medical Sciences, Poland
[6]Medical University of Lodz, Poland
[7]Medical University of Gdansk, Poland
[8]Jagiellonian University Medical College, Krakow, Poland

ABSTRACT

Introduction. Stroke remains one of the main causes of death and the most common cause of long-term disability in adults. Embolic strokes of undetermined source (ESUS) amount to a significant proportion of all ischaemic strokes. Detection of atrial fibrillation (AF) in this group of patients would allow for a major therapeutic decision to switch from antiplatelets to oral anticoagulants and therefore significantly reduce the risk of recurrence.

State of the Art. Current technology allows long-term continuous ECG monitoring with different systems, including implantable cardiac monitors (ICM). However, in Poland lack of reimbursement does not allow their use in everyday clinical practice.

Clinical Implications. This is a statement by a Working Group conceived by the Polish National Consultants in Cardiology and Neurology addressing the use of ICM in patients after ischaemic embolic strokes of undetermined source. The aim was to develop reasonable and comprehensive guidance on how to select and manage candidates for ICM in order to obtain the maximum benefit for Polish public health.

Future Directions. This expert opinion is not intended as a guideline but it provides advice as to how to optimise the potential use of ICM in patients after ESUS in the Polish setting.

Key words: acute ischaemic stroke, embolic stroke of undetermined source, atrial fibrillation, ECG monitoring
(*Neurol Neurochir Pol 2019; 53 (3): 181–189*)

Address for correspondence: Michał A. Karlinski, Institute of Psychiatry and Neurology, Warsaw, Poland, e-mail: mkarlinski@ipin.edu.pl

Therapeutic problem

Despite continuous progress in prevention and treatment observed over recent decades, stroke remains one of the main causes of death, and the most common cause of long-term disability, in adults in developed countries [1, 2].

In about 80% of cases stroke is ischaemic [2]. According to the map of health needs related to hospital treatment in Poland developed by the Ministry of Health, ischaemic stroke was the main cause of 64,400 hospital stays in Polish stroke units in 2016 [3]. Only about 9% of patients with the principal diagnosis of acute ischaemic stroke were treated in non-stroke departments [3].

The mortality rate in Polish patients after ischaemic stroke was 14.5% within 30 days, 21.5% within 90 days, and reached 30.2% at 12 months [3].

In terms of aetiology, stroke is a heterogeneous condition. Therefore, in order to implement optimal secondary prevention, it is necessary to individually identify its most probable cause in each patient. According to the generally applicable TOAST (Trial of Org 10172 in Acute Stroke Treatment) classification, the main causes of ischaemic stroke may be [4]:

- Large artery atherosclerosis (about 25% of ischaemic strokes worldwide [5], and 18% in Poland [6]; 5-year recurrence 23%, 5-year risk of death 31% [7]). Diagnosed if there is ≥ 50% stenosis or occlusion of a large artery or its branches supplying the infarct area with no evidence of a cardiac source of embolism.
- Cardioembolism (about 20% of ischaemic strokes worldwide [5], and 28% in Poland [6]; 5-year recurrence 25%, 5-year risk of death 65% [7]). Diagnosed if there is at least one potential source of embolic material (e.g. atrial fibrillation, prosthetic cardiac valve, left ventricular or atrial thrombus, sick sinus syndrome, recent myocardial infarction, dilated cardiomyopathy, akinetic left ventricular segment, atrial myxoma, infective endocarditis) with no advanced atherosclerosis of the supplying arteries.
- Small vessel disease (about 25% of ischaemic strokes worldwide [5], and 12% in Poland [6]; 5-year recurrence 20%, 5-year risk of death about 20% [7]). Diagnosed if there is no clinical evidence of cerebral cortical dysfunction and no evident infarct focus or a relevant brain stem lesion or a relevant subcortical lesion measures < 1.5 cm (so called lacunar lesion).
- Other determined causes (about 5% of ischaemic strokes worldwide [5], about 4% in Poland). Most frequently diagnosed in the presence of nonatherosclerotic vasculopathies (e.g. dissection, fibrous dysplasia, vasculitis, moyamoya disease) or hypercoagulable states.
- No clear cause or more than one probable cause (about 25% of ischaemic strokes worldwide [5], and up to 39% of ischaemic strokes in Poland [6]; 5-year recurrence 23%, 5-year risk of death 25% [7]).

Identification of a cardioembolism is of primary importance for secondary prevention. Randomised studies have not revealed any clear benefits of using anti-platelet agents in this group, which are an implicit standard of treatment of each ischaemic stroke in the acute phase [8]. However, long term treatment with vitamin K antagonists is known to reduce the relative risk of another ischaemic stroke by 64% (NNT 12 in 1 year) [8]. A similar or even higher efficacy in preventing stroke compared to warfarin, together with a superior safety profile, has been shown for novel oral anticoagulants (NOAC) [9, 10]. Moreover, a subsequent ischaemic stroke which occurs despite treatment with an oral anticoagulant is milder and has more favourable outcome [11].

Therefore, cardiological diagnostic workup, especially screening for cardiac arrhythmias, is one of the key elements of a hospital stay in the stroke unit [12]. A positive history of atrial fibrillation or its identification after ischaemic stroke is a clear indication for implementation of oral anticoagulation, preferably with the use of a NOAC [13].

Research data suggests that a major proportion of strokes of unknown aetiology, so called 'cryptogenic' strokes, have in fact an embolic origin [5]. For this reason, in 2014, a new subtype of cryptogenic stroke was introduced: embolic strokes of undetermined source (ESUS) [5]. The diagnosis of ESUS requires combination of all following criteria:

- Non-lacunar ischaemic lesion responsible for the symptoms detected by computed tomography (CT) or magnetic resonance imaging (MRI)
- Absence of extracranial or intracranial atherosclerosis causing ≥ 50% luminal stenosis in arteries supplying the area of ischaemia (ultrasound, angio-CT or angio-MRI)
- No major risk cardioembolic source of embolism (12-lead ECG, at least 24-hour Holter ECG monitoring and transthoracic echocardiography)
- No other specific cause of stroke identified

It is estimated that 9–25% of patients with acute ischaemic stroke meet the criteria of ESUS [6, 14]. Compared to the other types of ischaemic stroke, patients with ESUS are younger, have milder neurological deficits, and a better chance of remaining independent in everyday activities [6, 14]. Therefore, in this group of patients optimal and intense secondary prevention is especially justified.

The results of a prospective analysis of patients hospitalised due to acute stroke at the Institute of Psychiatry and Neurology between 2001 and 2015 show that the real proportion of ESUS in Poland is probably between 10% and 20% of all acute ischaemic strokes [6].

With regard to recurrence (3–6% within one year) and the potential therapeutic benefit of safe anticoagulation with NOAC, two randomised clinical trials were conducted to evaluate the safety and efficacy of long term treatment with rivaroxaban (NAVIGATE ESUS, terminated prematurely in 2017, N = 7,213) or dabigatran (RE-SPECT ESUS,

completed in 2018, N = 5,390) compared to standard dose aspirin [14]. Unfortunately, neither of the studies showed NOAC superiority in preventing strokes [15, 16] (World Stroke Conference 2018). Moreover, the use of rivaroxaban was associated with an increased risk of haemorrhagic complications [16].

As a consequence, it must be recognised that the current concept of ESUS has proved to be clinically impractical. *Post hoc* analyses of the abovementioned trials are likely to provide information as to which ESUS subpopulations might potentially benefit from oral anticoagulation, based on additional demographic, clinical, imaging and electrophysiological criteria. Nevertheless, the hypotheses generated in this way will have to be verified in further randomised trials. Considering the duration of such potential trials, new solutions may appear no sooner than in a few years.

Therefore, it is reasonable to subject patients currently classified as having ESUS based on standard diagnostic criteria to further diagnostic workup. Due to the potential therapeutic implications, targeting confirmation of a suspected cardioembolism seems to be of particular importance. This will allow the identification of patients with a potentially higher risk of recurrence than the average for the whole ESUS group, and subsequently reduce this risk by the introduction of an oral anticoagulant.

It is desirable that ECG monitoring initiated shortly after ESUS be prolonged, especially in the subpopulation with additional signs of atrial disease [17–22]. Supplementary diagnostic procedures should be initiated as soon as possible following the occurrence of stroke, in order to maximise the benefits of potentially indicated anticoagulation. A delayed diagnosis of atrial fibrillation after the first ischaemic stroke is related to a 1.5-fold higher risk of recurrence [23]. It also needs to be emphasised that the curves of survival free of another stroke diverge already in the first year of follow-up, later becoming almost parallel [23].

Standard procedures in the acute phase of ischaemic stroke

Acute stroke is a life-threatening condition, and as such requires urgent admission to a stroke unit. The diagnosis of stroke is based on symptoms and clinical signs with the support of brain imaging. In Poland, the hospital stay of an acute stroke patient lasts in most cases eight days or longer. This time is fully sufficient to conduct the standard diagnostic process recommended by guidelines, including the guidelines from the Section of Vascular Diseases at the Polish Neurological Society [12, 24, 25]:

- Brain imaging: CT (usually), CT and MRI (sometimes), or only MRI (rarely); performed at least once on admission to hospital; allows a determination to be made as to whether the stroke is ischaemic or haemorrhagic; it can reveal an acute lesion, silent brain infarcts, and signs of small vessel disease
- Vascular imaging: carotid ultrasound (always), transcranial Doppler (usually), CT angiography or MRI angiography (sometimes additionally); performed to assess atherosclerosis and confirm or exclude other less common vascular pathologies
- Screening for cardiac arrhythmias: resting ECG (at least once), monitoring of heart rate with a cardiomonitor for at least 24 hours (almost always), 24-hour Holter monitoring (usually); may detect previously undiagnosed atrial fibrillation
- Echocardiography: transthoracic echocardiography (usually), transoesophageal echocardiography (as a supplementary examination is some cases); may detect source of cardiac embolism

Reperfusion therapy is the gold standard of treatment in all eligible cases. Intravenous thrombolysis is available at all Polish stroke units and is fully reimbursed. Currently, such treatment is used in about 13% of patients. Mechanical thrombectomy as a therapy supporting thrombolytic treatment, or as the therapy of choice in patients not eligible to thrombolysis, is indicated for strokes caused by occlusion or critical stenosis. In Poland it is not reimbursed and is therefore used in less than 1% of patients. A pilot project launched by the Ministry of Health in January 2019 should enable reasonable nationwide access to thrombectomy within the next few years.

All acute patients who are not eligible for reperfusion therapy should receive anti-platelet therapy (usually 150-300 mg of aspirin, or sometimes a combination of aspirin and clopidogrel). Aspirin is also initiated 24 hours after reperfusion therapy [12, 24, 25].

After the acute phase, long-term treatment with aspirin 75–150 mg is maintained unless the stroke has been considered to be cardioembolic. In such cases, aspirin should be replaced with an oral anticoagulant as soon as it is safe for the patient [12, 24–26].

Atrial fibrillation and ischaemic stroke

According to the guidelines, atrial fibrillation (AF) is diagnosed on an electrocardiogram showing completely irregular R-R intervals with the absence of marked P waves, lasting at least 30 s [13, 27]. AF is the most common arrhythmia in the population. Its prevalence in the general population is about 1–2% of patients on average. In selected risk groups (e.g. old age, ESUS, numerous general and cardiological diseases), this proportion is much higher [13, 27].

AF aetiology is believed to be multifactorial. It entails genetic conditioning, as well as comorbidities and lifestyle [27].

AF may become manifest with general weakness, the sensation of skipping beats, reduced exercise tolerance, chest discomfort, sleeping disorders or anxiety. Basic AF therapy

involves a strategy of rhythm control or ventricular rate control [13]. AF may result in serious complications leading to death or significant disability: cardiac insufficiency, ischaemic stroke or peripheral embolism [13]. The basis of primary and secondary prevention of stroke is oral anticoagulant therapy (OAT). Each patient should undergo risk stratification regarding vascular events with the use of a CHA_2DS_2-VASc scale, and if a score of 2 or higher is achieved – oral anticoagulation should be introduced [13]. It must be remembered that a history of ischaemic stroke adds 2 points to the total CHA_2DS_2-VASc score [13]. This means in practice that oral anticoagulation is indicated for every patient with a history of atrial fibrillation and ischaemic stroke, regardless of the time of its detection.

ECG monitoring

Due to the potentially serious embolic consequences of AF and the possibility of their effective prevention, all scientific societies and expert groups find it justified to screen for AF patients with a high risk of stroke [13, 27]. ESUS patients also belong in the group of high risk of both AF and recurrent stroke. Therefore prolonged ECG monitoring after ESUS is recommended both during the stroke unit stay and in the outpatient setting.

Monitoring may be non-invasive (e.g. prolonged Holter monitoring, external arrhythmia recorders, electronic devices) or invasive, in the form of an implantable cardiac monitor (ICM) [27].

Clinical trials have shown that the longer the monitoring, the greater the chance of detecting AF. In CRYSTAL-AF, the use of ICM in patients after cryptogenic stroke resulted in diagnosing AF in an additional 7.5% of patients (8.9% *vs* 1.4%) within six months, in an additional 10.4% (12.4% *vs* 2.0%) within 12 months, and in an additional 27.0% (30.0% vs 3.0%) within three full years of follow-up [28, 29]. In another clinical trial, during a one year follow-up, ICM implantation yielded an additional 15.3% (17% *vs* 1.7%) AF diagnoses compared to 7-day Holter monitoring [30]. Unfortunately, there are no randomised studies confirming the clinical benefits of anticoagulation therapy in AF diagnosis made with the use of ICM. However, there are no reasons to believe that they will significantly differ from the benefits experienced by patients with AF diagnosed with the use of standard ECG monitoring.

In current clinical practice, prolonged ECG monitoring after a stroke is rare, and qualification for such monitoring is highly individualised [19]. Such practice results from limited financial and human resources and definitely brings no benefit on the level of public health [19]. On the other hand, the high direct cost of prolonged ECG monitoring require the proper selection of patients to maximise the proportion of screenings yielding positive results.

Currently, Polish patients have very limited access to long-term ECG monitoring. ICM implantation and follow-up visits are not reimbursed, and the National Health Fund does not account for the number of days of Holter ECG monitoring, nor does it provide separate financing of external or implantable arrhythmia recorders.

Considering these limitations, and the uncertainty about long-term benefit, it is suggested that only patients with the highest risk of AF occurrence should be referred for such diagnostic workup [18]. Observational studies consistently point to older age as the main risk factor of the occurrence/recognition of AF after cryptogenic stroke [20].

Currently there are three initially validated scoring systems used to stratify the risk of occurrence/recognition of AF in patients scheduled for long-term ECG monitoring after ESUS that are worth mentioning. These are: MrWALLETS (from -2 to 5 points) [31], HAVOC (from 0 to 14 points) [32], and Brown ESUS-AF score (from 0 to 4 points) [33]. According to a group of experts from the German Cardiac Society and the German Stroke Society there are several predictors of AF in patients after ischaemic stroke, including age ≥ 75 years, left atrial diameter > 45 mm, detection of supraventricular arrhythmias and increased serum BNP or NT-proBNP level [18]. In contrast, age < 60 years, left atrial diameter < 40 mm, low number of supraventricular arrhythmias and low serum BNP or NT-proBNP level suggest a low probability of detecting AF [18].

This set of variables overlaps with the Brown ESUS-AF score (age 65–74 years = 1 point, age ≥ 75 years = 2 points, moderate or severe left atrial enlargement = 2 points). The Brown ESUS-AF score has been developed based on the analysis of 296 ESUS patients subjected to prolonged ECG monitoring (initial 30-day external monitoring followed by optional ICM implantation). Atrial fibrillation was detected in 21% of patients in a subgroup scoring 2 points (sensitivity 63%, specificity 71%), in 22% of patients scoring 3 points, and in 56% of patients scoring 4 points [33].

In our opinion, ICM implantation is especially justified in two groups of patients after an ESUS that did not result in a permanent loss of independence in performing daily activities:

- Age 65–74 years with left atrial enlargement ≥ 45 mm
- Age ≥ 75 years with left atrial enlargement > 40 mm

It may be assumed that after such selection ICM monitoring should result in the detection of AF in about 30% of patients (similarly to the group with ≥ 2 points in the Brown ESUS-AF score).

Clinical aspects of the use of ICM

Modern cardiac implantable electronic devices (CIED: cardiac pacemakers, cardioverter defibrillators, resynchronisation therapy systems), if they enable direct recording of atrial electrical activity, are the best model for identifying supraventricular tachyarrhythmias, since they can do it continuously, 24 hours a day. The system should allow for an

intracardiac electrogram (IEGM). Based only on the criterion of atrial electrical activity, episodes with a rate exceeding 160–170 beats/min are usually considered to be atrial high rate episodes (AHRE). Such episodes may include various supraventricular tachycardias, not only episodes of atrial flutter/fibrillation. Therefore, confirmation of the latter is only possible via a careful analysis of IEGM. It must be emphasised that CIEDs are implanted based on a set of well-described indications, and a diagnosis of AHRE is just a side effect of the primary function of the device.

The 2016 guidelines of the European Society of Cardiology on atrial fibrillation recommend (as class I indications) a regular CIED memory interrogation in order to identify AHRE [13]. Patients with diagnosed AHRE should undergo further ECG monitoring in order to document potential AF episodes before the onset of oral anticoagulant therapy, while IEGM recording is enough to document the arrhythmia. The same recommendations for patients after stroke suggest the consideration of additional (more than 72 hours) long-term ECG monitoring with the use of non-invasive ECG recorders or ICM in order to document AF. Implantable cardiac monitors are small devices [mm] 45–88.4 x 7–15.2 x 3–6.2, depending on the manufacturer and model. The recorders are implanted subcutaneously in the parasternal region, in the 4th intercostal space. The battery allows operation of the device for 2–4 years. The implantation procedure is minimally invasive and performed under local anaesthesia, in the setting of an operating room or treatment room, and is characterised by 100% efficacy. The device is oriented to achieve the highest possible amplitude of ventricular complexes, usually at a 45 degree angle to the sternal long axis, along the sternum or in any other position between the above two.

Another element of the system is the possibility of telemonitoring. A special modem enables automatic transmission of arrhythmic episodes to a dedicated server. The episodes are available for a physician taking care of the patient within 24 hours of their occurrence. ICMs record only ventricular electrical activity (QRS complexes), so episodes of atrial fibrillation may be suspected only thanks to special algorithms which assess irregularities of R-R intervals on the basis of the analysis of Lorentz plots. Detection of atrial fibrillation is possible when the arrhythmia lasts for at least two minutes. The algorithms detecting atrial fibrillation based on the analysis of changes in R-R intervals are also available in some models of single chamber cardioverter defibrillators. Basic technical data of particular ICMs are presented in Table 1.

Device interrogation (including device memory) is usually conducted every 3–12 months in the device control clinic or by means of remote control (based on the telemonitoring technology) with the same time intervals as controls in the clinic. In the latter case, it is recommended that once a year the interrogation is performed during a visit to the clinic. As previously mentioned, the remote control of devices enables not only automatic reporting at pre-programmed time intervals, but also immediate transmission of information about a significant clinical event (e.g. episode of atrial fibrillation) within 24 hours of its occurrence.

Asymptomatic episodes of atrial fibrillation are much more frequent than symptomatic ones. In a study by Orlow et al., which included 427 patients with an implanted pacemaker in accordance with applicable indications, the risk of an atrial high rate episode after two years of follow-up was 53.8% and 88.6% in a subgroup without and with a history of supraventricular tachyarrhythmias, respectively [34]. Moreover, the episodes were asymptomatic in these groups in 94.7% and 75.3% of cases, respectively. The symptoms reported by patients were not consistent with arrhythmia episodes in most of the enrolled patients. Importantly, as much as 93% of AHREs were, in fact, supraventricular tachyarrhythmias and not AFs. In another study involving patients with an implanted CIED, it was found that as much as 95% of AF episodes are asymptomatic [35]. The percentage of correct AF diagnoses based on the analysis of AHRE in the ICM memory increases with the episode duration: starting from 83% for episodes > 6 minutes up to 97% for episodes > 6 hours [34]. False positive AHRE diagnoses are usually caused by episodes of: repetitive non-reentrant ventriculo-atrial synchrony (RNRVAS) – 80.4%, R-wave oversensing on the atrial lead – 7.5%, interference – 6.9%, and other factors – 5.2%.

A subanalysis of the CRYSTAL-AF trial, which included patients after ischaemic stroke with ICM, compared the sensitivity of detecting AF episodes between ICM and other ECG recording methods [36]. Compared to ICM, one 24-hour Holter examination showed a sensitivity of 1.3%, and a continuous 30-day examination 22.8%. With a 24-hour Holter examination repeated every three months this figure was 3.1%, and with a 7-day examination it was 20.8%. It is apparent that compared to an AF diagnosis based on implantable episode recorders, all other analysed methods of ECG registration allow detection of only one in every four AF episodes.

The latest algorithms of atrial fibrillation implemented in ICMs are characterised by over 99% sensitivity and a positive predictive value of 95% [37].

Optimal patient pathway for ICM implantation

To ensure early detection and quick therapeutic decision after the occurrence of clinically significant arrhythmia the process of qualification, implantation and outpatient follow-up needs to be standardised.

a) Tasks of the stroke centre
   - Identification of an ESUS patient eligible for ICM implantation
   - Brief explanation of the whole procedure and obtaining patient's initial consent to a possible ICM implantation
   - Initiation of the process of final qualification for ICM implantation at the collaborating cardiological centre

Table 1. Basic technical data of selected implantable arrhythmic episode recorders

Manufacturer	Abbott	Biotronik	Medtronic
Model	Confirm Rx™[1] DM3500	Biomonitor 2	Reveal LINQ LNQ1
Dimensions (mm): length x width x thickness	49 x 9 x 3	88.4 x 15.2 x 6.2	45 x 7 x 4
Volume (cm^3)	1.4	5	1.2
ECG storage capacity (min)	60	66	59
Diagnosed episodes	Asystole, Brady, Tachy, AF	Asystole, Brady, AF, HVR, SRD	Asystole, Brady, Tachy, AT, AF
Mean time of operation (years)	2	4	3

AF – atrial fibrillation; AT – atrial tachycardia; HVR – high ventricular rate; SRD – sudden rate drop

b) Tasks of the cardiological centre
- Verification of indications for ICM implantation based on patient's medical records and discussing alternative methods of long-term ECG monitoring that are currently available
- ICM implantation
  - ICM implantation in the CIED operating room; perioperative antibiotic prophylaxis in accordance with local standards is required; the procedure should be performed by a cardiologist experienced in CIED implantations
  - ICM interrogation before discharge
- Schedule of follow-up visits
  - Permanent remote monitoring in accordance with the standard of a given centre, but allowing everyday assessment of ICM report. If remote monitoring is not possible, additional visits should be scheduled to ensure that the device is interrogated every three months.
  - Follow-up visit 3 months after implantation: assessment of the implantation site and ICM function
  - Follow-up visits every 12 months
  - Emergency visit in the case of recorded arrhythmia requiring a therapeutic decision

Observational studies show that the real-life diagnostic workup in Polish stroke units may not be sufficient to clearly determine if a given cryptogenic stroke may be classified as ESUS [6]. Therefore, if the patient has an opportunity of cost-free long-term ECG monitoring, it is especially important to start by making a diagnosis of ESUS as described in the previous section. It should also be considered to introduce an additional procedure of 48–72-hour ECG Holter monitoring or to equip stroke units with telemetric systems capable of automated detection of arrhythmias and adding it to the NHF list of procedures for stroke.

Follow-up visits should be performed by a cardiologist capable of addressing different cardiac conditions. It is important to provide the possibility of a telemetric rhythm control to ensure quick diagnosis of arrhythmias and immediate implementation of adequate treatment. ICM telemonitoring was an integral part of the diagnostic strategy used in clinical trials and therefore influenced the outcomes [28–30].

In our opinion, it is reasonable to maintain ICM and continue follow-up visits until battery depletion even in patients with AF detected by the device. This strategy is justified by the risk coincidence of clinically significant arrhythmias other than AF, and by the possibility of monitoring the AF treatment efficacy or diagnosing syncopes. The real costs of outpatient ICM visits may be considered similar to pacemaker visits, since they require a detailed overview and verification of all automatically detected and recorded episodes. The annual cost of telemedical follow-up is estimated to equal the cost of four pacemaker visits.

Recommended conditions of arrhythmia monitoring with ICM following ESUS

a) Neurological centres
- Stroke unit which admits at least 200 patients with ischaemic stroke a year
- Equipment and human resources allowing full standard diagnostic workup necessary to diagnose ESUS in each patient with cryptogenic ischaemic stroke
- Ability to provide follow-up at the hospital outpatient neurological clinic

b) Cardiological centres
- Ability to implant ICM within 4 weeks from the first information received from the cooperating stroke centre about a patient meeting neurological criteria of qualification
- Resources ensuring comprehensive care of AF patient, i.e. a team experienced in CIED procedures and electrophysiology (EP), CIED/EP operating theatre, on-site transthoracic and transoesophageal echocardiography, on-site access to prolonged ECG examination (7-day Holter, external arrhythmia recorders), CIED outpatient clinic, on-site general cardiological outpatient clinic
- Experience in remote monitoring of CIED
- Possibility of delivering a cardiological consultation on a 24-hour basis

Health needs at the national level

In order to estimate the health needs in the area of ICM implantation after ESUS, an additional analysis was conducted based on the material used in the study of Bembenek et al., making the following assumptions [6].

- The results presented in the publication of Bembenek et al. may be extrapolated to the general Polish population
- Inclusion criteria are the first-ever ischaemic stroke, age ≥ 65 years, and left atrial enlargement
- Annual number of patients admitted to Polish stroke units for acute ischaemic stroke is 64,400
- At discharge from the stroke unit the patient is assessed as independent in daily activities (0–2 points on the modified Rankin Scale)

In the basic variant (i.e. assuming that the proportion of ESUS patients will be equal to the proportion of patients with a certain ESUS diagnosis), the annual number of patients eligible for intense prolonged ECG monitoring may amount to 800. In the maximum variant (i.e. including patients not classified as certain ESUS due to not having echocardiography), the annual number of cases may rise to 1,625.

Additionally, it must be emphasised that the data stored in the registry did not allow determination of the degree of left atrial enlargement. This means that the actual population size is probably less numerous. Moreover, not every patient will be willing to undergo a procedure that requires repeated visits to a specialised cardiological centre.

Conclusion

Adequate cardiological workup is one of the main factors determining the type of pharmacotherapy used in the secondary prevention of ischaemic stroke. In a large proportion of patients, standard diagnostics do not allow stroke aetiology to be determined. Therefore, there is a need for closer cooperation between stroke centres and cardiological centres and a need for systemic solutions that would facilitate such cooperation.

Research data indicates, that early initiation of prolonged ECG monitoring in a properly selected group of patients after embolic stroke of undetermined source could provide the chance of detecting atrial fibrillation, consequently reducing the risk of recurrence by timely introduction of oral anticoagulation.

Current technology allows long-term continuous ECG monitoring with the use of ICM. Due to high patient cost and the lack of dedicated financing from the NHF, this medical technology is not available to a Polish stroke patient. Nevertheless, considering the health benefits in the context of the whole population, efforts should be made to implement long term ECG monitoring after ESUS in reasonably selected patients.

Conflict of interest *MMF received consultancy, proctoring or lecturer fees from Medtronic, Abbott, Boston Scientific, Pfizer; MK received lecturer fees from Boehringer Ingelheim, Ever Pharma, Bayer, travel grants for scientific conferences from Boehringer Ingelheim and Ever Pharma, consultancy fees from Medtronic; JK received lecturer fees from Medtronic, Biotronik, Abbott and proctoring fees from Medtronic; PK received lecturer fees from Medtronic, Biotronik, Abbott; PM received honoraria from Medtronic, Biotronik, Abbott, Boston Scientific and investigator fees from Medtronic, Abbott; PP received lecturer fees from Medtronic, Abbott and grants from Medtronic; DR received an honorarium for an advisory board meeting of Medtronic; JS received lecturer fees from Medtronic; AS received honoraria for advisory board meetings of Boehringer Ingelheim and advisory meetings of Bayer, Boehringer Ingelheim, Novartis, MERCK, lecturer fees from Bayer, Boehringer Ingelheim, Novartis, Polpharma, Bristol-Myers Squipp, Novartis, Biogen, Teva, Medtronic, MERCK; MS received consultancy and lecturer fees from Abbott, Adamed, Biotronik, Boehringer Ingelheim, Boston Scientific, Medtronic, Novartis, Pfizer and investigator fees from Biotronik, Medtronic, Zoll.*

Ethics *Ethical approval was not necessary for preparation of this article.*

References

1. Kim AS, Cahill E, Cheng NT. Global Stroke Belt: Geographic Variation in Stroke Burden Worldwide. Stroke. 2015; 46(12): 3564–3570, doi: 10.1161/STROKEAHA.115.008226, indexed in Pubmed: 26486867.
2. Krishnamurthi RV, Feigin VL, Forouzanfar MH, et al. Global Burden of Diseases, Injuries, Risk Factors Study 2010 (GBD 2010), GBD Stroke Experts Group. Global and regional burden of first-ever ischaemic and haemorrhagic stroke during 1990-2010: findings from the Global Burden of Disease Study 2010. Lancet Glob Health. 2013; 1(5): e259–e281, doi: 10.1016/S2214-109X(13)70089-5, indexed in Pubmed: 25104492.
3. Mapa potrzeb zdrowotnych w zakresie lecznictwa szpitalnego dla Polski. Ministerstwo Zdrowia 2018. http://www.mpz.mz.gov. pl/mapy-szpitalne-ustawowe-2018/, dostęp 06. ; 12: 2018.
4. Adams HP, Bendixen BH, Kappelle LJ, et al. Classification of subtype of acute ischemic stroke. Definitions for use in a multicenter clinical trial. TOAST. Trial of Org 10172 in Acute Stroke Treatment. Stroke. 1993; 24(1): 35–41, indexed in Pubmed: 7678184.
5. Hart RG, Diener HC, Coutts SB, et al. Cryptogenic Stroke/ESUS International Working Group. Embolic strokes of undetermined source: the case for a new clinical construct. Lancet Neurol. 2014; 13(4): 429–438, doi: 10.1016/S1474-4422(13)70310-7, indexed in Pubmed: 24646875.
6. Bembenek JP, Karlinski MA, Kurkowska-Jastrzebska I, et al. Embolic strokes of undetermined source in a cohort of Polish stroke patients. Neurol Sci. 2018; 39(6): 1041–1047, doi: 10.1007/s10072-018-3322-5, indexed in Pubmed: 29556872.
7. Li L, Yiin GS, Geraghty OC, et al. Oxford Vascular Study. Incidence, outcome, risk factors, and long-term prognosis of cryptogenic transient ischaemic attack and ischaemic stroke: a population-based study. Lancet Neurol. 2015; 14(9): 903–913, doi: 10.1016/S1474-4422(15)00132-5, indexed in Pubmed: 26227434.
8. Hart R, Pearce L. Antithrombotic Therapy To Prevent Stroke in Patients with Atrial Fibrillation. Annals of Internal Medicine. 2000; 132(10): 841, doi: 10.7326/0003-4819-132-10-200005160-00017.

9. Ruff CT, Giugliano RP, Braunwald E, et al. Comparison of the efficacy and safety of new oral anticoagulants with warfarin in patients with atrial fibrillation: a meta-analysis of randomised trials. Lancet. 2014; 383(9921): 955–962, doi: 10.1016/S0140-6736(13)62343-0, indexed in Pubmed: 24315724.
10. López-López JA, Sterne JAC, Thom HHZ, et al. Oral anticoagulants for primary prevention, treatment and secondary prevention of venous thromboembolic disease, and for prevention of stroke in atrial fibrillation: systematic review, network meta-analysis and cost-effectiveness analysis. Health Technol Assess. 2017; 21(9): 1–386, doi: 10.3310/hta21090, indexed in Pubmed: 28279251.
11. Hellwig S, Grittner U, Audebert H, et al. Non-vitamin K-dependent oral anticoagulants have a positive impact on ischaemic stroke severity in patients with atrial fibrillation. Europace. 2018; 20(4): 569–574, doi: 10.1093/europace/eux087, indexed in Pubmed: 28460024.
12. Boulanger JM, Lindsay MP, Gubitz G, et al. Canadian Stroke Best Practice Recommendations for Acute Stroke Management: Prehospital, Emergency Department, and Acute Inpatient Stroke Care, 6th Edition, Update 2018. Int J Stroke. 2018; 13(9): 949–984, doi: 10.1177/1747493018786616, indexed in Pubmed: 30021503.
13. Kirchhof P, Benussi S, Kotecha D, et al. ESC Scientific Document Group. 2016 ESC Guidelines for the management of atrial fibrillation developed in collaboration with EACTS. Eur Heart J. 2016; 37(38): 2893–2962, doi: 10.1093/eurheartj/ehw210, indexed in Pubmed: 27567408.
14. Hart RG, Catanese L, Perera KS, et al. Embolic Stroke of Undetermined Source: A Systematic Review and Clinical Update. Stroke. 2017; 48(4): 867–872, doi: 10.1161/STROKEAHA.116.016414, indexed in Pubmed: 28265016.
15. Diener HC, Easton JD, Granger CB, et al. RE-SPECT ESUS Investigators. Design of Randomized, double-blind, Evaluation in secondary Stroke Prevention comparing the EfficaCy and safety of the oral Thrombin inhibitor dabigatran etexilate vs. acetylsalicylic acid in patients with Embolic Stroke of Undetermined Source (RE-SPECT ESUS). Int J Stroke. 2015; 10(8): 1309–1312, doi: 10.1111/ijs.12630, indexed in Pubmed: 26420134.
16. Hart RG, Sharma M, Mundl H, et al. NAVIGATE ESUS Investigators. Rivaroxaban for Stroke Prevention after Embolic Stroke of Undetermined Source. N Engl J Med. 2018; 378(23): 2191–2201, doi: 10.1056/NEJMoa1802686, indexed in Pubmed: 29766772.
17. Carmona-Puerta R, Castro-Torres Y. Atrial fibrillation and cryptogenic stroke. What is the current evidence? Role of electrocardiographic monitoring. J Arrhythm. 2018; 34(1): 1–3, doi: 10.1002/joa3.12016, indexed in Pubmed: 29721107.
18. Haeusler KG, Gröschel K, Köhrmann M, et al. Expert opinion paper on atrial fibrillation detection after ischemic stroke. Clin Res Cardiol. 2018; 107(10): 871–880, doi: 10.1007/s00392-018-1256-9, indexed in Pubmed: 29704214.
19. Haeusler KG, Tütüncü S, Schnabel RB. Detection of Atrial Fibrillation in Cryptogenic Stroke. Curr Neurol Neurosci Rep. 2018; 18(10): 66, doi: 10.1007/s11910-018-0871-1, indexed in Pubmed: 30090997.
20. Sanna T, Ziegler P, Crea F. Detection and management of atrial fibrillation after cryptogenic stroke or embolic stroke of undetermined source. Clinical Cardiology. 2018; 41(3): 426–432, doi: 10.1002/clc.22876.
21. Widimsky P, Doehner W, Diener HC, et al. ESC Council on Stroke. The role of cardiologists in stroke prevention and treatment: position paper of the European Society of Cardiology Council on Stroke. Eur Heart J. 2018; 39(17): 1567–1573, doi: 10.1093/eurheartj/ehx478, indexed in Pubmed: 29020357.
22. Jonas D, Kahwati L, Yun J, et al. Screening for Atrial Fibrillation With Electrocardiography. JAMA. 2018; 320(5): 485, doi: 10.1001/jama.2018.4190.
23. Chou PS, Ho BL, Chan YH, et al. Delayed diagnosis of atrial fibrillation after first-ever stroke increases recurrent stroke risk: a 5-year nationwide follow-up study. Intern Med J. 2018; 48(6): 661–667, doi: 10.1111/imj.13686, indexed in Pubmed: 29193638.
24. Powers WJ, Rabinstein AA, Ackerson T, et al. American Heart Association Stroke Council. 2018 Guidelines for the Early Management of Patients With Acute Ischemic Stroke: A Guideline for Healthcare Professionals From the American Heart Association/American Stroke Association. Stroke. 2018; 49(3): e46–e4e110, doi: 10.1161/STR.0000000000000158, indexed in Pubmed: 29367334.
25. Grupa Ekspertów Sekcji Chorób naczyniowych Polskiego Towarzystwa Neurologicznego. Postępowanie w udarze mózgu. Neurol Neurochir Pol. 2012; 46: s1–116.
26. Steffel J, Verhamme P, Potpara TS, et al. ESC Scientific Document Group, ESC Scientific Document Group . The 2018 European Heart Rhythm Association Practical Guide on the use of non-vitamin K antagonist oral anticoagulants in patients with atrial fibrillation. Eur Heart J. 2018; 39(16): 1330–1393, doi: 10.1093/eurheartj/ehy136, indexed in Pubmed: 29562325.
27. Mairesse GH, Moran P, Van Gelder IC, et al. ESC Scientific Document Group. Screening for atrial fibrillation: a European Heart Rhythm Association (EHRA) consensus document endorsed by the Heart Rhythm Society (HRS), Asia Pacific Heart Rhythm Society (APHRS), and Sociedad Latinoamericana de Estimulación Cardíaca y Electrofisiología (SOLAECE). Europace. 2017; 19(10): 1589–1623, doi: 10.1093/europace/eux177, indexed in Pubmed: 29048522.
28. Brachmann J, Morillo CA, Sanna T, et al. Uncovering Atrial Fibrillation Beyond Short-Term Monitoring in Cryptogenic Stroke Patients: Three-Year Results From the Cryptogenic Stroke and Underlying Atrial Fibrillation Trial. Circ Arrhythm Electrophysiol. 2016; 9(1): e003333, doi: 10.1161/CIRCEP.115.003333, indexed in Pubmed: 26763225.
29. Sanna T, Diener HC, Passman RS, et al. CRYSTAL AF Investigators. Cryptogenic stroke and underlying atrial fibrillation. N Engl J Med. 2014; 370(26): 2478–2486, doi: 10.1056/NEJMoa1313600, indexed in Pubmed: 24963567.
30. Ritter M, Kochhäuser S, Duning T, et al. Occult Atrial Fibrillation in Cryptogenic Stroke. Stroke. 2013; 44(5): 1449–1452, doi: 10.1161/strokeaha.111.676189.
31. Muscari A, Bonfiglioli A, Faccioli L, et al. Usefulness of the MrWALLETS Scoring System to Predict First Diagnosed Atrial Fibrillation in Patients With Ischemic Stroke. Am J Cardiol. 2017; 119(7): 1023–1029, doi: 10.1016/j.amjcard.2016.12.009, indexed in Pubmed: 28153345.
32. Kwong C, Ling AY, Crawford MH, et al. A Clinical Score for Predicting Atrial Fibrillation in Patients with Cryptogenic Stroke or Transient Ischemic Attack. Cardiology. 2017; 138(3): 133–140, doi: 10.1159/000476030, indexed in Pubmed: 28654919.
33. Ricci B, Chang AD, Hemendinger M, et al. A Simple Score That Predicts Paroxysmal Atrial Fibrillation on Outpatient Cardiac Monitoring after Embolic Stroke of Unknown Source. J Stroke Cerebrovasc Dis. 2018; 27(6): 1692–1696, doi: 10.1016/j.jstrokecerebrovasdis.2018.01.028, indexed in Pubmed: 29501269.
34. Orlov MV, Ghali JK, Araghi-Niknam M, et al. Atrial High Rate Trial Investigators. Asymptomatic atrial fibrillation in pacemaker recipients:

incidence, progression, and determinants based on the atrial high rate trial. Pacing Clin Electrophysiol. 2007; 30(3): 404–411, doi: 10.1111/j.1540-8159.2007.00682.x, indexed in Pubmed: 17367361.
35. Strickberger SA, Ip J, Saksena S, et al. Relationship between atrial tachyarrhythmias and symptoms. Heart Rhythm. 2005; 2(2): 125–131, doi: 10.1016/j.hrthm.2004.10.042, indexed in Pubmed: 15851283.
36. Choe WC, Passman RS, Brachmann J, et al. CRYSTAL AF Investigators. A Comparison of Atrial Fibrillation Monitoring Strategies After Cryptogenic Stroke (from the Cryptogenic Stroke and Underlying AF Trial). Am J Cardiol. 2015; 116(6): 889–893, doi: 10.1016/j.amjcard.2015.06.012, indexed in Pubmed: 26183793.
37. Pürerfellner H, Sanders P, Sarkar S, et al. Adapting detection sensitivity based on evidence of irregular sinus arrhythmia to improve atrial fibrillation detection in insertable cardiac monitors. Europace. 2018; 20(FI_3): f321–f328, doi: 10.1093/europace/eux272, indexed in Pubmed: 29036652.

REVIEW ARTICLE

Neurologia i Neurochirurgia Polska
Polish Journal of Neurology and Neurosurgery
2019, Volume 53, no. 3, pages: 190–193
DOI: 10.5603/PJNNS.a2019.0022

ISSN 0028–3843

Prevention of epilepsy in humans – truth or myth? The experience from Sturge-Weber syndrome and Tuberous Sclerosis Complex

Monika Słowińska[1], Weronika Golec[1], Sergiusz Jóźwiak[1, 2]

[1]Department of Child Neurology, Medical University of Warsaw, Warsaw, Poland
[2]Department of Neurology and Epileptology, The Children's Memorial Health Institute, Warsaw, Poland

Abstract

Introduction. Epilepsy is a chronic neurological disease, usually decreasing the quality of life and often resulting in other comorbidities e.g. cognitive impairment in children. Despite the recent discovery of new antiepileptic drugs, roughly one in three patients suffers from drug-resistant seizures. Therefore, the prevention of epilepsy is becoming one of the most important challenges in medicine. Is it, however, in fact possible to prevent epilepsy?

Clinical reflections and implications. We present the results of preventive antiepileptic treatment in children with Sturge-Weber syndrome and Tuberous Sclerosis Complex as examples of the possible prevention of epilepsy and epilepsy-associated cognitive impairment in children.

Key words: epilepsy, prevention, tuberous sclerosis, Sturge-Weber

(Neurol Neurochir Pol 2019; 53 (3): 190–193)

Epilepsy affects approximately 50 million patients worldwide, with an incidence in paediatric patients that varies from 3.4 to 5.8 per 1,000 [1]. Effective epilepsy treatment and swift seizure cessation are especially important in children in whom uncontrolled seizures deteriorate the psychomotor functions, which leads to cognitive impairment and reduced quality of life in adulthood [2, 3]. Regardless of the immense progress in epilepsy treatment that has been made in recent years, drug-resistant epilepsy still afflicts roughly 30% of patients [4]. Therefore to the goal should be to try to prevent epilepsy. The question is whether the prevention of epilepsy is truly possible?

It has been documented that the process of epilepsy development (epileptogenesis) begins with an insulting/triggering factor (i.e. genetic mutation, injury, metabolic disease). This is followed by a latent period of changes in protein expression and ion channel functioning, and finally manifests with clinical seizures [5]. However, the epileptogenic process does not end with the occurrence of clinical epilepsy, but persists beyond the initial seizures, leading to the development of drug-resistant epilepsy and epilepsy-related comorbidities [5]. Thus, a better understanding of epileptogenesis may lead to the development of new, antiepileptogenic (AEG) therapies. There is an important difference between the terms antiepileptic (AED) and antiepileptogenic (AEG) drugs. AEDs (e.g. phenytoin, carbamazepine) are implemented after seizure onset and reduce seizure frequency and severity but do not influence epileptogenesis [5, 6]. On the other hand, AEGs may be introduced before or after epilepsy onset, and they change the natural course of epilepsy by counteracting epileptogenesis by prevention, seizure modification, reduction or prevention of the progression of epilepsy, or curing. Therefore, currently, the terms antiseizure (ASD) or anticonvulsant, rather than antiepileptic drug (AED) are beginning to be used in order to better distinguish the antiepileptogenic from the antiseizure effects of action [6].

In the light of recent studies on epileptogenesis, a first step to prevent epilepsy is to identify patients with a high risk of epilepsy development before the occurrence of clinical

Address for correspondence: Monika Słowińska, Department of Child Neurology, Medical University of Warsaw, Warsaw, Poland, e-mail: monikaslowinska91@gmail.com

seizures. It is well known that patients after traumatic brain injury or stroke have an increased risk of epilepsy [7, 8]. However, objective studies on epileptogenesis and the possibility of its prevention are difficult in these groups of patients due to their considerable heterogeneity in terms of their aetiology, epilepsy risk, and the variety of environmental and individual factors that influence epileptogenesis [5, 7, 8].

On the other hand, some paediatric genetic diseases are highly associated with early-onset epilepsy, leading to more homogenous groups, and patients may be diagnosed before the development of clinical seizures, which enables a preventive intervention. Therefore, such children may be a perfect group for possible preventive antiepileptogenic treatment and studies of epileptogenesis.

Sturge-Weber syndrome (SWS) is a vascular neurocutaneous disorder with an incidence of 1 in 20,000–50,000 live births and it is characterised by a very high overall risk of epilepsy, that reaches 80-90% in the first two years of life [9, 10]. Due to a characteristic facial naevus, SWS can be diagnosed early, before epilepsy [11]. The study of Ville et al. demonstrated that preventive treatment with phenobarbital in SWS patients significantly decreased the incidence of epilepsy and delayed development compared to the control SWS group treated after first seizures [12]. The presence of developmental venous anomalies and decreased brain tissue perfusion leading to anoxic brain injury are the major contributory factors to epileptogenesis in SWS [13–15]. Early identification of potential predicting factors, combined with prophylactic antiepileptogenic therapy, may significantly improve the clinical outcome and life quality of patients.

Another paediatric model for possible antiepileptogenic intervention is tuberous sclerosis complex (TSC). This is a genetic neurocutaneous disorder with a high risk of early onset epilepsy (70–90%) associated with cognitive impairment (50–60% of TSC patients) and autistic behaviour [16]. TSC is more frequent than SWS, affecting 1 in 6,000 people and can be diagnosed very early, before clinical seizures, and even prenatally [16, 17]. The first seizures in TSC usually occur within first two years of life, mostly at the age of 4–6 months, and it has been proved that epileptiform discharges in electroencephalography (EEG) precede clinical seizures in TSC infants, being a good predictive factor for preventive treatment [18–20]. Based on the evolution pattern from epileptic EEG record to clinical seizures, we performed in our previous study regular EEG studies in infants with TSC and introduced preventive treatment with vigabatrin when ictal discharges occurred in EEG, but before clinical seizures [21]. At the age of 24 months, significantly more children in the preventive group were seizure-free compared to the standard group treated after clinical seizures (35% *vs* 93%, $p = 0.004$). Moreover, fewer children in the preventive cohort had drug-resistant epilepsy (7% *vs* 42%, $p = 0.021$). Also, of great importance for parents and children, the cognitive functioning of children treated before clinical seizures was significantly better (mean IQ: 92.3 *vs* 68.7, $p < 0.05$) and intellectual disability was also less frequent (14.3% *vs* 48.4%, $p = 0.031$) [21].

Besides the abovementioned treatment implications, new and interesting therapy approaches are emerging. Mutations in TSC1 or TSC2, encoding two tumour suppressor proteins of the mammalian target of rapamycin (mTOR) pathway, are known to cause TSC [22]. The mTOR signalling pathway is recognised as regulating a number of cellular processes required in the growth, metabolism, structure and interactions of neuronal cells [23]. Inactivation of one of the TSC genes results in overactivation of the mTOR pathway, leading to the development of benign tumours or hamartomas in multiple organs. In the majority of patients, the brain is one of the most affected organs, which results in epilepsy, developmental delay, and neurobehavioural or neuropsychiatric disorders [24]. The establishment of a connection between TSC1/TSC2 mutations and mTOR led to the clinical use of drugs known as mTOR inhibitors: sirolimus and everolimus. These are becoming an increasingly interesting tool in the management of TSC-associated symptoms and epileptogenesis [23, 25]. It has been demonstrated that mTOR inhibitors can be used in the treatment of many features of TSC, including subependymal giant cell astrocytomas (SEGA), renal angiomyolipomas (AML), lymphangioleiomyomatosis (LAM), and skin lesions [26–29]. Moreover, EXIST-3, a recent prospective, randomised, multicentre, placebo-controlled study, established that everolimus can be used as adjunctive therapy for the treatment of refractory seizures associated with TSC [30]. Everolimus reduces seizure frequency in a dose-dependent manner with a tolerable safety profile in TSC patients with refractory epilepsy [30]. The odds for response in patients treated with everolimus were 2.2–3.9 times higher than with a placebo [30]. Furthermore, a positive effect of everolimus has been observed in a variety of seizure types [30].

In conclusion, we feel that the mTOR pathway represents a great opportunity for future novel antiepileptogenic drugs. Moreover, another benefit of the use of mTOR inhibitors in TSC is the possibility of simultaneously improving not only one manifestation, e.g. SEGA or seizures, but also other TSC symptoms. The currently available findings regarding mTOR inhibitors, both clinical and pre-clinical, are intriguing and highly supportive of future experiments.

Currently, TSC is considered to be one of the best models for prospective studies of epileptogenesis in humans due to a homogenous group of patients, the possibility of a diagnosis before seizures, and the possibility of early (before clinical seizures) and easy detection of epileptogenesis based on ictal discharges on EEG.

Hence, at present there are two large, multicentre studies on epilepsy prevention in TSC in Europe and the US ongoing: EPISTOP (ClinicalTrials.gov Identifier: NCT02098759) (www.epistop.eu) and PREVENT (ClinicalTrials.gov Identifier:

NCT02849457). The EPISTOP project is focused not only on the prevention of epilepsy but also on the identification of the clinical and molecular biomarkers of epileptogenesis in humans. The project ended in April 2019 and the results of EPISTOP may shed new light on the management and prevention of epilepsy in humans.

Undoubtedly, the prevention of epilepsy is a serious challenge. However, prevention is possible, and it has been proved that preventive treatment may be particularly effective and important in epileptic encephalopathies such as TSC and SWS, reducing not only seizures but also their comorbidities [31]. Future studies using predictive biomarkers will demonstrate the extent to which this may be useful in other types of seizures, and in adult patients.

Acknowledgments and funding

This study was in part supported by the 7th Framework Programme of the European Commission within the Large-scale Integrating Project EPISTOP (Proposal No: 602391–2; Proposal title: 'Long term, prospective study evaluating clinical and molecular biomarkers of epileptogenesis in a genetic model of epilepsy – tuberous sclerosis complex'; www.EPISTOP.eu), the Polish Ministerial Funds for Science (years 2014–2018) for the implementation of international co-financed projects, and the grant EPIMARKER of the Polish

National Centre for Research and Development No STRATEGMED3/306306/4/2016.

Conflict of interest: *The authors declare no conflict of interest.*

References

1. Behr C, Goltzene MA, Kosmalski G, et al. Epidemiology of epilepsy. Rev Neurol (Paris). 2016; 172(1): 27–36, doi: 10.1016/j.neurol.2015.11.003, indexed in Pubmed: 26754036.
2. Garcia-Ramos C, Dabbs K, Meyerand E, et al. Psychomotor slowing is associated with anomalies in baseline and prospective large scale neural networks in youth with epilepsy. Neuroimage Clin. 2018; 19: 222–231, doi: 10.1016/j.nicl.2018.04.020, indexed in Pubmed: 30035016.
3. Lenck-Santini PP, Scott RC. Mechanisms Responsible for Cognitive Impairment in Epilepsy. Cold Spring Harb Perspect Med. 2015; 5(10), doi: 10.1101/cshperspect.a022772, indexed in Pubmed: 26337111.
4. Kalilani L, Sun X, Pelgrims B, et al. The epidemiology of drug-resistant epilepsy: A systematic review and meta-analysis. Epilepsia. 2018; 59(12): 2179–2193, doi: 10.1111/epi.14596, indexed in Pubmed: 30426482.
5. Pitkänen A, Lukasiuk K, Dudek FE, et al. Epileptogenesis. Cold Spring Harb Perspect Med. 2015; 5(10), doi: 10.1101/cshperspect.a022822, indexed in Pubmed: 26385090.
6. Clossen BL, Reddy DS. Novel therapeutic approaches for disease-modification of epileptogenesis for curing epilepsy. Biochim Biophys Acta Mol Basis Dis. 2017; 1863(6): 1519–1538, doi: 10.1016/j.bbadis.2017.02.003, indexed in Pubmed: 28179120.
7. Graham N, Crichton S, Koutroumanidis M, et al. Incidence and Associations of Poststroke Epilepsy. Stroke. 2013; 44(3): 605–611, doi: 10.1161/strokeaha.111.000220.
8. Englander J, Bushnik T, Duong TT, et al. Analyzing risk factors for late posttraumatic seizures: a prospective, multicenter investigation. Arch Phys Med Rehabil. 2003; 84(3): 365–373, doi: 10.1053/apmr.2003.50022, indexed in Pubmed: 12638104.
9. Comi AM. Update on Sturge-Weber syndrome: diagnosis, treatment, quantitative measures, and controversies. Lymphat Res Biol. 2007; 5(4): 257–264, doi: 10.1089/lrb.2007.1016, indexed in Pubmed: 18370916.
10. Comi AM. Sturge-Weber syndrome. Handb Clin Neurol. 2015; 132: 157–168, doi: 10.1016/B978-0-444-62702-5.00011-1, indexed in Pubmed: 26564078.
11. Sudarsanam A, Ardern-Holmes SL. Sturge-Weber syndrome: from the past to the present. Eur J Paediatr Neurol. 2014; 18(3): 257–266, doi: 10.1016/j.ejpn.2013.10.003, indexed in Pubmed: 24275166.
12. Ville D, Enjolras O, Chiron C, et al. Prophylactic antiepileptic treatment in Sturge-Weber disease. Seizure. 2002; 11(3): 145–150, doi: 10.1053/seiz.2001.0629, indexed in Pubmed: 12018956.
13. Kaseka ML, Bitton JY, Décarie JC, et al. Predictive Factors for Epilepsy in Pediatric Patients With Sturge-Weber Syndrome. Pediatr Neurol. 2016; 64: 52–58, doi: 10.1016/j.pediatrneurol.2016.08.009, indexed in Pubmed: 27637568.
14. Pinto A, Sahin M, Pearl PL. Epileptogenesis in neurocutaneous disorders with focus in Sturge Weber syndrome. F1000Res. 2016; 5, doi: 10.12688/f1000research.7605.1, indexed in Pubmed: 27019697.
15. Alkonyi B, Chugani HT, Juhász C. Transient focal cortical increase of interictal glucose metabolism in Sturge-Weber syndrome: implications for epileptogenesis. Epilepsia. 2011; 52(7): 1265–1272, doi: 10.1111/j.1528-1167.2011.03066.x, indexed in Pubmed: 21480889.
16. Curatolo P, Bombardieri R, Jozwiak S. Tuberous sclerosis. Lancet. 2008; 372(9639): 657–668, doi: 10.1016/S0140-6736(08)61279-9, indexed in Pubmed: 18722871.
17. Słowińska M, Jóźwiak S, Peron A, et al. Early diagnosis of tuberous sclerosis complex: a race against time. How to make the diagnosis before seizures? Orphanet J Rare Dis. 2018; 13(1): 25, doi: 10.1186/s13023-018-0764-z, indexed in Pubmed: 29378663.
18. Chu-Shore CJ, Major P, Camposano S, et al. The natural history of epilepsy in tuberous sclerosis complex. Epilepsia. 2010; 51(7): 1236–1241, doi: 10.1111/j.1528-1167.2009.02474.x, indexed in Pubmed: 20041940.
19. Domańska-Pakieła D, Kaczorowska M, Jurkiewicz E, et al. EEG abnormalities preceding the epilepsy onset in tuberous sclerosis complex patients - a prospective study of 5 patients. Eur J Paediatr Neurol. 2014; 18(4): 458–468, doi: 10.1016/j.ejpn.2013.12.006, indexed in Pubmed: 24412076.
20. Whitney R, Jan S, Zak M, et al. The Utility of Surveillance Electroencephalography to Guide Early Antiepileptic Drug Therapy in Infants With Tuberous Sclerosis Complex. Pediatr Neurol. 2017; 72: 76–80, doi: 10.1016/j.pediatrneurol.2017.04.009, indexed in Pubmed: 28506505.
21. Jóźwiak S, Kotulska K, Domańska-Pakieła D, et al. Antiepileptic treatment before the onset of seizures reduces epilepsy severity and risk of mental retardation in infants with tuberous sclerosis complex. Eur J Paediatr Neurol. 2011; 15(5): 424–431, doi: 10.1016/j.ejpn.2011.03.010, indexed in Pubmed: 21507691.

22. Caban C, Khan N, Hasbani DM, et al. Genetics of tuberous sclerosis complex: implications for clinical practice. Appl Clin Genet. 2017; 10: 1–8, doi: 10.2147/TACG.S90262, indexed in Pubmed: 28053551.
23. Sadowski K, Kotulska-Jóźwiak K, Jóźwiak S. Role of mTOR inhibitors in epilepsy treatment. Pharmacol Rep. 2015; 67(3): 636–646, doi: 10.1016/j.pharep.2014.12.017, indexed in Pubmed: 25933981.
24. Salussolia CL, Klonowska K, Kwiatkowski DJ, et al. Genetic Etiologies, Diagnosis, and Treatment of Tuberous Sclerosis Complex. Annu Rev Genomics Hum Genet. 2019 [Epub ahead of print], doi: 10.1146/annurev-genom-083118-015354, indexed in Pubmed: 31018109.
25. Schubert-Bast S, Rosenow F, Klein KM, et al. The role of mTOR inhibitors in preventing epileptogenesis in patients with TSC: Current evidence and future perspectives. Epilepsy Behav. 2019; 91: 94–98, doi: 10.1016/j.yebeh.2018.05.039, indexed in Pubmed: 29941212.
26. Franz DN, Belousova E, Sparagana S, et al. Efficacy and safety of everolimus for subependymal giant cell astrocytomas associated with tuberous sclerosis complex (EXIST-1): a multicentre, randomised, placebo-controlled phase 3 trial. Lancet. 2013; 381(9861): 125–132, doi: 10.1016/S0140-6736(12)61134-9, indexed in Pubmed: 23158522.
27. Bissler JJ, Kingswood JC, Radzikowska E, et al. Everolimus for angiomyolipoma associated with tuberous sclerosis complex or sporadic lymphangioleiomyomatosis (EXIST-2): a multicentre, randomised, double-blind, placebo-controlled trial. Lancet. 2013; 381(9869): 817–824, doi: 10.1016/S0140-6736(12)61767-X, indexed in Pubmed: 23312829.
28. McCormack FX, Inoue Y, Moss J, et al. National Institutes of Health Rare Lung Diseases Consortium, MILES Trial Group. Efficacy and safety of sirolimus in lymphangioleiomyomatosis. N Engl J Med. 2011; 364(17): 1595–1606, doi: 10.1056/NEJMoa1100391, indexed in Pubmed: 21410393.
29. Jóźwiak S, Sadowski K, Kotulska K, et al. Topical Use of Mammalian Target of Rapamycin (mTOR) Inhibitors in Tuberous Sclerosis Complex--A Comprehensive Review of the Literature. Pediatr Neurol. 2016; 61: 21–27, doi: 10.1016/j.pediatrneurol.2016.04.003, indexed in Pubmed: 27222056.
30. French JA, Lawson JA, Yapici Z, et al. Adjunctive everolimus therapy for treatment-resistant focal-onset seizures associated with tuberous sclerosis (EXIST-3): a phase 3, randomised, double-blind, placebo-controlled study. Lancet. 2016; 388(10056): 2153–2163, doi: 10.1016/S0140-6736(16)31419-2, indexed in Pubmed: 27613521.
31. Jóźwiak S, Kotulska K. Prevention of epileptogenesis–a new goal for epilepsy therapy. Pediatr Neurol. 2014; 51(6): 758–759, doi: 10.1016/j.pediatrneurol.2014.08.019, indexed in Pubmed: 25283750.

RESEARCH PAPER

Neurologia i Neurochirurgia Polska
Polish Journal of Neurology and Neurosurgery
2019, Volume 53, no. 3, pages: 194–198
DOI: 10.5603/PJNNS.a2019.0019

ISSN 0028–3843

Association between polymorphisms of a folate – homocysteine – methionine – SAM metabolising enzyme gene and multiple sclerosis in a Polish population

Monika Chorąży[1], Natalia Wawrusiewicz-Kurylonek[2], Joanna Gościk[3], Renata Posmyk[4], Agata Czarnowska[1], Marta Więsik[5], Katarzyna Kapica-Topczewska[1], Adam Jacek Krętowski[2], Jan Kochanowicz[1], Alina Kułakowska[1]

[1]Department of Neurology, Medical University in Bialystok, Bialystok, Poland
[2]Department of Endocrinology, Diabetology and Internal Medicine, Medical University in Bialystok, Bialystok, Poland
[3]Faculty of Computer Science, Bialystok University of Technology, Bialystok, Poland
[4]Department of Perinatology, Medical University in Bialystok, Bialystok, Poland
[5]Alab Diagnostic Laboratory Company, Warsaw, Poland

ABSTRACT

Background and Objectives. Multiple sclerosis (MS) is a chronic inflammatory, autoimmune disease with a still unknown aetiology. The main initial mechanism of demyelination and injury to the central nervous system (CNS) appears to be inflammation. Neurotoxicity induced by homocysteine (Hcy) may be a factor affecting this process. 5,10-methylenetetrahydrofolate reductase (MTHFR) is an essential enzyme involved in Hcy metabolism. It leads to Hcy remethylation to methionine. In the present study, we aimed to investigate a possible association between two variants of MTHFR gene in patients with MS in Poland and healthy individuals.

Methods. In this study, we genotyped 174 relapsing-remitting MS patients and 186 healthy controls using the TaqMan technique.

Results and Conclusions. It was found that, regardless of the presence of a specific allele, the gender of MS patients affects age at the time of the clinical onset of the disease: in rs1801133 for the C allele and T, the average age was 35 years for women and 29 for men ($p = 0.0004$; $p = 0.034$ respectively). Similarly for the second polymorphism rs1801131 for the A allele and C, the average age was 35 years for women and 29 for men ($p = 0.001$; $p = 0.01$ respectively). No significant allelic / genotypic frequency differences have been observed between the studied groups (c.677C > T, CT/TT $p = 0.719$, $p = 0.262$; c.1298A > C, AC/CC of $p = 0.686$; $p = 0.66$). We found no association between polymorphisms of a folate-homocysteine-methionine-SAM metabolising gene enzyme and multiple sclerosis in a Polish population.

Key words: multiple sclerosis, polymorphism, MTHFR gene, folate
(*Neurol Neurochir Pol 2019; 53 (3): 194–198*)

Introduction

Multiple sclerosis (MS) is a chronic inflammatory, autoimmune disease with a still unknown aetiology. The main initial mechanism of demyelination and injury to the central nervous system (CNS) appears to be inflammation [1]. The neurotoxicity induced by homocysteine (Hcy) action is considered to be one of the factors that triggers this process. Several studies have shown an increase in Hcy levels in patients with MS [2, 3], which leads to reactive oxygen species generation as a result of sulfhydryl group oxidation. The effect of this process is excessive N-methyl-D-aspartate receptor stimulation leading to neuronal damage through the exaggerated calcium ion influx [4, 5]. An important factor necessary for CNS myelination is

Address for correspondence: Monika Chorąży, Department of Neurology, Medical University in Bialystok, Bialystok, Poland, e-mail: chorazym@op.pl, tel.: +48 85 746 83 26

an appropriate level of S-Adenosylmethionine (SAM). 5,10 – methylenetetrahydrofolate reductase (*MTHFR*) is an essential enzyme in Hcy metabolism that leads to its remethylation to methionine, which is a precursor of SAM. *MTHFR* is coded by a gene localised in one chromosome (gene ID 4524, 1p36.22) and is a key folate – homocysteine – methionine – SAM metabolising enzyme [1]. Two common polymorphic variants influence *MTHFR* activity, which can lead to hyperhomocysteinemia. This metabolic effect is considered to be a possible mechanism predisposing for myelin pathology in MS. The C677T and A1289C of *MTHFR* gene polymorphisms are a missense mutation leading to aminoacid change and subsequent reduction in enzyme activity. This has been reported as a genetic susceptibility factor in a few population studies of relapsing – remitting MS patients [6–8]. The relationship between *MTHFR* polymorphisms and multiple sclerosis has not been investigated in a Polish population thus far. In the present study, we investigated a possible association between two variants of the *MTHFR* gene in a Polish multiple sclerosis population and a control group.

Materials and Methods

Study population

The study population consisted of 174 unrelated patients (124 women and 50 men) with clinically defined relapsing – remitting MS according to McDonald's criteria [9]. All patients were recruited from the Department of Neurology, Medical University of Bialystok. The average age of the patients at the time of diagnosis was 40 years (41.14 ± 0.79), and the mean disease duration was 8 years (8.12 ± 0.42). MS patients were treated with interferon β (a/b), glatiramer acetate, natalizumab, or fingolimod. Physical disability was assessed using the Expanded Disability Status Scale (EDSS) score. The control group included 186 healthy volunteers (mean age 38.7 + 1.23; 75 women and 111 men) with no family history of any autoimmune disease. The study was approved by the local Bioethics Committee (Medical University of Bialystok) and written informed consent was obtained from all the participants.

MTHFR Genotyping

DNA was extracted from peripheral whole blood leukocytes. Genotyping through a single nucleotide polymorphism (SNP) was performed using the 7900HT Fast Real-Time PCR System (Applied Biosystems, USA). All SNPs in the *MTHFR* gene (rs1801133 – C677T, rs1801131 – A1298C) were genotyped by TaqMan assay, SNP technology, from a ready-to-use human probes library (Applied Biosystems, Foster City, CA, USA) with the TaqMan Genotyping Master Mix (Applied Biosystems, Foster City, CA, USA) in a 20μl reaction volume. The final concentration of genomic DNA for all samples in the experiment sample was 10ng/μl. The reactions were carried out under the following conditions: 10 min at 95°C for starting Hot-Start Taq polymerase activity, 40 cycles of 92°C for 15 s and 60°C for 1 min.

Statistical analysis

Descriptive statistics including mean, standard error of the mean and the median were calculated for selected clinical measurements, henceforth called features. To determine whether the features' distributions statistically significantly differed between the defined groups, either the parametric [10] or the non-parametric [11] approach was used. The choice of appropriate method was made based upon the fulfillment of normality and homogeneity of variance assumptions, and the non-parametric approach was chosen in the case of violation of at least one of the conditions. The normality of the features' distributions was checked using the Shapiro-Wilk test [12] and the homogeneity of variances using Levene's test [13]. To address the problem of multiple testing appearing in post-hoc analyses, the false discovery rate (FDR) p-value adjustment method [14] was applied. Median unbiased estimator (mid-p) of the odds ratio, the exact confidence interval and the associated p-value, both obtained using the mid-p method [15], were used to assess the strength of a relationship between genotype or allele occurrence and the patient's status. Significance level was set at 0.05 for all calculations. The R software environment [16] was exploited for all calculations.

Results

The distribution of alleles and genotypes in the two analysed groups, MS patients and healthy controls, is shown in Table 1. There were no significant differences between the presence of the polymorphic variants, allele T and genotypes

Table 1. Distributions of genotypes and alleles in *MTHFR* gene polymorphisms rs1801133 and rs1801131 in multiple sclerosis and healthy groups

SNP	MS group N = 174	Control group N = 186	P (95% CI)
rs 1801133			
CC	94 (54%)	99 (53.2%)	NS
CT	67 (38.5%)	80 (43%)	NS
TT	13 (7.5%)	7 (3.8%)	NS
C	255 (73.3%)	278 (74.7%)	NS
T	93 (26.7%)	94 (25.3%)	NS
rs 1801131			
AA	77 (44.2%)	83 (44.6%)	NS
AC	73 (41.9%)	83 (44.6%)	NS
CC	24 (13.8%)	20 (10.8%)	NS
A	227 (69.6%)	249 (67%)	NS
C	121 (30.4%)	123 (33%)	NS

Table 2. Distributions of genotypes and alleles in *MTHFR* gene polymorphisms rs1801133 and rs1801131 in multiple sclerosis and healthy groups with sex stratification

SNP	MS group		Control group		P (95% CI)
	Female N = 124	Male N = 50	Female N = 75	Male N = 111	
rs 1801133					
CC	69 (55.6%)	24 (48%)	41 (54.6%)	58 (52.3%)	NS
CT	43 (34.7%)	22 (44%)	34 (45.4%)	46 (41.4%)	NS
TT	9 (7.3%)	4 (8%)	-	7 (6.3%)	NS
C	181 (73%)	70 (70%)	116 (77.3%)	162 (73%)	NS
T	61 (27%)	30 (30%)	34 (22.7%)	60 (27%)	NS
rs 1801131					
AA	56 (45.2%)	23 (46%)	38 (50.6%)	45 (40.5%)	NS
AC	48 (38.7%)	23 (46%)	29 (38.7%)	54 (48.6%)	NS
CC	20 (16.1%)	4 (8%)	8 (10.7%)	12 (10.9%)	NS
A	154 (63.6%)	69 (69%)	105 (70%)	144 (65%)	NS
C	88 (36.4%)	31 (31%)	45 (30%)	78 (34%)	NS

CT/TT of rs1801133 (p = 0.719; p = 0.262), and allele C and genotypes AC/CC of rs1801131 (p = 0.686; p = 0.66) in the *MTHFR* gene in both studied groups. We observed a very similar count in the MS cases and the controls in allele distribution in both assessed polymorphisms (C - 73.2% *vs* 74.7%; T – 26.7% *vs* 25.3%; A – 65.2% *vs* 66.9%; C – 34.7% *vs* 33%). The MS patients and the control group did not significantly differ after stratification into sexes (Tab. 2). Nevertheless, sex stratification of patients with MS showed statistically significant differences in the age of disease onset. Regardless of the presence of a specific allele, the sex of patients with MS affected the age differences at the time of clinical onset of the disease: in rs1801133 polymorphism for the C allele, the average age was 35 for women and 29 for men (p = 0.0004); for the T allele, the average age was 35 for women and 29 for men (p = 0.034). In the rs1801131 polymorphism for the A allele, the average age was 35 for women and 29 for men (p = 0.001); for the C allele, the average age was 35 for women and 29 for men (p = 0.01) (Tab. 3).

There was no statistically significant association between *MTHFR* gene C677T and A1298C polymorphisms and any other clinical characteristic features of MS patients (except for duration of disease and EDSS scale score).

Table 3. Mean age in years at disease onset of MS and distributions of alleles in MTHFR gene polymorphisms rs1801133 and rs1801131 in female and male patients

SNP	Female MS	Male MS	P (95% CI)
rs1801133			
C	34.6 (± 0.80)	29.13 (± 0.94)	0.0004
T	34.57 (± 1.37)	29.3 (± 1.59)	0.034
rs1801131			
A	34.13 (± 0.86)	29.47 (± 0.99)	0.001
C	34.13 (± 1.15)	28.53 (± 1.41)	0.01

Discussion

The strong influences of environmental and genetic factors are considered in the pathogenesis of MS [17]. In many case-control studies in different populations, particular genes have been found to be possible genetic factors that can increase the risk of MS [18–21]. In our study, we investigated the possible link between two variants of the *MTHFR* gene in Polish patients with MS and a control group.

The reduction of the enzyme activity encoded by the *MTHFR* gene, 5.10 methylenetetrahydrofolate reductase, disturbs the folate acid metabolism cycle and nucleic acid synthesis, as a result of single nucleotide polymorphisms. *MTHFR* reduces 5.10 –methylenetetrahydrofolate to 5-methylenetetrahydrofolate which is a key factor of remethylation of neurotoxic homocysteine to methionine. The inhibition of this process leads to hyperhomocysteinemia and causes the formation of free radicals damaging the myelin. Methionine is a precursor of S-Adenosylmethionine, which is essential for CNS myelination [1, 5].

We assessed the two molecular variants of the *MTHFR* gene, c.677C > T and c.1298A > C, which lead to decreased product activity encoded by this gene. To the best of our knowledge, this is the first study based on a Polish population. In both analysed polymorphisms, regardless of the presence of the wild type or polymorphic allele, the average age at diagnosis with MS in women was higher than in men (35 years

vs 29 years). This means that sex is a modulating factor that can influence the age of multiple sclerosis onset. This result is consistent with data published by Confavreux and Vukusic from a French population [22]. However, there is some evidence that women have earlier onset of MS than men [23]. These differences may be related to the existence of various demographic, geographic, genetic, or environmental factors that affect the age of MS onset in both women and men.

The results of the presented study did not show an association between the studied polymorphisms and multiple sclerosis in our population. There were no significant differences between the distribution of missense variants in the *MTHFR* gene in both studied groups. We also analysed the association of SNPs between the chosen clinical features of patients with MS, but they did not bring the expected effect. Our results are comparable with some earlier published studies in other populations. Szvetko et al. did not find any link between the c.1298A > C variant of the *MTHFR* gene in an Australian multiple sclerosis population. The analysed group of patients had lower results than in our investigation [15]. In a Tunisian population, Mrissa et al. obtained similar results as in the present study in relation to variant C677T, but opposite results in terms of variant A1298C. They observed an association of the c.1298A > C missense variant with the studied MS population [7]. In another case-control study in Turkish MS patients, the authors demonstrated statistically significant differences between the analysed groups. These associations were observed when patients were compared with the controls according to CC genotype versus CT + TT genotypes [8]. Klotz et al. published very interesting data. They found the occurrence of the wild type of a homozygosity AA variant in a group of healthy controls with a higher frequency than in patients with MS. This may suggest that the presence of this genotype is a protective factor against MS development. In addition, the authors did not show a relationship of variant C677T with the MS group [6]. Among the studies described above, none of them revealed a relationship with the age of disease onset or sex stratification of the studied polymorphisms.

The discrepancies between the data of other studies and our results may be due to various reasons, with the most notable being inter-ethnic and geographical genetic differences. These discrepancies may also depend on allele frequency, genome location on chromosomes, various LD patterns (linkage disequilibrium) in the populations, different evolutionary histories of genes affecting complex diseases, and the effect of numerous environmental factors. Our results could also have been affected by the small study groups, which may explain the lack of statistical significance. Moreover, the overall statistical approach could be impacted by the research design and criteria for patient inclusion. Replication in a larger sample set, and other populations, is necessary to confirm these findings and to expand our knowledge in this area.

Clinical implications

The results of our research are contradictory to those of some reports, but they also confirm others. The recently published results of a meta-analysis clearly indicate a lack of a relationship between both polymorphic variants c.677C > T and c.1298A > C of *MTHFR* gene with MS. The analysed population consisted of approximately 2,500 patients with MS and almost 3,000 healthy individuals [25].

Our results encourage us to do further research. We found that, regardless of the presence of a specific allele, the sex of MS patients affects the age differences at the time of the clinical onset of the disease. We plan to expand the study group in the future and include patients with other types of MS (i.e. primary progressive and secondary progressive).

Acknowledgement *The authors would like to thank the physicians and patients who participated in this study.*
Conflicts of interest *The authors have no conflict of interest to declare.*
Funding *Prepared as part of the Medical University of Bialystok statutory work number N/ST/ZB/16/001/1144.*

References

1. Surtees R, Leonard J, Austin S. Association of demyelination with deficiency of cerebrospinal-fluid S-adenosylmethionine in inborn errors of methyl-transfer pathway. Lancet. 1991; 338(8782-8783): 1550–1554, indexed in Pubmed: 1683972.
2. Vrethem M, Mattsson E, Hebelka H, et al. Increased plasma homocysteine levels without signs of vitamin B12 deficiency in patients with multiple sclerosis assessed by blood and cerebrospinal fluid homocysteine and methylmalonic acid. Mult Scler. 2003; 9(3): 239–245, doi: 10.1191/1352458503ms918oa, indexed in Pubmed: 12814169.
3. Ramsaransing GSM, Fokkema MR, Teelken A, et al. Plasma homocysteine levels in multiple sclerosis. J Neurol Neurosurg Psychiatry. 2006; 77(2): 189–192, doi: 10.1136/jnnp.2005.072199, indexed in Pubmed: 16421120.
4. Kruman II, Culmsee C, Chan SL, et al. Homocysteine elicits a DNA damage response in neurons that promotes apoptosis and hypersensitivity to excitotoxicity. J Neurosci. 2000; 20(18): 6920–6926, indexed in Pubmed: 10995836.
5. Lipton SA, Kim WK, Choi YB, et al. Neurotoxicity associated with dual actions of homocysteine at the N-methyl-D-aspartate receptor. Proc Natl Acad Sci U S A. 1997; 94(11): 5923–5928, doi: 10.1073/pnas.94.11.5923, indexed in Pubmed: 9159176.
6. Klotz L, Farkas M, Bain N, et al. The variant methylenetetrahydrofolate reductase c.1298A>C (p.E429A) is associated with multiple sclerosis in a German case-control study. Neurosci Lett. 2010; 468(3): 183–185, doi: 10.1016/j.neulet.2009.10.057, indexed in Pubmed: 19854238.
7. Fekih Mrissa N, Mrad M, Klai S, et al. Association of methylenetetrahydrofolate reductase A1298C polymorphism but not of C677T with multiple sclerosis in Tunisian patients. Clin Neurol Neurosurg. 2013; 115(9): 1657–1660, doi: 10.1016/j.clineuro.2013.02.025, indexed in Pubmed: 23523621.

8. Cevik B, Yigit S, Karakus N, et al. Association of methylenetetrahydrofolate reductase gene C677T polymorphism with multiple sclerosis in Turkish patients. J Investig Med. 2014; 62(8): 980–984, doi: 10.1097/JIM.0000000000000107, indexed in Pubmed: 25203152.
9. Polman CH, Reingold SC, Banwell B, et al. Diagnostic criteria for multiple sclerosis: 2010 revisions to the McDonald criteria. Ann Neurol. 2011; 69(2): 292–302, doi: 10.1002/ana.22366, indexed in Pubmed: 21387374.
10. Chambers J, Freeny A, Heiberger R. Analysis of Variance; Designed Experiments. Statistical Models in S. 2017: 145–193, doi: 10.1201/9780203738535-5.
11. Wilcoxon F. Individual Comparisons by Ranking Methods. Biometrics Bulletin. 1945; 1(6): 80, doi: 10.2307/3001968.
12. SHAPIRO SS, WILK MB. An analysis of variance test for normality (complete samples). Biometrika. 1965; 52(3-4): 591–611, doi: 10.1093/biomet/52.3-4.591.
13. Levene H. Robust tests for equality of variances. Contributions to Probability and Statistics: Essays in Honor of Harold Hotelling. Stanford University Press. ; 1960: 278–292.
14. Benjamini Y, Hochberg Y. Controlling the False Discovery Rate: A Practical and Powerful Approach to Multiple Testing. Journal of the Royal Statistical Society: Series B (Methodological). 2018; 57(1): 289–300, doi: 10.1111/j.2517-6161.1995.tb02031.x.
15. Lydersen S, Fagerland MW, Laake P. Recommended tests for association in 2 x 2 tables. Stat Med. 2009; 28(7): 1159–1175, doi: 10.1002/sim.3531, indexed in Pubmed: 19170020.
16. R Co. R: A language and environment for statistical computing. R Foundation for Statistical Computing, Vienna, Austria. Foundation for Statistical Computing, Vienna, Austria. URL https://www R-project org. 2018.
17. Thompson A, Baranzini S, Geurts J, et al. Multiple sclerosis. The Lancet. 2018; 391(10130): 1622–1636, doi: 10.1016/s0140-6736(18)30481-1.
18. Hadjigeorgiou GM, Kountra PM, Koutsis G, et al. Replication study of GWAS risk loci in Greek multiple sclerosis patients. Neurol Sci. 2019; 40(2): 253–260, doi: 10.1007/s10072-018-3617-6, indexed in Pubmed: 30361804.
19. Gil-Varea E, Urcelay E, Vilariño-Güell C, et al. Exome sequencing study in patients with multiple sclerosis reveals variants associated with disease course. J Neuroinflammation. 2018; 15(1): 265, doi: 10.1186/s12974-018-1307-1, indexed in Pubmed: 30217166.
20. Simsek H, Geckin H, Sensoz NP, et al. Association Between IL7R Promoter Polymorphisms and Multiple Sclerosis in Turkish Population. J Mol Neurosci. 2019; 67(1): 38–47, doi: 10.1007/s12031-018-1205-0, indexed in Pubmed: 30443838.
21. Wawrusiewicz-Kurylonek N, Chorąży M, Posmyk R, et al. The FOXP3 rs3761547 Gene Polymorphism in Multiple Sclerosis as a Male-Specific Risk Factor. Neuromolecular Med. 2018; 20(4): 537–543, doi: 10.1007/s12017-018-8512-z, indexed in Pubmed: 30229436.
22. Confavreux C, Vukusic S. Age at disability milestones in multiple sclerosis. Brain. 2006; 129(Pt 3): 595–605, doi: 10.1093/brain/awh714, indexed in Pubmed: 16415309.
23. Harbo HF, Gold R, Tintoré M. Sex and gender issues in multiple sclerosis. Ther Adv Neurol Disord. 2013; 6(4): 237–248, doi: 10.1177/1756285613488434, indexed in Pubmed: 23858327.
24. Szvetko AL, Fowdar J, Nelson J, et al. No association between MTHFR A1298C and MTRR A66G polymorphisms, and MS in an Australian cohort. J Neurol Sci. 2007; 252(1): 49–52, doi: 10.1016/j.jns.2006.10.006, indexed in Pubmed: 17113603.
25. Lee YHo, Seo YHo, Kim JH, et al. Meta-analysis of associations between MTHFR and GST polymorphisms and susceptibility to multiple sclerosis. Neurol Sci. 2015; 36(11): 2089–2096, doi: 10.1007/s10072-015-2318-7, indexed in Pubmed: 26150166.

RESEARCH PAPERS

Neurologia i Neurochirurgia Polska
Polish Journal of Neurology and Neurosurgery
2019, Volume 53, no. 2, pages: 199–204
DOI: 10.5603/PJNNS.a2019.0009

ISSN 0028–3843

Quantitative volumetric analysis of primary glioblastoma multiforme on MRI and 11C-methionine PET: initial study on five patients

Jingwang Zhao[1], Zhijuan Chen[2], Li Cai, Shaoya Yin[3], Weidong Yang[1], Zengguang Wang[4]

[1] Department of Neurosurgery, Tianjin Huanhu Hospital, No. 6 Jizhao Road, Jinnan District, Tianjin, China
[2] Department of Neurosurgery, Tianjin Medical University General Hospital, Tianjin, China
[3] Department of PET-CT Diagnostic, Tianjin Medical University General Hospital, No. 154 Anshan Road, Heping District, Tianjin, China
[4] Tianjin Neurological Institute, No. 154 Anshan Road, Heping District, Tianjin, China

ABSTRACT

To investigate the discrepancy between 11C-methionine (MET) positron emission tomography (PET) and MRI results in primary glioblastoma multiforme (GBM) through three-dimensional (3D) volumetric analysis, we retrospectively analysed patients with primary GBM who underwent preoperative 3D MRI and MET PET and were operated between June 2016 and January 2017. Tumour delineation and volumetric analysis were conducted using MRIcron software. Tumour volumes defined by MRI (VMRI) were manually drawn slice by slice in axial and sagittal or coronal images of enhanced T1 sequence, while metabolic tumour volumes were automatically segmented in MET PET (VMET) based on three (frontal, occipital and temporal) 3D reference volumes of interest (VOI). Discrepancies were evaluated in terms of both absolute volume and percentage on the combined images. MET PET contours contained and extended beyond MRI contours in all five patients; in a subset of cases, MET PET contours extended to the contralateral hemisphere. The discrepancy between MET uptake and MRI results was 27.67 cm^3 (4.20–51.20 cm^3), i.e. approximately 39.0% (17.4–64.3%) of the metabolic tumour volume was located outside the volumes of the Gd-enhanced area. Metabolic tumour volume is substantially underestimated by Gd-enhanced area in patients with primary GBM. Quantitative volumetric information derived from MET uptake is useful in defining tumour targets and designing individualised therapy strategies in primary GBM.

Key words: Volumetric analysis, glioblastoma multiforme, MRI, 11C-methionine
(*Neurol Neurochir Pol 2019; 53 (3): 199–204*)

Introduction

Glioma is the most common primary brain tumour of the central nervous system in adults (38%). The World Health Organisation (WHO) has established criteria for classifying glioma into four histological grades according to the tumour's pathological morphology [1]. Glioblastoma multiforme (GBM), the highest grade glioma, is intensively infiltrative and has a diffuse border with the brain parenchyma. As a consequence, defining tumour boundaries for treatment is challenging. Magnetic resonance imaging (MRI) is the most widely used imaging modality and the standard reference for diagnosis, therapy planning and follow-up of GBM tumours. Inhomogeneous enhancement and necrosis characterise the majority of GBM lesions [2]. The standard MRI sequence for calculating tumour volume and planning the extent of surgery for high-grade gliomas is gadolinium (Gd) enhanced T1-weighted imaging [3]. However, MRI cannot precisely delineate tumour volume and is insufficient in helping to achieve total resection of glioblastoma, because T2-weighted imaging can incorporate both tumour tissue and perifocal oedema [4], and high-grade glioma cells are not limited to the Gd-enhanced volume in MRI T1 images [5, 6] and in fact can be located up to 30 mm beyond the Gd-enhanced area [7].

Address for correspondence: Weidong Yang, Department of Neurosurgery, Tianjin Huanhu Hospital, No. 6 Jizhao Road, Jinnan District, Tianjin, China, e-mail: yangweidongshine@yahoo.cn

Positron emission tomography (PET) with metabolic tracers has played an important role in neurooncology [8, 9]. Radiolabelled amino acids, such as ^{11}C-methionine (MET) PET, reflect the extent of tumour boundaries in GBM more reliably than CT or MRI, because Gd-enhanced areas in MRI represent disruptions of the brain-blood barrier, while MET uptake correlates with tumour cell density or proliferative capability, thus more closely reflecting the properties of glioblastoma multiforme [10-13]. Complete resection of MET uptake areas has been shown to increase survival of high-grade glioma patients in previous studies [14, 15]. Both qualitative and semiquantitative analysis of Gd-enhanced T1 and MET PET in GBM have revealed discrepancies between the two modalities [7, 16, 17], but these studies reported neither volumetric analysis of entire tumours nor volume information of any sort. To date, only a few studies have conducted volumetric calculation [18, 19], and no 3D volumetric analysis of discrepancies between MRI and MET PET has been performed focusing on primary GBM.

The current study therefore aimed to investigate differences in estimates of primary GBM tumour volume based on 3D MRI and MET PET.

Materials and methods

Patients

Firstly, we retrospectively reviewed the neurosurgery database and found a total of 461 brain tumour operations performed between June 2016 and January 2017. Secondly, patients were screened for pathological confirmation of GBM, with 31 patients thereby selected. Finally, patients were required to meet all of the following inclusion criteria: (1) they had no prior biopsy or treatment; (2) they had available data from preoperative 3D whole brain contrast-enhanced MRI and MET PET; and (3) the interval between these two examinations was less than seven days. The final study population consisted of five patients, whose clinical data is set out in Table 1. The protocol of this study was approved by the Research Ethics Committee of the Hospital.

Image acquisition

MR images were obtained using a 3.0-Tesla MR scanner (Discovery MR750, General Electric, Milwaukee, WI, USA). Sagittal 3D T1-weighted images were acquired using a whole brain sequence with the following parameters: repetition time (TR) = 8.2 ms; echo time (TE) = 3.2 ms; inversion time (TI) = 450 ms; flip angle (FA) = 12°; field of view (FOV) = 256 mm × 256 mm; and matrix = 256 × 256; slice thickness = 1 mm, no gap.

PET images were acquired with a dedicated PET/CT scanner (Discovery LS, GE Medical Systems, Milwaukee, WI, USA). Patients fasted for at least six hours before examination; a dose of 555–740 MBq (15–20 mCi) MET was injected intravenously within one minute. Static emission scanning was performed for a minimum of 20 minutes after MET injection in 3D mode (FOV = 150 mm×150 mm, slice thickness = 5.0 mm, slice gap 4.5 mm, matrix = 128 × 128). For attenuation correction, we acquired a non-contrast-enhanced, low-dose CT scan (slice thickness = 2.5 mm, slice gap = 0, matrix = 512 × 512). MET uptake in the tumour and in normal cortex was expressed as standard uptake value (SUV). The ratio of tumour SUV to normal SUV in contralateral gray matter (TNR) was calculated for each tumour by a nuclear medicine physician trained in brain PET. For surgical planning, the TNR was adjusted to 1.3 to define the tumour target.

Image processing and volumetric analysis

The MET PET and MRI images were first transferred from DICOM to NIfTI format for viewing and processing using MRIcron software (http://www.mricro.com; University of South Carolina, Columbia, SC, USA). Images were then coregistered using Statistical Parametric Mapping 12 software (http://www.fil.ion.ucl.ac.uk/spm/; Wellcome Department of Cognitive Neurology, London, UK).

Tumour delineation and volumetric analysis of MRI and MET PET images were performed in MRIcron. The tumour was defined as previously described [18, 20]. Tumour volumes defined by MRI (VMRI) were manually drawn slice by slice in axial and sagittal or coronal images of the enhanced T1 sequence by two skilled radiologists. The metabolic tumour volume defined by MET uptake (VMET) was automatically segmented based on image thresholding. Firstly, three spherical regions of 10-mm radius were drawn in the unaffected contralateral frontal, occipital and temporal parenchyma as reference VOI in order to calculate normal SUV. Secondly, VMET was automatically segmented by image thresholding (TNR = 1.3) as defined above. For tumour volume comparisons between MET PET and the corresponding MRI, contours were extended to central areas without MET uptake related to necrosis. High uptake areas beyond the tumour were manually excluded in order to avoid inclusion of physiological MET uptake in normal tissues. Thirdly, in order to express tumour volume differences between the two modalities, volume of discrepancy-MET (dis-MET: VMET not included in VMRI) was evaluated (both in terms of absolute volume and percentage) using the 'Overlay Comparisons' and 'Descriptive' functions included in MRIcron.

Statistical analysis

Statistical analyses were performed using SPSS 19.0 software (SPSS Inc., Chicago, IL, USA). Descriptive statistics were expressed as median and range [median (range)]. Values of $p < 0.05$ (two-tailed) were considered statistically significant.

Results

Patient characteristics and volumetric data for the whole group are summarised in Table 1.

Table 1. Patient characteristics and volumetric analysis of MRI and MET PET

No.	Sex	Age	Location (side)	VMRI (cm^3)	VMET (cm^3)	dis-MET (cm^3)	dis-MET (%)
1	F	63	Frontal(R)	53.81	93.31	45.15	48.4
2	M	66	Temporal(L)	43.86	59.20	16.80	28.4
3	M	71	Occipital(L)	38.48	57.43	20.98	36.5
4	F	66	Frontal(R)	22.24	24.12	4.20	17.4
5	F	65	Frontal(L)	28.92	79.63	51.20	64.3

F femal, GBM glioblastoma multiforme, L left, M male, No. patient number, R right

On MET PET, uptake in the metabolically active tumour was clearly differentiated from that of normal brain tissue for all five patients. Visual analysis of coincidence and discrepancy between MET high uptake volumes and Gd-enhanced MRI demonstrated that MET PET contours contained and extended beyond most MRI contours. Furthermore, MET PET volumes even extended along commissural fibres to the contralateral cerebral hemisphere (Figure 1). Moreover, the overall shape of MET high uptake volumes was asymmetrical and irregular.

In volumetric analysis, the discrepancy of MET uptake was 27.67 cm^3 (4.20–51.20 cm^3), i.e. about 39.0% (17.4–64.3%) of metabolically defined tumour volumes were located beyond the Gd-enhanced regions (Figure 2).

Discussion

Glioblastoma multiforme is known for its invasive and aggressive behaviour, and there is no distinct margin with the brain parenchyma [1]. Gd-enhanced T1-weighted MRI is the standard MRI sequence for tumour delineation and defining resection targets for high-grade gliomas [3]. Timothy et al. conducted the largest systematic review and the only quantitative meta-analysis to investigate associations between the extent of resection and overall progression-free survival in GBM. They concluded that compared to subtotal resection, gross total resection substantially improved overall and progression-free survival [21]. Although cytoreductive surgery is the cornerstone of therapy in GBM, no consensus exists regarding the optimal extent of tumour resection necessary to improve survival [11]. Most GBM still recurs even after removal of all contrast-enhanced volumes on T1-weighted MRI. Therefore techniques such as metabolic imaging are needed to improve resection rates and the safety of surgery.

A subset of studies has reported that MET uptake reflects proliferation potential and angiogenic capability in gliomas [22, 23]. In these studies, MET uptake was compared to the Ki-67 labelling index and microvessel density non-stereotactically. To overcome this problem, Yoshiko et al. conducted a stereotactic comparison of MET PET images and the resulting histology; they confirmed that MET uptake correlates with tumour cell density rather than with microvessel density in glioma [10]. They concluded that MET uptake correlates with tumour cell density (proliferative capability). Moreover, Yoo et al. [15] reported that metabolic tumour volume on MET PET is a significant and independent prognostic factor for progression-free survival in high-grade glioma; they recommended volumetric analysis of MET for better prognostication. Singhal et al. [24] compared MET to ^{18}F-fluorodeoxyglucose (FDG) and contrast enhancement on MRI, suggesting that MET PET can predict prognosis in gliomas more accurately than FDG PET and MRI. In summary, MET is more accurate in delineating the tumour and defining the extent of resection targets.

Given the different physiological bases of Gd-enhanced MRI and MET uptake, discrepancies between MRI and

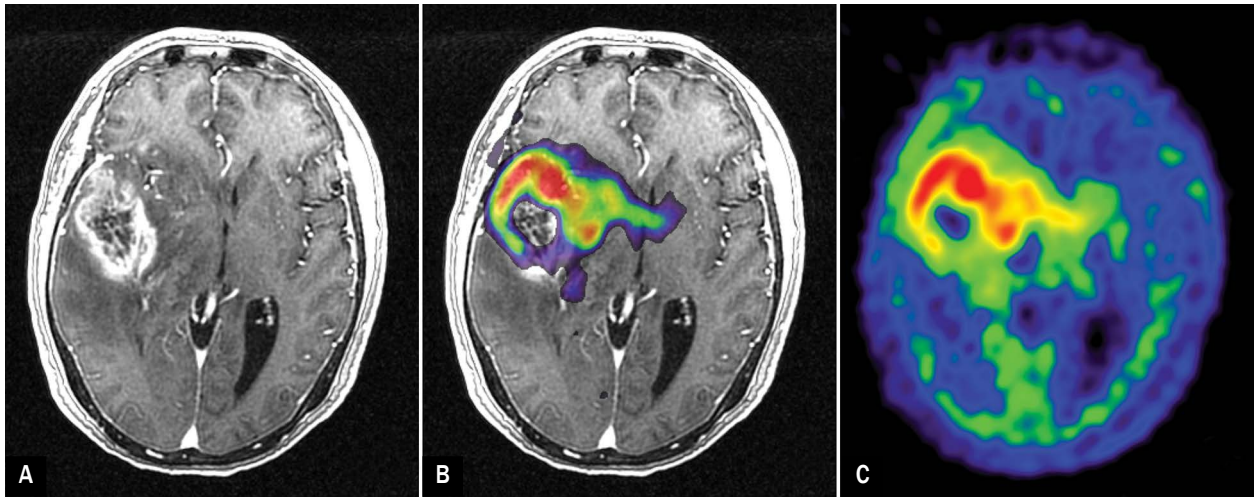

Figure 1. Visual comparison of enhanced MRI with MET PET of primary GBM. **A**: Tumour contours (green line) in Gd-enhanced T1 MRI. **B**: Tumour contours comparison in the overlap of MET (TNR = 1.3) and corresponding MRI demonstrated that MET-defined tumour volume extended along commissural fibres of fornix to the contralateral hemisphere. **C**: General MET PET image of GBM

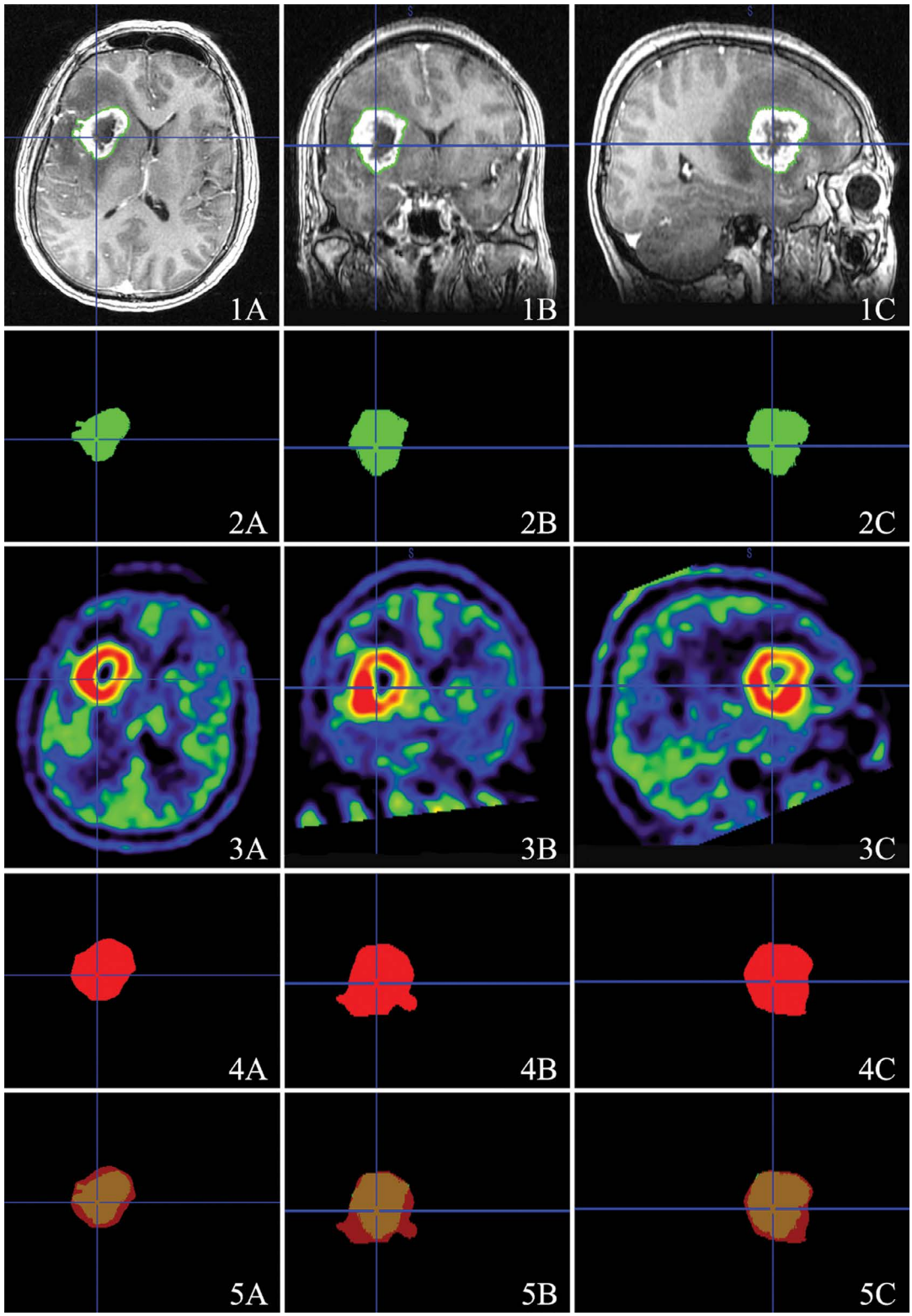

Figure 2. Volumetric analysis of enhanced MRI and MET PET in primary GBM (case 1). Letters A, B and C represent axial, coronal and sagittal views of the same origin, respectively. **Row 1**: tumour contour (green line) delineated manually in each slice of Gd-enhanced T1 MRI images. **Row 2**: tumour volume calculated by MRIcron (VMRI is 53.81 cm^3). **Row 3**: MET PET images minimally processed to show MET high uptake of GBM. **Row 4**: Automatically defined metabolic tumour volume (VMET) calculated as 93.31 cm^3 (setting threshold: TNR = 1.3). **Row 5**: tumour volume comparisons between MET PET and the corresponding MRI, dis-MET (volumes contained in MET but not in MRI) is 48.4%

corresponding MET PET images are to be expected. PET metabolic imaging using radiolabelled amino acids, such as MET, has been successfully combined with MRI to produce a powerful and reliable technique for defining GBM target volumes in neuronavigation surgery and radiotherapy [17].

To examine the distribution of metabolic abnormalities associated with glioblastoma multiforme relative to MRI, Miwa et al. superimposed contemporaneous MRI on corresponding MET-PET images in 10 patients with newly diagnosed GBM prior to treatment. They found that the MET volume included and exceeded the entire Gd-enhanced volume and that 99.8% of the MET-enhanced area was located within 30 mm surrounding of the Gd-enhanced area [7], although the MET volume was assessed by qualitative visual analysis. Galldiks et al. investigated the relationship between MET and Gd-enhanced MRI through volumetric calculation. They reported that the metabolically active tumour volume may be substantially underestimated by Gd-enhanced volume, and they also showed a positive correlation between MET uptake and the volumes of Gd-enhanced area [19]. However, the reference ROI in that study was a two-dimensional circular area that contained limited volumetric information. Moreover, all 12 patients were recurrent GBM. Qualitative, semiquantitative and quantitative methods have all been applied to analyse discrepancies and coincidences between MET PET and MRI; these methods have illustrated the importance of including those areas in the treatment plan [7, 19]. To date, there has been no precise 3D volumetric study focused on primary GBM.

The aim of the present study was to investigate discrepancies of tumour volumes in primary GBM based on precise volumetric analysis of two imaging modalities. In particular, we investigated tumour volumes metabolically estimated using MET PET that extended regions of Gd-enhanced area. To improve precision and recall, we set strict inclusion criteria. Due to the high proliferation rate of tumour cells, we limited the interval between the MRI and the PET examinations to seven days; this minimised discrepancies between the two image modalities due to tumour growth. This interval was significantly shorter than those used in previous studies [18, 19]. Furthermore, to obtain representative reference VOI and to segment V_{MET}, we selected three spherical regions with a 10 mm radius in the unaffected contralateral frontal, occipital and temporal parenchyma. Compared to image processing software in previous studies [19], MRIcron is convenient to acquire and simple to operate. These properties make it suitable and popular for practical clinical use.

As described above, we found that MET PET contours contained and extended beyond most MRI contours in all five patients; this finding was in accordance with the study of Miwa et al. [7]. However, in our study, volumes of high MET uptake were not limited to within 30 mm of the Gd-enhanced area. Rather, they extended along commissural fibres to the contralateral cerebral hemisphere. This also explains why GBM may exhibit higher proliferation rates in some regions, resulting in asymmetrical and irregular MET PET images.

In volumetric analyses, approximately 39.0% (17.4–64.3%) of metabolic tumour volume was located beyond the Gd-enhanced area. Javier et al. previously performed volumetric research to analyse the contributions of MRI and MET PET to tumour target volume estimates in both high- and low-grade glioma. According to this study, approximately 30.22% (17.4–64.3%) of MET-defined tumour volume did not overlap with MRI-defined volumes in GBM [18]. However, it must be noted that seven out of ten (70%) patients were recurrent GBM. This clinical profile significantly affected the analysis, as the authors included the resection cavity when defining tumour volume. These MET-specific volumes are especially important. Recently, John et al. reported findings that support the interpretation that MET delineates non-contrast enhancing tumour regions at high risk for recurrence [12]. Although we performed no statistical estimation, due to our limited sample size, our results nevertheless indicated larger V_{MET} estimates associated with VMRI, in line with a previous study [19].

Concerning the specific results in the volumetric analysis observed in our group, it is relevant to discuss the inclusion of volumes with a lack of MET uptake related to central necrosis in the final volume of MET PET. These areas were included in order to facilitate comparison with MRI, which typically includes these areas defining the final surgical target volume.

Limitations

Our study was performed in a clinical setting, and therefore may reflect a natural bias. Additionally, exact volumetric calculation and comparison could only be performed on patients with presurgical 3D acquisition of both Gd-enhanced MRI and MET PET. As a consequence, the number of patients limits further statistical calculation, and may constrain our conclusions. Although we selected skilled radiologists to delineate MRI volume, there will have been subjective error due to the manually drawn contours.

Conclusion

GBM is a diffusely infiltrating and widespread malignant neoplasm that, even at the time of diagnosis, typically invades multiple lobes and both hemispheres of the brain. Metabolic tumour volume is substantially underestimated by Gd-enhanced area in primary GBM. MET PET contours contain and extend beyond most MRI contours. In our experience, approximately 40% of MET high uptake volumes are not included in MRI tumour volumes. Quantitative volumetric information derived from MET uptake is helpful in defining tumour targets and designing individualised therapy strategies for primary GBM.

References

1. Komori T, Sasaki H, Yoshida K. [Revised WHO Classification of Tumours of the Central Nervous System:Summary of the Revision and Perspective]. No Shinkei Geka. 2016; 44(8): 625–635, doi: 10.11477/mf.1436203347, indexed in Pubmed: 27506840.
2. Faguer R, Tanguy JY, Rousseau A, et al. Early presentation of primary glioblastoma. Neurochirurgie. 2014; 60(4): 188–193, doi: 10.1016/j.neuchi.2014.02.008.
3. Stupp R, Tonn JC, Brada M, et al. High-grade malignant glioma: ESMO Clinical Practice Guidelines for diagnosis, treatment and follow-up. Annals of Oncology. 2010; 21(Supplement 5): v190–v193, doi: 10.1093/annonc/mdq187.
4. Grosu AL, Weber WA, Riedel E, et al. L-(methyl-11C) methionine positron emission tomography for target delineation in resected high-grade gliomas before radiotherapy. Int J Radiat Oncol Biol Phys. 2005; 63(1): 64–74, doi: 10.1016/j.ijrobp.2005.01.045, indexed in Pubmed: 16111573.
5. Kelly P, Daumas-Duport C, Kispert D, et al. Imaging-based stereotaxic serial biopsies in untreated intracranial glial neoplasms. Journal of Neurosurgery. 1987; 66(6): 865–874, doi: 10.3171/jns.1987.66.6.0865.
6. Watanabe M, Tanaka R, Takeda N. Magnetic resonance imaging and histopathology of cerebral gliomas. Neuroradiology. 1992; 34(6): 463–469, doi: 10.1007/bf00598951.
7. Miwa K, Shinoda J, Yano H, et al. Discrepancy between lesion distributions on methionine PET and MR images in patients with glioblastoma multiforme: insight from a PET and MR fusion image study. J Neurol Neurosurg Psychiatry. 2004; 75(10): 1457–1462, doi: 10.1136/jnnp.2003.028480, indexed in Pubmed: 15377696.
8. Jacobs AH, Li H, Winkeler A, et al. PET-based molecular imaging in neuroscience. European Journal of Nuclear Medicine and Molecular Imaging. 2003; 30(7): 1051–1065, doi: 10.1007/s00259-003-1202-5.
9. Ogawa T, Shishido F, Kanno I, et al. Cerebral glioma: evaluation with methionine PET. Radiology. 1993; 186(1): 45–53, doi: 10.1148/radiology.186.1.8380108, indexed in Pubmed: 8380108.
10. Okita Y, Kinoshita M, Goto T, et al. 11C-methionine uptake correlates with tumor cell density rather than with microvessel density in glioma: A stereotactic image-histology comparison. NeuroImage. 2010; 49(4): 2977–2982, doi: 10.1016/j.neuroimage.2009.11.024.
11. Jiang H, Cui Y, Liu X, et al. Patient-Specific Resection Strategy of Glioblastoma Multiforme: Choice Based on a Preoperative Scoring Scale. Annals of Surgical Oncology. 2017; 24(7): 2006–2014, doi: 10.1245/s10434-017-5843-1.
12. Lucas J, Serrano N, Kim H, et al. 11C-Methionine positron emission tomography delineates non-contrast enhancing tumor regions at high risk for recurrence in pediatric high-grade glioma. Journal of Neuro-Oncology. 2017; 132(1): 163–170, doi: 10.1007/s11060-016-2354-z.
13. Susheela SP, Revannasiddaiah S, Madhusudhan N, et al. The demonstration of extension of high-grade glioma beyond magnetic resonance imaging defined edema by the use of (11) C-methionine positron emission tomography. J Cancer Res Ther. 2013; 9(4): 715–717, doi: 10.4103/0973-1482.126464, indexed in Pubmed: 24518724.
14. Pirotte B, Levivier M, Goldman S, et al. POSITRON EMISSION TOMOGRAPHY-GUIDED VOLUMETRIC RESECTION OF SUPRATENTORIAL HIGH-GRADE GLIOMAS. Neurosurgery. 2009; 64(3): 471–481, doi: 10.1227/01.neu.0000338949.94496.85.
15. Yoo M, Paeng J, Cheon G, et al. Prognostic Value of Metabolic Tumor Volume on 11C-Methionine PET in Predicting Progression-Free Survival in High-Grade Glioma. Nuclear Medicine and Molecular Imaging. 2015; 49(4): 291–297, doi: 10.1007/s13139-015-0362-0.
16. Tanaka Y, Nariai T, Momose T, et al. Glioma surgery using a multimodal navigation system with integrated metabolic images. Journal of Neurosurgery. 2009; 110(1): 163–172, doi: 10.3171/2008.4.17569.
17. Pirotte B, Goldman S, Dewitte O, et al. Integrated positron emission tomography and magnetic resonance imaging–guided resection of brain tumors: a report of 103 consecutive procedures. Journal of Neurosurgery. 2006; 104(2): 238–253, doi: 10.3171/jns.2006.104.2.238.
18. Arbizu J, Tejada S, Marti-Climent JM, et al. Quantitative volumetric analysis of gliomas with sequential MRI and 11C-methionine PET assessment: patterns of integration in therapy planning. European Journal of Nuclear Medicine and Molecular Imaging. 2012; 39(5): 771–781, doi: 10.1007/s00259-011-2049-9.
19. Galldiks N, Ullrich R, Schroeter M, et al. Volumetry of [(11)C]-methionine PET uptake and MRI contrast enhancement in patients with recurrent glioblastoma multiforme. Eur J Nucl Med Mol Imaging. 2010; 37(1): 84–92, doi: 10.1007/s00259-009-1219-5, indexed in Pubmed: 19662410.
20. Kracht LW, Miletic H, Busch S, et al. Delineation of brain tumor extent with [11C]L-methionine positron emission tomography: local comparison with stereotactic histopathology. Clin Cancer Res. 2004; 10(21): 7163–7170, doi: 10.1158/1078-0432.CCR-04-0262, indexed in Pubmed: 15534088.
21. Brown T, Brennan M, Li M, et al. Association of the Extent of Resection With Survival in Glioblastoma. JAMA Oncology. 2016; 2(11): 1460, doi: 10.1001/jamaoncol.2016.1373.
22. Kracht L, Friese M, Herholz K, et al. Methyl-[11C]-l-methionine uptake as measured by positron emission tomography correlates to microvessel density in patients with glioma. European Journal of Nuclear Medicine and Molecular Imaging. 2003; 30(6): 868–873, doi: 10.1007/s00259-003-1148-7.
23. Kato T, Shinoda J, Nakayama N, et al. Metabolic Assessment of Gliomas Using11C-Methionine, [18F] Fluorodeoxyglucose, and11C-Choline Positron-Emission Tomography. American Journal of Neuroradiology. 2008; 29(6): 1176–1182, doi: 10.3174/ajnr.a1008.
24. Singhal T, Narayanan TK, Jacobs MP, et al. 11C-Methionine PET for Grading and Prognostication in Gliomas: A Comparison Study with 18F-FDG PET and Contrast Enhancement on MRI. Journal of Nuclear Medicine. 2012; 53(11): 1709–1715, doi: 10.2967/jnumed.111.102533.

RESEARCH PAPER

Neurologia i Neurochirurgia Polska
Polish Journal of Neurology and Neurosurgery
2019, Volume 53, no. 3, pages: 205–211
DOI: 10.5603/PJNNS.a2019.0020

ISSN 0028–3843

Assessment of relationship between C-reactive protein to albumin ratio and 90-day mortality in patients with acute ischaemic stroke

Mehtap Kocatürk[1], Özcan Kocatürk[1]

[1]Department of Neurology, Harran University, Şanlıurfa, TURKEY

Abstract

Aim and clinical rationale for the study. It is now known that inflammation is involved in the pathophysiology of acute ischaemic stroke (AIS). It has been proven that CRP and albumin alone are useful in predicting a prognosis for stroke patients. A combination of these two parameters, namely the ratio of CRP to albumin (CAR), is believed to be a more accurate indicator of inflammatory status than CRP or albumin alone, and may be more valuable than either of them separately in predicting the prognosis of ıschaemic stroke patients. However, the role of CAR as a predictor of mortality in patients with AIS remains unclear.

Materials and methods. We retrospectively enrolled 260 patients who were referred to our clinic within the first 24 hours of symptom presentation and who were diagnosed with AIS between January 2015 and December 2018. The patient group was classified into two groups according to 90-day mortality. These groups were compared in terms of C-reactive protein, albumin, and CAR.

Results. The C-reactive protein and CAR values were higher, and the albumin level was lower, in non-surviving patients. The CAR value was also found to be a significant independent variable of 90-day mortality in patients with AIS ($p < 0.001$). The optimum cut-off value of CAR in predicting the 90-day mortality for patients with AIS was 0.50, with 64.1% sensitivity and 56.2% specificity.

Conclusions and clinical implications. Our study demonstrated that a high CAR value is an independent predictor of 90-day mortality in patients with AIS

Key words: stroke, C-reactive protein to albumin ratio, mortality
(*Neurol Neurochir Pol 2019; 53 (3): 205–211*)

Introduction

Acute Ischaemic Stroke (AIS) has a high rate of worldwide mortality and disability. Intravenous rtPA and endovascular therapy, which are effective treatments for ischaemic stroke, have narrow therapeutic windows and therefore patient selection criteria are important for these treatments. Also, there is as yet no treatment known to have neuroprotective properties. This situation prompted us to search for a biomarker to accelerate the diagnosis, predict the prognosis for patient selection, better understand the pathophysiology, and offer new treatment options.

Inflammation is known to occur in the pathophysiology of ischaemic stroke [1, 2]. Necrotic cells, which are formed in the brain due to vascular occlusion, trigger inflammation. CRP and albumin is an acute phase protein. CRP is increased in inflammation, while albumin is decreased in inflammation as a negative phase reactant.

Many studies have investigated the relationship between CRP and disease severity, functional outcome, in-hospital mortality, long-term mortality, and infarct volume in patients with ischaemic stroke [3–6]. Increased plasma levels of CRP may affect coagulation by inducing tissue factor expression

Address for correspondence: Özcan Kocatürk, Osman Bey Campus, Mardin Yolu, Şanlıurfa, TURKEY tel.: +905074191621 e-mail: ozcankocaturk@gmail.com

[7]. Activation of coagulation in patients with ischaemic stroke may increase mortality [8]. In addition to that, post-ischaemic inflammation increases neuronal injury [9], which may explain the poor outcome in patients with high CRP.

Albumin, which is synthesised from the liver, acts as a carrier of endogenous and exogenous substances in the blood. The neuroprotective properties of albumin have been shown in animal models of ischaemic stroke [10]. It has also been reported to be an important inhibitor of platelet aggregation, scavenging free oxygen radicals, and acting as an antioxidant [11]. Albumin, like CRP, has been shown to be an independent prognostic factor, and has been used to predict recurrence, prognosis and mortality in ischaemic stroke [10, 12, 13].

Clinical rationale for the study

Although it has been shown that CRP and albumin individually are useful in predicting prognosis [14, 15], the combination of these two parameters, namely the ratio of CRP to albumin (CAR), has not been studied in detail. CAR may be a more accurate indicator of inflammatory status than CRP or albumin alone, and it may be of greatervalue than either of them separately in predicting the prognosis of ıschaemic stroke patients. Although CRP and albumin have been separately demonstrated to be associated with increased poor prognostic events in patients with ischaemic stroke, no study to date has investigated the prognostic importance of the CRP to albumin ratio in patients with ischaemic stroke. In this study, we hypothesise that an elevated CAR increases the risk of mortality in patients with ischaemic stroke. We assessed the association between the CAR at admission and 90-day mortality in patients with ischaemic stroke.

Methods

Study design and data collectionThe files of patients who were admitted to the neurology clinic of Harran University Faculty of Medicine Training and Research Hospital, Sanlıurfa, Turkey between January 2015 and December 2018 with the diagnosis of acute ischaemic stroke (AIS) were retrospectively screened from electronic medical records. The diagnosis of AIS was based on the World Health Organisation definition [16]. Patients were aetiologically classified according to the Trial of Org 10,172 in Acute Stroke Treatment (TOAST) criteria: cardioembolic, atherosclerotic, small vessel/lacunar, and cryptogenic/others [17].

Exclusion criteria for the patients were the following: 1) those patients with trauma or a history of surgery within the previous 12 months; 2) those with an active infection before stroke onset or within 72 h after admission; 3) previously known haematological disorders (e.g. anaemia, bleeding disorder, leukaemia); 4) pre-existing kidney disease with serum creatinine > 1.5 mg/dL and pre-existing liver disease with abnormal liver function test; 5) intoxication; 6) patients with previous history of cerebrovascular diseases (ıschaemic and haemorrhagic); 7) a history of cancer at any time or the use of steroids or immunosuppressant agents within the previous 12 months; and 8) an absence of medical, demographic, clinical, laboratory, and/or radiological data. Our study was conducted in full accordance with the Declaration of Helsinki and was approved by the local ethics committee. Informed consent was not required due to its retrospective design.

Baseline clinical data including age, gender, and risk factors such as hypertension (HT), diabetes mellitus (DM), hyperlipidemia (HL), heart failure, and atrial fibrillation (AF) were recorded from patients' medical records for all patients. HT was defined as systolic blood pressure (BP) ≥ 140 mmHg, and/or diastolic BP ≥ 90 mmHg, taking anti-hypertensive medications, and/or previously diagnosed hypertension. DM was defined as fasting serum glucose of ≥ 126 mg/dL (7 mmol/L), non-fasting glucose of ≥ 200 mg/dL (11.1 mmol/L), use of anti-diabetic medications, or a previously established diagnosis. HL was diagnosed if low-density lipoproteins (LDL)-cholesterol level was ≥ 100 mg/dL or in cases of the use of lipid-lowering agents after being diagnosed with HL. Congestive heart failure was defined as left ventricular ejection fraction (LVEF) < 40% and typical symptoms e.g. breathlessness, ankle swelling, and fatigue [18]. Atrial fibrillation was defined as AF recorded at the time of the electrocardiography, or any previously known episode of AF.

Laboratory measurements

Venous blood samples for a complete blood count and serum chemistry, including serum albumin and CRP levels, were drawn when admitted to our hospital emergency service in all patients with a suspicion of acute ischaemic stroke. CAR was calculated by dividing the serum CRP level by the serum albumin level, while the neutrophil to lymphocyte ratio (NLR) was calculated by dividing the neutrophil count by the lymphocyte count. CAR, NLR, CRP, albumin, neutrophil, lymphocyte, and thrombocyte levels were recorded.

Statistical analysis

Data was expressed as the median for continuous variables and percentages for categorical variables. Mann-Whitney U test for continuous variables and x2 test for categorical variables were performed. To determine the factors associated with 90-day mortality, univariate analyses were performed firstly, followed by multivariate logistic regression analysis. Variables with P-values < 0.05 were put into the multivariate logistic regression model. To assess the association of the CRP/albumin ratio with mortality outcome, the CRP/albumin ratio was examined as a continuous variable. To determine the best cutoff values for the albumin and CRP levels and CRP/albumin ratio, a receiver operating characteristic curve was generated and Youden's index was calculated; sensitivities, specificities,

Table 1A. Baseline characteristics and laboratory data of categorical variables of patients with or without 90-day mortality

	Death at 90 days n: 45 (17.3%)	Surviving patient n: 215 (82.6%)	p
Male, n (%)	15 (33.3)	129 (60)	0.028
Hypertension, n (%)	17 (37.8)	131 (60.9)	0.0047
DM, n (%)	11 (24.4)	62 (28.8)	0.295
Hyperlipidemia, n (%)	4 (8.9)	65 (30.2)	0.029
Heart failure, n (%)	9 (20)	12 (6)	0.000
Coronary artery disease	4 (7)	14 (7)	0.326
Atrial fibrillation, n (%)	13 (28.9)	31 (14.1)	0.011
Stroke aetiologic subtypes, n (%)			
Cardioembolic	24 (53.3)	52 (24.2)	0.001
Atherosclerotic	4 (9)	39 (18)	
Small vessel/ lacunar	3 (6.7)	34 (16)	
Cryptogenic/others	14 (31)	90 (41.9)	
Therapy strategy			
Endovascular / thrombolitic	10 (22.2)	33 (15.3)	0.188
Antiaggregant only	35 (77.8)	182 (84.7)	
Anterior circulation, (%)	34 (75.6)	155 (72.1)	0.635
Stroke severity (NIHSS)			
Mild (0–4)	2 (4)	55 (26)	< 0,001
Moderate (5–15)	29 (64)	143 (67)	
Severe (> 16)	14 (31.1)	17 (8)	

Values are shown as median (interquartile range) or number (%) DM – diabetes mellitus; NIHSS – National Institutes of Health Stroke Scale

Table 1B. Baseline characteristics and laboratory data of continuous variables of patients with or without 90-day mortality

	Death at 90 days n: 45 (17.3%)	Surviving patient n: 215 (82.6)	p
Age, years	75 (15)	66 (17)	< 0.001
Albumin, g/dL	3.40 (0.4)	3.80 (0.6)	< 0.001
CRP	1.32 (2.99)	0.53 (1.13)	< 0.001
CRP / albumin	0.40 (0.87)	0.14 (0.31)	< 0.001
NIHSS	7 (6)	13 (9)	< 0.001
LDL, mg/dL	141 (108.05)	117 (72)	0.20
HDL, mg/dL	39.3 (11)	39 (11)	0.117
Triglyceride, mg/dL	133 (41.46)	169 (80)	0.016
Total cholesterol, mg/dL	183 (24.6)	183 (46)	0.875
Creatinine	0.75 (0.3)	0.81 (0.27)	0.875
Glucose, mg/dL	151 (50)	123 (58)	0.022
White blood cell, 10^3/mc	11.5 (4.56)	10.1 (3.63)	0.006
Platelet, 10^3/mc	240 (108)	256 (105)	0.263
Haemoglobin, g/dL	13.4 (2.34)	14 (2.97)	0.014
Neurophil / lymphocyte	5.51 (5.67)	3.8 (3.12)	< 0.001
Platelet / lymphocyte	152.27 (142.87)	129.5 (90.62)	0.088

Values are shown as median (interquartile range) LDL – low density lipoprotein; HDL – high density lipoprotein; CRP – C-reactive protein; NIHSS – National Institutes of Health Stroke Scale

positive and negative predictive values, and their 95% CIs were also calculated. We determined predictive performance using receiver operating characteristic curves with logistic regression models to compare and assess for equality of the area under the curve using the DeLong test. Statistical analyses were performed by the use of SPSS, NSCC, Stata, and Gretl. P values ≤ 0.05 were considered statistically significant.

Results

A total of 413 patients with suspected acute ischaemic stroke were admitted to our hospital during the study period. Of those, 153 were excluded because they had a history of previous stroke (n: 19), had liver or kidney disease (n: 20), were admitted more than 24 hours after the onset of symptoms (n: 52), had a recent history of surgery, acute infection and malignancy (n: 14), or had missing data (n: 48).

The remaining 260 patients were finally included in this study. The median age was 68 (18) years and 144 patients (55.4%) were male. Forty-five patients (17.3%) died within 90 days. Female were more common in the non-survivor group. Hypertension was the most common comorbidity. A history of atrial fibrillation and heart failure were more common among non-survivors, while hypertension was more common among survivors. There was no association between CAR and stroke subtypes. Baseline characteristics and laboratory data of categorical variables are set out in Table 1A and continuous variables are set out in Table 1B.

The CAR ranged from zero to 3.47 [0.170 (0.36)]. The CAR was higher in non-survivors than in survivors [0.40 (0.87) *vs* 0.14 (0.31)]. In the univariate analyses, age, female sex, hypertension, hyperlipidemia, atrial fibrillation, congestive heart failure, stroke severity, triglyceride, white blood cell count, haemoglobin level, neutrophil count, total cholesterol, CRP, albumin, CAR, neutrophil to lymphocyte ratio, and platelet to lymphocyte ratio revealed statistically significant associations with 90-day mortality. After adjusting for all these variables, the CAR still revealed an association with 90-mortality of

Table 2. Odds ratios for all-cause 90 day mortality events

	Univariate			p	Multivariate			p
	Odds ratio	CI lower	CI upper		Odds ratio	CI lower	CI upper	
Age	1.067	1.033	1.101	0.000	1.064	1.010	1.122	0.020
Sex, female	3	0.0681	0.1985	0.000	4.437	1.265	15.560	0.020
Diabetes mellitus	0.798	0.3805	1.675	0.552				
Hypertension	0.389	0.2008	0.755	0.005	0.891	0.282	2.820	0.844
Hyperlipidemia	0.225	0.078	0.655	0.006	0.524	0.086	3.180	0.482
Coronary artery disease	1.401	0.439	4.472	0.569				
Atrial fibrillation	2.41	1.140	5.097	0.021	0.160	0.022	1.169	0.071
Congestive heart failure	8.323	3.254	21.289	0.000	3.176	0.464	21.734	0.239
NIHSS	1.201	1.131	1.291	0.000	1.257	1.113	1.419	< 0.001
Stroke severity (NIHSS)	1			–				
Mild (0–4)								
Stroke severity (NIHSS)	5.577	1.29	24.16	0.022	13.918	1.591	121.744	0.017
Moderate (5–15)								
Stroke severity (NIHSS)	22.647	4.672	109.760	0.000	57.907	5.061	662.580	< 0.001
Severe (> 16)								
Stroke aetiology (cardio-embolic)	1			–				
Stroke aetiology (athero-sclerotic)	0.440	0.149	1.301	0.138				
Stroke aetiology (small vessel/lacunar)	0.380	0.149	1.301	0.123				
Stroke aetiology (crypto-genic/other)	0.627	0.316	1.247	0.183				
LDL cholesterol, mg/dL	1.001	0.998	1.012	0.155				
HDL cholesterol, mg/dL	1.010	0.985	1.037	0.448				
Triglyceride, mg/dL	0.994	0.988	0.999	0.018	0.996	0.807	1.009	0.664
White blood cell, 103/mL	1.199	1.05	1.367	0.006	1.749	0.997	4.335	0.227
Haemoglobin, g/dL	0.837	0.721	0.973	0.020	1.110	0.629	1.527	0.522
Platelet count, 103/mL	1.000	0.997	1.003	0.931				
Mean platelet volume, fL	1.016	0.838	1.233	0.869				
Neutrophil count, 103/mL	1.226	1.085	1.385	0.001	0.652	0.995	1.513	0.320
Lymphocyte count, 103/mL	0.725	0.508	1.035	0.077				
Glucose, mg/dL	1.003	0.998	1.007	0.297				
Creatinine, mg/dL	1.351	0.457	3.995	0.586				
Total cholesterol, mg/dL	0.991	0.983	0.999	0.026	0.975	0.098	1.007	0.055
CRP	1.672	1.355	2.064	0.000	1.771	1.010	2.486	0.001
Albumin	0.279	0.138	0.566	0.000	0.325	0 .996	1.075	0.066
CRP/albumin	4.998	2.497	10.005	0.000	6.345	2.201	18.295	0.001
Neutrophil to lymphocyte ratio	1.138	1.059	1.223	0.000	0.835	0.660	1.057	0.134

CRP – C-reactive protein; CI – confidence interval

Table 3. Sensitivity, specificity, positive predictive value (PPV), and negative predictive value (NPV) of albumin, CRP, and CRP / albumin ratio (CAR)

	Cutoff	Sensitivity	Specificity	PPV	NPV
Albumin	2.2	0.366 (0.225–0.069)	0.501 (0.362–0.068)	0.101 (0.081–0.122)	0.771 (0.743–0.800)
CRP	1.92	0.560 (0.525–0.018)	0.656 (0.616–0.020)	0.362 (0.331–0.394)	0.883 (0.880–0.886)
CRP / albumin ratio	0.50	0.641 (0.609–0.016)	0.562 (0.525–0.019)	0.431 (0.386–0.477)	0.878 (0.874–0.883)

Table 4. Area under curve of CRP, albumin, and CRP / albumin ratio

	Area	Std. Error	p	95% Lower Bound	95% Upper Bound
CRP	0.689	0.048	0.000	0.595	0.783
Albumin	0.694	0.041	0.000	0.614	0.775
CRP / albumin ratio	0.696	0.047	0.000	0.604	0.788

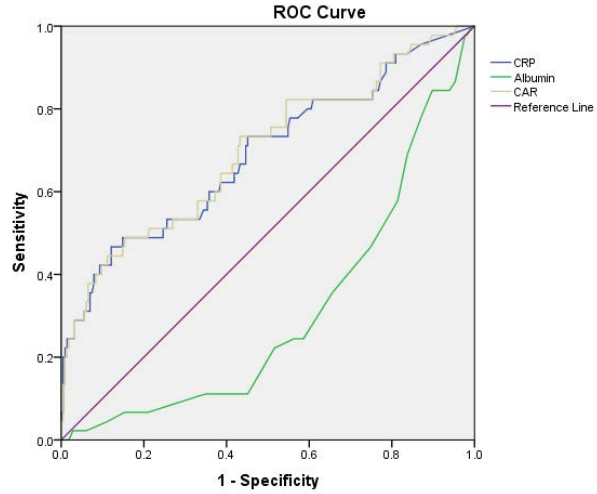

Figure 1. Receiver operating curve of CRP, albumin level and CAR in predicting 90-day mortality

stroke patients. The CAR showed an association with 90-day mortality (odds ratio, 6.345; 95% CI, 2.201 to 18.295) (Tab. 2).

Table 3 reveals the sensitivity, specificity, positive and negative predictive values of the albumin level, CRP level and CAR. The best cutoff value of the CAR was 0.50, with 64.1% sensitivity and 56.2% specificity. The area under the curve of the CAR was greater than that of albumin and CRP alone (Tab. 4, Fig. 1).

Discussion

Ourstudy showed that CAR at the time of admission is an independent predictor of mortality in the third month of acute ischaemic stroke patients. To the best of our knowledge, CAR has not been previously evaluated in predicting prognosis in patients with acute ischaemic stroke. The present study is the first to show that CAR is an independent predictor of three--month mortality of ischaemic stroke patients. In addition, CAR may have a greater prognostic value than CRP and albumin alone. The odds ratio of CAR (6.35) was higher than the CRP's odds ratio (1.8) for predicting three month mortality. For intance, after adjusting for all confounding factors, every whole-number increase in CAR increased by 6.35 the probability of mortality in the third month. On the other hand, while each whole-number increase in CRP increased by 1.8, each whole number decrease in albumin level affected mortality by 3.07 (Tab. 2).

If a patient had a CAR of > 0.5, the risk of 90-day mortality was 43.1%. If a patient had a CAR of < 0.5, the probability of survival at 90 days was 87.8% (Tab. 3).

CRP and albumin are both independently affected by inflammatory conditions, As CRP increases in inflammation, albumin metabolism increases and synthesis decreases [19]. Albumin is also affected by nutritional deficiency. With increasing age, malnutrition increases and this causes albumin deficiency [20]. We tried to exclude conditions that might affect CRP and albumin, but we could not exclude chronic hypoalbumin due to a lack of information about the nutritional status of patients. In our study, similar to previous studies, elevated CRP level was statistically significant at 90-day mortality (p: 0.001), and decreasing albumin did not reach significance but trended toward significance at three month mortality (p: 0.06) (Tab. 2). CAR, which collects CRP and albumin under a single index, has been recently considered as a novel marker. In different disease groups, especially in prognostic predictive studies, some have used CAR as only one marker, while others have compared the values of CAR to those of albumin and CRP alone to predict prognosis.

In our study, CRP was found to be statistically significant. Albumin did not reach significance but trended toward significance. As shown in ROC analysis, we found CAR was more significant compared to the area under the curve (Tab. 4). The fact that albumin was not statistically significant may be due to the limited number of patients. Furthermore, although albumin is an acute phase reactant, its response is slightly delayed. In this study, we obtained albumin at the time of admission, and this may be another reason why albumin did not reach statistical significance.

In a systematic review of five studies, CRP elevation was significantly related to functional outcome in ischaemic stroke [21]. One study found that follow-up CRP had a greater predictive value than that of CRP on admission [22]. In another study, CRP taken within two weeks of admission to hospital was associated with poor functional disability at one year [5]. We thought that the marker (CAR) obtained at the time of admission could be more useful in making a quick decision about the treatment to be chosen. So in this study we used admission CRP and albumin to predict 90-day mortality.

CAR is a new inflammation marker and is believed to reflect inflammatory status better than albumin and CRP alone. In our study, the predictive accuracy of CAR was better than that of CRP and albumin, according to the comparison of ROC curves. Recently, the relationship between CAR and critical diseases, malignancy, post-op patients, and cardiovascular diseases has been studied [23, 24]. CAR has emerged as an independent indicator of poor prognosis in various malignancies, including liver, lung, pancreatic, oesophageal and cervical malignancies [25]. A significant relationship was found between the CAR and the severity of coronary artery disease in patients with acute coronary syndrome [26]. One study showed that CAR measured after admission to the intensive care unit was an independent risk factor for 30-day and one-year mortality in postoperative patients [27]. To the best of our knowledge, no previous study has investigated the relationship between prognosis, disease severity or mortality, and CAR in stroke patients.

Neutrophil to lymphocyte ratio (NLR) has emerged as a novel marker of systemic inflammation. Previous studies have reported that NLR was associated with poor outcomes and predicted short-term mortality in patients with AIS [28]. In our study, although NLR was associated with an increased risk of mortality in univariate analysis, it did not reach statistical significance in multivariate analysis. However, CAR was an independent predictor of mortality in multivariate analysis. Therefore, CAR may be more valuable than NRL in predicting prognosis in acute ischaemic stroke. In accordance with the previous report, age, sex (female) and stroke severity also affected 90-day mortality independently ın our study [29] (Tab. 2).

In this study, we could not detect a relationship between stroke subtypes and CAR. For this reason, it is not yet clear how CAR works in each stroke subtype. In order to clarify the relationship between CAR and stroke subtypes, we think that there is a need for further studies with broader participation.

The primary limitation of this study is its retrospective observational design from a single centre. We do not know the exact cause of death of our study population, and cannot provide serial measurements of CRP and albumin. Also in our study we used conventional CRP rather than hsCRP, which can detect smaller changes in inflammation.

In conclusion, CAR at admission to hospital was associated with 90-day mortality among stroke patients. CAR may serve as a surrogate marker of disease severity. Moreover, CAR at the time of admission may be more helpful in predicting mortality at three months compared to CRP. A high CAR at initial presentation to the hospital in a stroke patient may aid decision making regarding treatment. However, the prognostic value of CAR needs to be verified by larger studies with different populations.

Conflict of interest: *The authors declare no conflict of interest.*
Funding information: *The authors received no external sources of funding for the research or authorship of this publication.*
Ethical statement: *This study was approved by the Institutional Review Boards and Ethical Committee.*

References

1. Shichita T, Sakaguchi R, Suzuki M, et al. Post-ischemic inflammation in the brain. Front Immunol. 2012; 3: 132, doi: 10.3389/fimmu.2012.00132, indexed in Pubmed: 22833743.
2. Kawabori M, Yenari MA. Inflammatory responses in brain ischemia. Curr Med Chem. 2015; 22(10): 1258–1277, indexed in Pubmed: 25666795.
3. Idicula TT, Brogger J, Naess H, et al. Admission C-reactive protein after acute ischemic stroke is associated with stroke severity and mortality: the ‚Bergen stroke study'. BMC Neurol. 2009; 9: 18, doi: 10.1186/1471-2377-9-18, indexed in Pubmed: 19400931.
4. Napoli MDi, Papa F, Bocola V. C-Reactive Protein in Ischemic Stroke. Stroke. 2001; 32(4): 917–924, doi: 10.1161/01.str.32.4.917.
5. Ye Z, Zhang Z, Zhang H, et al. Prognostic Value of C-Reactive Protein and Homocysteine in Large-Artery Atherosclerotic Stroke: a Prospective Observational Study. J Stroke Cerebrovasc Dis. 2017; 26(3): 618–626, doi: 10.1016/j.jstrokecerebrovasdis.2016.11.016, indexed in Pubmed: 27979431.
6. Rallidis LS, Vikelis M, Panagiotakos DB, et al. Inflammatory markers and in-hospital mortality in acute ischaemic stroke. Atherosclerosis. 2006; 189(1): 193–197, doi: 10.1016/j.atherosclerosis.2005.11.032, indexed in Pubmed: 16388807.
7. Cermak J, Key NS, Bach RR, et al. C-reactive protein induces human peripheral blood monocytes to synthesize tissue factor. Blood. 1993; 82(2): 513–520, indexed in Pubmed: 8329706.
8. Feinberg WM, Erickson LP, Bruck D, et al. Hemostatic markers in acute ischemic stroke. Association with stroke type, severity, and outcome. Stroke. 1996; 27(8): 1296–1300, indexed in Pubmed: 8711789.
9. Wang ZK, Xue Li, Wang T, et al. Infiltration of invariant natural killer T cells occur and accelerate brain infarction in permanent ischemic stroke in mice. Neurosci Lett. 2016; 633: 62–68, doi: 10.1016/j.neulet.2016.09.010, indexed in Pubmed: 27637387.
10. Idicula TT, Waje-Andreassen U, Brogger J, et al. Serum albumin in ischemic stroke patients: the higher the better. The Bergen Stroke Study. Cerebrovasc Dis. 2009; 28(1): 13–17, doi: 10.1159/000215938, indexed in Pubmed: 19420917.
11. Arques S. [Serum albumin and cardiovascular diseases: A comprehensive review of the literature]. Ann Cardiol Angeiol (Paris). 2018; 67(2): 82–90, doi: 10.1016/j.ancard.2018.02.002, indexed in Pubmed: 29544976.
12. Babu MS, Kaul S, Dadheech S, et al. Serum albumin levels in ischemic stroke and its subtypes: correlation with clinical outcome. Nutrition. 2013; 29(6): 872–875, doi: 10.1016/j.nut.2012.12.015, indexed in Pubmed: 23422540.

13. Abubakar S, Sabir A, Ndakotsu M, et al. Low admission serum albumin as prognostic determinant of 30-day case fatality and adverse functional outcome following acute ischemic stroke. Pan Afr Med J. 2013; 14: 53, doi: 10.11604/pamj.2013.14.53.1941, indexed in Pubmed: 23565300.
14. Idicula TT, Brogger J, Naess H, et al. Admission C-reactive protein after acute ischemic stroke is associated with stroke severity and mortality: the ‚Bergen stroke study'. BMC Neurol. 2009; 9: 18, doi: 10.1186/1471-2377-9-18, indexed in Pubmed: 19400931.
15. Zhang Q, Lei YX, Wang Q, et al. Serum albumin level is associated with the recurrence of acute ischemic stroke. Am J Emerg Med. 2016; 34(9): 1812–1816, doi: 10.1016/j.ajem.2016.06.049, indexed in Pubmed: 27364646.
16. Stroke--1989. Recommendations on stroke prevention, diagnosis, and therapy. Report of the WHO Task Force on Stroke and other Cerebrovascular Disorders. Stroke. 1989; 20(10): 1407–1431, indexed in Pubmed: 2799873.
17. Adams HP, Bendixen BH, Kappelle LJ, et al. Classification of subtype of acute ischemic stroke. Definitions for use in a multicenter clinical trial. TOAST. Trial of Org 10172 in Acute Stroke Treatment. Stroke. 1993; 24(1): 35–41, doi: 10.1161/01.str.24.1.35.
18. Ponikowski P, Voors AA, Anker SD, et al. Authors/Task Force Members; Document Reviewers. Eur J Heart Fail. 2016 Aug. ; 18(8): 891–975.
19. Don BR, Kaysen G. Serum albumin: relationship to inflammation and nutrition. Semin Dial. 2004; 17(6): 432–437, doi: 10.1111/j.0894--0959.2004.17603.x, indexed in Pubmed: 15660573.
20. Cabrerizo S, Cuadras D, Gomez-Busto F, et al. Serum albumin and health in older people: Review and meta analysis. Maturitas. 2015; 81(1): 17–27, doi: 10.1016/j.maturitas.2015.02.009, indexed in Pubmed: 25782627.
21. VanGilder RL, Davidov DM, Stinehart KR, et al. C-reactive protein and long-term ischemic stroke prognosis. J Clin Neurosci. 2014; 21(4): 547––553, doi: 10.1016/j.jocn.2013.06.015, indexed in Pubmed: 24211144.
22. Rocco A, Ringleb PA, Grittner U, et al. Follow-up C-reactive protein level is more strongly associated with outcome in stroke patients than admission levels. Neurol Sci. 2015; 36(12): 2235–2241, doi: 10.1007/s10072-015-2342-7, indexed in Pubmed: 26208640.
23. Kim MH, Ahn JY, Song JeE, et al. The C-Reactive Protein/Albumin Ratio as an Independent Predictor of Mortality in Patients with Severe Sepsis or Septic Shock Treated with Early Goal-Directed Therapy. PLoS One. 2015; 10(7): e0132109, doi: 10.1371/journal.pone.0132109, indexed in Pubmed: 26158725.
24. Park JiE, Chung KS, Song JH, et al. The C-Reactive Protein/Albumin Ratio as a Predictor of Mortality in Critically Ill Patients. J Clin Med. 2018; 7(10), doi: 10.3390/jcm7100333, indexed in Pubmed: 30297655.
25. Wu M, Guo J, Guo L, et al. The C-reactive protein/albumin ratio predicts overall survival of patients with advanced pancreatic cancer. Tumour Biol. 2016; 37(9): 12525–12533, doi: 10.1007/s13277-016-5122-y, indexed in Pubmed: 27344157.
26. Çağdaş M, Rencüzoğullari I, Karakoyun S, et al. Assessment of Relationship Between C-Reactive Protein to Albumin Ratio and Coronary Artery Disease Severity in Patients With Acute Coronary Syndrome. Angiology. 2019; 70(4): 361–368, doi: 10.1177/0003319717743325, indexed in Pubmed: 29172653.
27. Oh TK, Ji E, Na HS, et al. C-Reactive Protein to Albumin Ratio Predicts 30-Day and 1-Year Mortality in Postoperative Patients after Admission to the Intensive Care Unit. J Clin Med. 2018; 7(3), doi: 10.3390/jcm7030039, indexed in Pubmed: 29495423.
28. Xue J, Huang W, Chen X, et al. Neutrophil-to-Lymphocyte Ratio Is a Prognostic Marker in Acute Ischemic Stroke. J Stroke Cerebrovasc Dis. 2017; 26(3): 650–657, doi: 10.1016/j.jstrokecerebrovasdis.2016.11.010, indexed in Pubmed: 27955949.
29. Corso G, Bottacchi E, Tosi P, et al. Outcome Predictors in First-Ever Ischemic Stroke Patients: A Population-Based Study. Int Sch Res Notices. 2014; 2014: 904647, doi: 10.1155/2014/904647, indexed in Pubmed: 27437502.

RESEARCH PAPER

Neurologia i Neurochirurgia Polska
Polish Journal of Neurology and Neurosurgery
2019, Volume 53, no. 3, pages: 212–216
DOI: 10.5603/PJNNS.a2019.0021

ISSN 0028–3843

Seasonal variations in the occurrence of transient global amnesia (TGA)

Justyna Chojdak-Łukasiewicz[1], Edyta Dziadkowiak[1], Leszek Noga[2], Małgorzata Wieczorek[3], Bogusław Paradowski[1]

[1]Department of Neurology, Wrocław Medical University, Wroclaw, Poland
[2]Department of Pathophysiology, Wrocław Medical University, Wroclaw, Poland
[3]Department of Geoinformatics and Cartography, University of Wrocław, Wroclaw, Poland

Abstract

Background. Transient global amnesia (TGA) is a rare, benign condition characterised by a sudden deficit of anterograde and retrograde memory that usually lasts for a few hours and is not accompanied by other focal neurological symptoms or signs. Its aetiology is still unclear. Various events or activities may trigger TGA. Evidence of seasonal variations in the appearance of TGA is inconsistent.

Methods. We retrospectively analysed the medical history of 114 adult patients with diagnosed TGA, hospitalised at two neurology departments in Wrocław from 2008 to 2014. We reviewed risk factors, trigger points, and occurrence in each month of the year in our patient population.

Results. Over this seven-year period, 114 patients were diagnosed with TGA. The annual occurrence ranged from 13 to 22 hospitalisations. The mean age of the patients was 64 years. There were 36 TGA events in men and 78 in women. TGA occurred most frequently in spring (36%) and summer (30%), with the incidence peaking during March.

Conclusions. Our findings suggest that there is a relationship between the season of the year and the probability of TGA.

Key words: transient global amnesia, seasonal variations
(*Neurol Neurochir Pol 2019; 53 (3): 212–216*)

Introduction

Transient global amnesia (TGA) is a rare condition characterised by a sudden deficit of anterograde and retrograde memory that lasts up to 24 hours. The episodes are sudden, transient, benign and not accompanied by other neurological symptoms [1]. The incidence varies between 3 and 8 cases per 100,000 people per year; the majority of cases occur in people aged between 50 and 70 years and only rarely in patients younger than 40 [2]. The rate of recurrent attacks within one year varies between 6% and 10% [3]. The aetiology and pathomechanism of TGA are not clearly defined. Transient ischaemic attack (TIA), venous congestion with subsequent ischaemia, epilepsy, and migraine have been suggested as possible causes [3–5]. Magnetic resonance imaging (MRI) studies indicate that CA1 neurons of the hippocampal area play a role in the pathomechanism of TGA [6–9]. These areas are sensitive to metabolic stress, oxidative stress, and cytotoxic glutamate. One in three patients experiences a preceding event immediately before a TGA episode, especially emotional stress, physical activity, acute pain, or immersion in cold water [3]. Atmospheric factors such as air pollution, UV radiation, temperature, and air pressure also play an important role in the pathogenesis of TGA.

The aim of this study was to evaluate the seasonality of TGA and the possible influence of the seasons on the incidence of TGA.

Address for correspondence: Justyna Chojdak-Łukasiewicz, Department of Neurology, Wrocław Medical University, Wroclaw, Poland, e-mail: justyna.ch.lukasiewicz@gmail.com

Table 1. Criteria of TGA according to Hodge and Warlow [2]

Sudden anterograde and retrograde amnesia in the presence of witnesses of the event
No disturbance of consciousness; awareness of personal identity is preserved
Cognitive impairment limited to amnesia
No focal neurological signs
Exclusion of head or neck injury, or other causes of amnesia; lack of epilepsy in medical history
Attack resolves within 24 hours

Table 2. Demographic data of patients

Time of observation: 2008–2014				
n = 114, mean age 64.32 ± 10.52 years				
F: n = 78, mean age 65.36 ± 10.29 years				
M: n = 36; mean age 62.06 ± 10.80 years				
Risk factors				
Hyperten-sion	Diabetes	Ischaemic disease	Thyroid dysfunction	Hyper-lipidemia
61 / 114	5 / 114	13 / 114	15 / 114	30 / 114

Material and methods

We retrospectively analysed the medical history of 114 adult patients with diagnosed TGA, hospitalised at two departments of neurology in Wrocław between 1 January 2008 and 31 December 2014. TGA was diagnosed according to the criteria created by Hodge and Warlow in 1990 (Tab. 1) [10]. All participants in the study underwent a neurological examination, brain CT scan without contrast, laboratory tests, EEG, and Doppler scanning of vessels. We excluded patients with transient ischaemic attack (TIA) and stroke.

In addition, in 2016 patients who had experienced a TGA in the previous one to seven years were sent a questionnaire asking about their vascular diseases and past TGA incidents.

Ethical approval and patient consent were not required.

All analyses were performed using Statistica 10 software. Pearson's chi-square test was used for categorical variables. The threshold of statistical significance was $\alpha = 0.05$.

Results

TGA was diagnosed in 114 patients (78 women, 36 men) with a mean age of 64.3 ± 10.52 years (range 27–87) and with a median of 63.0. In our group, the annual occurrence of TGA ranged from 13 to 22 hospitalisations. Table 2 shows the demographics, basic clinical data, and risk factors. Loss of memory lasted between 30 minutes and 13 hours. A precipitating event was noted in 37 cases (65.6%). In 21 patients, an increase of blood pressure may have been the triggering factor. In other cases, the attacks were precipitated by stressors such as physical activity, medical appointment, insect bite, trauma, exposure to the sun, sauna, gastroscopy, headache, and nutritional factors.

According to the modified Rankin scale, all patients had a score of 0. In 63.1% of the cases (72 patients) the neurological examination was normal. The remaining patients had some abnormalities. The most common abnormality was weakened ankle jerk reflex. Nineteen patients who had suffered TGA in the summer had an abnormal neurological state, in most cases asymmetrical deep tendon reflexes without paresis. Non-contrast head CT performed on admission was normal in 46.5% of the patients. The remaining 53.5% of patients had changes in the white matter characteristic of cerebral small vessels disease.

Figures 1 and 2 show, respectively, the incidence of TGA in each month and season. The highest incidence was during the spring and summer months, with the peak incidence occurring during March (17 patients) and the lowest rate in September (five patients) (Tab. 3). Seasonal peaks in the incidence of TGA were noted in spring and summer (Tab. 4).

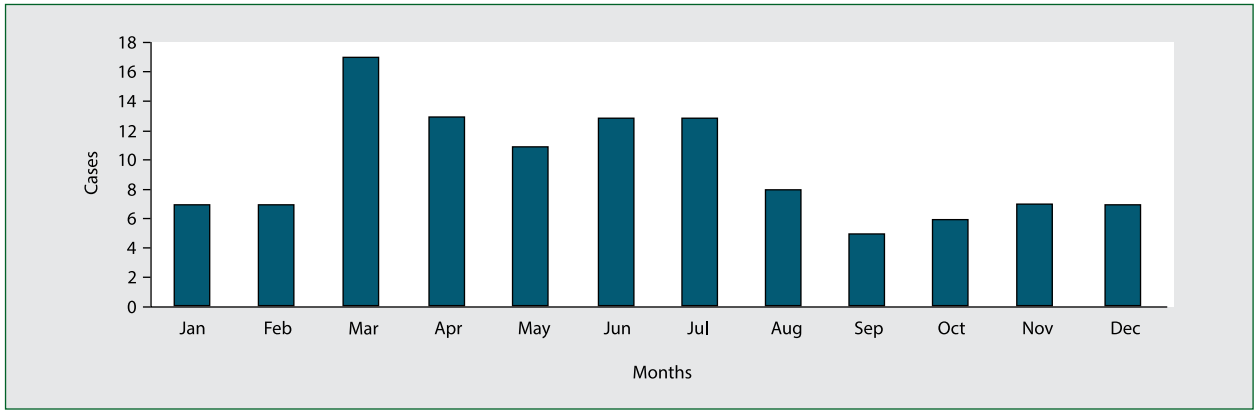

Figure 1. Incidence of TGA per month

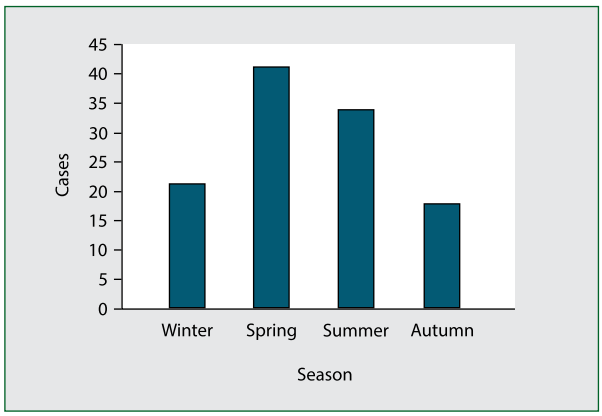

Figure 2. Incidence of TGA per season

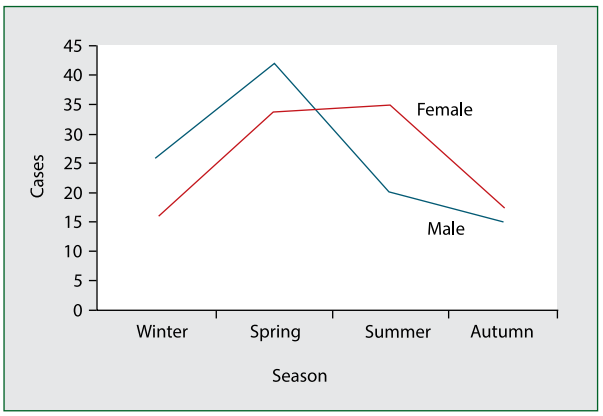

Figure 3. Incidence of TGA per gender (F/M) and season

Table 3. Percentage of TGA incidence according to season

Season	Mean	Convidence interval	Median	STD
Winter	17.4	9.5–25.4	21	8.6
Spring	34.4	21.4–47.5	30	14.1
Summer	30.9	18.5–43.4	35	13.4
Autumn	17.2	7.5–26.9	17	10.5

Table 4. Percentage of TGA incidence according to month

	Mean	Convidence interval	Median	STD
Jan	6.4	1.4–11.3	7.1	5.4
Feb	5.0	0–11.6	0.0	7.1
Mar	14.3	3.8–24.8	11.1	11.4
Apr	10.3	3.1–17.4	14.3	7.7
May	9.9	6.5–13.3	9.1	3.7
Jun	13.1	3.2–23.1	14.3	10.7
Jul	10.5	0–22.9	0.0	13.4
Aug	7.3	2.7–11.8	7.1	4.9
Sep	5.0	1.8–8.3	7.1	3.5
Oct	5.7	1.1–10.3	5.6	5.0
Nov	6.5	2.2–10.8	5.6	4.7
Dec	6.0	0–12.6	7.1	7.2

The Chi-square test indicates the largest incidence in the spring and summer months ($p = 0.013$). There was a predominance of women in all months of the year except for May and December. Among women, the largest (30%) incidence of TGA was in summer and in spring; among men more than 40% of incidence took place in spring (Fig. 3).

Based on the 37 questionnaire results, recurrent TGA occurred in three cases, one person had ischaemic stroke, and one case occurred with transient ischaemic attack.

Discussion

TGA is a neurological disorder with an unknown and complex pathogenesis. Its mechanisms are still unclear, including vascular aetiology, seizure and migraine. The presence of focal-high-signals abnormalities in the hippocampus on diffusion-weighted imaging (DWI) is very suggestive of TGA [11, 12]. The frequency of DWI signal abnormalities in patients with TGA varies widely, from 0% to 84% [13]. Also, silent small lacunar infarcts are detectable on conventional MRI [14, 15].

Its seasonal appearance, with a peak in March (which was confirmed in our retrospective study), may imply an atmospheric influence. In a six-year study involving a group of 223 patients in northern Italy, Akkawi et al found the peak incidence to be in the autumn–winter period, which indicates a correlation with low temperatures [16]. By contrast, the authors of an Israeli study observed an increase in TGA incidence in the winter-spring months, peaking in December and March [17]. These differences may result from different geographical locations or the coexistence of other atmospheric factors. We know from electrophysiological and biochemical studies that several functions of the nervous system change periodically. It has also been confirmed that the morbidity of several diseases is dependent on meteorological and climatological factors. The meteorological factors activate the autonomic nervous system, which may lead to certain diseases or exacerbate some symptoms by affecting the homeostasis. The climatological factors that are present in a given geographical region may stimulate a disease or weaken the human organism. In epidemiological studies, it has been shown that as much as 90% of strokes are correlated with the movement of weather fronts [18]. Seasonal diseases include depression (peaking in autumn-winter), epilepsy, and vascular brain disorders. Migraine is dependent on daily as well as annual cycles (with the peak in January) and atmospheric factors (for example, local winds). Multiple sclerosis patients have symptoms that change throughout the day. This disease is also known to spread differently in different geographic locations. Vascular

brain diseases are dependent on meteorological factors, such as air temperature and pressure [19, 20]. Haemorrhagic and subarachnoid strokes are also seasonal diseases, with peak incidence in autumn and winter [21].

In our TGA patient group, there were significantly more women than men (similar to other studies e.g. Melo et al. 1992, Lauria et al. 1997, and Keret et al. 2016) [17, 22, 23]. The relationship between patient gender and TGA is very unclear. Brigio et al. observed a higher incidence among men [24]. Other studies found no correlation. TGA-precipitating factors were observed only in 30% of the patients, and they were higher blood pressure and increased stress. In other studies, such factors were observed in 50–90% of the patients [6, 25]. Surveys have not shown an increased risk of recurrent TGA (similarly as with other vascular diseases).

In our study, the most frequent TGA comorbidity was hypertension, present in 54% of the patients. Epidemiological studies do not clarify which vascular disease risk factors are significant for TGA (unlike for stroke and TIA). Nevertheless, the following factors are thought to increase the likelihood of TGA: hypertension, diabetes, hypercholesterolemia, migraine, and psychological factors [3, 5]. In addition, Patoni mentions personality disorders, emotional instability and depressive anxiety, and a history of psychiatric disease in the family [26].

Our study confirmed the seasonal character of TGA, and the potential influence of geographic location and climate. The seasonality of TGA requires more clinical research in cooperation with weather stations in order to precisely determine the air pressure, humidity, and temperature fluctuations.

Conflict of interest: *There is no conflict of interest in this publication.*

Funding: *This publication was prepared with no external sources of funding. We declare that none of the authors have any financial agreement with any organisation or other financial relationships (e.g. stock ownership in medically-related fields, intellectual property rights, consultancies, advisory boards, expert testimony, employment partnerships contracts, honoraria, royalties grants) now or in the past three years, either related or unrelated to the current research.*

References:

1. Szabo K. Front Neurol Neurosci. 2014; 34: 143–9.
2. Hodges JR, Warlow CP. The aetiology of transient global amnesia. A case-control study of 114 cases with prospective follow-up. Brain. 1990; 113 (Pt 3): 639–657, doi: 10.1093/brain/113.3.639, indexed in Pubmed: 2194627.
3. Owen D, Paranandi B, Sivakumar R, et al. Classical diseases revisited: transient global amnesia. Postgrad Med J. 2007; 83(978): 236–239, doi: 10.1136/pgmj.2006.052472, indexed in Pubmed: 17403949.
4. Quinette P, Guillery-Girard B, Dayan J, et al. What does transient global amnesia really mean? Review of the literature and thorough study of 142 cases. Brain. 2006; 129(Pt 7): 1640–1658, doi: 10.1093/brain/awl105, indexed in Pubmed: 16670178.
5. Hunter G. Transient global amnesia. Neurol Clin. 2011; 29(4): 1045–1054, doi: 10.1016/j.ncl.2011.07.004, indexed in Pubmed: 22032672.
6. Bartsch T, Deuschl G. Transient global amnesia: functional anatomy and clinical implications. Lancet Neurol. 2010; 9(2): 205–214, doi: 10.1016/S1474-4422(09)70344-8, indexed in Pubmed: 20129169.
7. Spiegel DR, Mccroskey AL, Deyerle BA. A Case of Transient Global Amnesia: A Review and How It May Shed Further Insight into the Neurobiology of Delusions. Innov Clin Neurosci. 2016; 13(3-4): 32–41, indexed in Pubmed: 27354927.
8. Calabresi P, Centonze D, Pisani A, et al. Synaptic plasticity in the ischaemic brain. Lancet Neurol. 2003; 2(10): 622–629, indexed in Pubmed: 14505584.
9. Kosuge Y, Imai T, Kawaguchi M, et al. Subregion-specific vulnerability to endoplasmic reticulum stress-induced neurotoxicity in rat hippocampal neurons. Neurochem Int. 2008; 52(6): 1204–1211, doi: 10.1016/j.neuint.2007.12.010, indexed in Pubmed: 18280615.
10. Hodges JR, Warlow CP. Syndromes of transient amnesia: towards a classification. A study of 153 cases. J Neurol Neurosurg Psychiatry. 1990; 53(10): 834–843, doi: 10.1136/jnnp.53.10.834, indexed in Pubmed: 2266362.
11. Enzinger C, Thimary F, Kapeller P, et al. Transient global amnesia: diffusion-weighted imaging lesions and cerebrovascular disease. Stroke. 2008; 39(8): 2219–2225, doi: 10.1161/STROKEAHA.107.508655, indexed in Pubmed: 18583561.
12. Alberici E, Pichiecchio A, Caverzasi E, et al. Transient global amnesia: hippocampal magnetic resonance imaging abnormalities. Funct Neurol. 2008; 23(3): 149–152, indexed in Pubmed: 19152736.
13. Huber R, Aschoff AJ, Ludolph AC, et al. Transient Global Amnesia. Evidence against vascular ischemic etiology from diffusion weighted imaging. J Neurol. 2002; 249(11): 1520–1524, doi: 10.1007/s00415-002-0881-3, indexed in Pubmed: 12420091.
14. Himeno T, Kuriyama M, Takemaru M, et al. Vascular Risk Factors and Internal Jugular Venous Flow in Transient Global Amnesia: A Study of 165 Japanese Patients. J Stroke Cerebrovasc Dis. 2017; 26(10): 2272–2278, doi: 10.1016/j.jstrokecerebrovasdis.2017.05.010, indexed in Pubmed: 28669658.
15. Güngör Tunçer Ö, Aksay Koyuncu B, Vildan Okudan Z, et al. Vascular Ischemia as a Cause of Transient Global Amnesia: A Patient Series. Noro Psikiyatr Ars. 2015; 52(1): 59–63, doi: 10.5152./npa.2015.7444, indexed in Pubmed: 28360677.
16. Akkawi NM, Agosti C, Grassi M, et al. Weather conditions and transient global amnesia. A six-year study. J Neurol. 2006; 253(2): 194–198, doi: 10.1007/s00415-005-0952-3, indexed in Pubmed: 16133724.
17. Keret O, Lev N, Shochat T, et al. Seasonal Changes in the Incidence of Transient Global Amnesia. J Clin Neurol. 2016; 12(4): 403–406, doi: 10.3988/jcn.2016.12.4.403, indexed in Pubmed: 27095523.
18. Nyquist PA, Brown RD, Wiebers DO, et al. Circadian and seasonal occurrence of subarachnoid and intracerebral hemorrhage. Neurology. 2001; 56(2): 190–193, doi: 10.1212/wnl.56.2.190, indexed in Pubmed: 11160954.
19. Fares A. Winter cardiovascular diseases phenomenon. N Am J Med Sci. 2013; 5(4): 266–279, doi: 10.4103/1947-2714.110430, indexed in Pubmed: 23724401.
20. Wang X, Cao Y, Hong D, et al. Ambient Temperature and Stroke Occurrence: A Systematic Review and Meta-Analysis. Int J Environ Res Public Health. 2016; 13(7), doi: 10.3390/ijerph13070698, indexed in Pubmed: 27420077.
21. de Steenhuijsen Piters WAA, Algra A, van den Broek MFM, et al. Seasonal and meteorological determinants of aneurysmal subarach-

noid hemorrhage: a systematic review and meta-analysis. J Neurol. 2013; 260(2): 614–619, doi: 10.1007/s00415-012-6687-z, indexed in Pubmed: 23070464.
22. Melo TP, Ferro JM, Ferro H. Transient global amnesia. A case control study. Brain. 1992; 115 Pt 1: 261–270, doi: 10.1093/brain/115.1.261, indexed in Pubmed: 1559158.
23. Lauria G, Gentile M, Fassetta G, et al. Transient global amnesia and transient ischemic attack: a community-based case-control study. Acta Neurol Scand. 1998; 97(6): 381–385, indexed in Pubmed: 9669471.
24. Brigo F, Lochner P, Tezzon F, et al. Incidence of transient global amnesia in Merano, province of Bolzano, Italy. Acta Neurol Belg. 2014; 114(4): 293–296, doi: 10.1007/s13760-014-0281-3, indexed in Pubmed: 24515914.
25. Lewis SL. Aetiology of transient global amnesia. Lancet. 1998; 352(9125): 397–399, doi: 10.1016/S0140-6736(98)01442-1, indexed in Pubmed: 9717945.
26. Pantoni L, Bertini E, Lamassa M, et al. Clinical features, risk factors, and prognosis in transient global amnesia: a follow-up study. Eur J Neurol. 2005; 12(5): 350–356, doi: 10.1111/j.1468-1331.2004.00982.x, indexed in Pubmed: 15804264.

RESEARCH PAPER

Neurologia i Neurochirurgia Polska
Polish Journal of Neurology and Neurosurgery
2019, Volume 53, no. 3, pages: 217–226
DOI: 10.5603/PJNNS.a2019.0025

ISSN 0028–3843

Autoimmune response in lung cancer patients with neurological paraneoplastic syndromes

Sławomir Michalak[1], Tomasz Piorunek[2], Mikołaj Zaborowski[3], Joanna Rybacka-Mossakowska[1], Patrycja Stefens-Stawna[4], Alicja Kalinowska-Łyszczarz[1], Wojciech Kozubski[4], Halina Batura-Gabryel[2]

[1]Department of Neurology, Division of Neurochemistry and Neuropathology, Poznan University of Medical Sciences, Poznan, Poland
[2]Department of Pulmonology, Allergology and Respiratory Oncology, Poznan University of Medical Sciences, Poznan, Poland
[3]Department of Gynaecologic Oncology, Chair of Gynaecology, Obstetrics and Gynaecologic Oncology, Poznan University of Medical Sciences, Poznan, Poland
[4]Department of Neurology, Poznan University of Medical Sciences, Poznan, Poland

Abstract

Aim of the study. The aim of this study was to evaluate granzyme B, perforin and FasL expression in peripheral blood mononuclear cells (PBMCs) in lung cancer patients and in paraneoplastic neurological syndromes (PNS).

Clinical rationale for the study. Cellular immune response is activated as part of anti-tumour reaction of the malignancy-bearing host. Paraneoplastic neurological syndromes (PNS) are defined as indirect effects of cancer on the nervous system and are considered immune-mediated. Such stimulation of the immune system may limit the aggressiveness of cancer and the development of metastasis, and thereby improve survival. Granzyme B and perforin pathway, and Fas ligand (FasL) – Fas receptor interaction play an important role in cytotoxic response.

Materials and Methods. Fifty-two patients were included in the study: 28 subjects with PNS and 24 subjects with lung cancer. PNS cases were diagnosed according to the Graus criteria. The presence of onconeural antibodies (anti-Hu/anti-Ri/anti-Yo/anti-Ma/Ta/anti-CV2/anti-amphiphysin/anti-myelin/anti-neuroendothelium/anti-MAG/anti-GAD) was detected with indirect immunofluorescence and confirmed with Line Blotting. The expression of granzyme B, perforin and FasL was detected in PBMCs with ELISA.

Results. PPBMC-FasL expression was increased in lung cancer compared to other patient groups. The granzyme to FasL ratio was significantly higher in lung cancer patients with peripheral than with central PNS involvement. In a multiple regression model, sex was an independent factor influencing PBMC expression of granzyme and perforin.

Conclusions. FasL expression in PBMCs is up-regulated in lung cancer patients. The interplay between granzyme B and FasL may be involved in the development of PNS at the level of the peripheral and the central nervous systems in different manners. Gender is associated with PBMC expression of granzyme B and perforin in lung cancer patients.

Clinical Implications. The novel findings that we report broaden the current knowledge on PNS pathomechanism, with aspects that have not been previously explored. Our findings provide a rationale for further exploration of the granzyme B/FasL pathway with regards to its potential diagnostic value. However, our study is preliminary and needs further research, especially in the context of the prognostic value of the proposed markers.

Key words: lung cancer, paraneoplastic neurological syndromes, cytotoxicity, onconeural antibodies, Fas ligand, granzyme B, perforin

(*Neurol Neurochir Pol 2019; 53 (3): 217–226*)

Address for correspondence: Sławomir Michalak, Department of Neurology, Division of Neurochemistry and Neuropathology, Poznan University of Medical Sciences, Poznan, Poland, e-mail: slamic@yahoo.com

Introduction

Paraneoplastic neurological syndromes (PNS) are defined as the pathology of the nervous system observed in the course of a neoplastic disease, but unrelated to the direct effects of the tumour mass, such as infiltration, compression or metastasis [1]. PNS diagnosis is based on detailed criteria that consider both the clinical manifestation and the presence of onconeural antibodies [1]. In general, PNS may affect central (encephalitis, limbic encephalitis, brain stem encephalitis, paraneoplastic cerebellar degeneration and opsoclonus/myoclonus) and peripheral (polyneuropathies) nervous systems, as well as the neuromuscular junction (myasthenic syndrome) and skeletal muscles (dermatomyositis). Among the most common malignancies associated with PNS are pulmonary pathologies, particularly small cell lung carcinoma (SCLC) [1, 2]. The clinical significance of PNS stems mainly from the fact that the diagnosis of the neurological pathology often precedes neoplastic manifestation. Patients affected with PNS undergo detailed oncological diagnostic procedures that frequently result in detection of the tumour at an early stage of development. It has been suggested that neoplasms associated with these syndromes are less advanced, that metastases are rare, and that the overall outcome is favourable [3]. Cases of SCLC regression have been reported [4]. Some studies have suggested that in the course of PNS an effective anti-tumour response may develop [3]. Nonetheless, neither the origin of PNS nor the pathophysiological basis of a potentially more favourable outcome of the neoplastic disease is known, and this remains a hypothesis.

The prevailing view on the pathogenesis of PNS is based on the assertion that the immune system attacks the tumour and nervous tissue cells that share common antigens. The humoral response, however, has an unclear role in the pathomechanism of the disease. In some cases in animal models, the passive transfer of antibodies did not lead to nervous system pathology [5]. It appears, in turn, that lymphocytes withdrawn from blood samples of PNS patients were active against the same antigens as the antibodies used in diagnostic procedures e.g. onconeural antibodies. Mononuclear infiltrates have been observed in neuropathological studies of affected nervous tissue [6]. Immunohistopathologically it has been defined that these infiltrates consist mainly of lymphocytes $CD3^+$ and $CD8^+$ as well as less numerous $CD4^+$ cells [7]. Cerebrospinal fluid analysis in PNS patients has revealed an increase of white blood cell count, including elevated T lymphocytes $CD8^+$ and $CD4^+$, natural killer cells (NK) and especially B cells [8]. Interestingly, patients afflicted with SCLC-associated anti-Hu syndrome with high pleocytosis have turned out to have a better overall survival rate [8]. The above-mentioned studies imply that a cell-mediated immune response takes part in the pathogenesis of PNS. One needs to recognise that the type of immune response may depend on the localisation of the antigens under attack. In classical paraneoplastic syndromes, where intracellular antigens (i.e. Hu, Ri, amphiphysin) are targeted by onconeural antibodies, the cellular response seems to play a key role. However, in cases of surface antigens (i.e. NMDA, GABA, AMPA), the humoral response, with antibody-mediated receptor dysfunction, may be of more significance. Apoptosis related to cytotoxic effect is mediated by Tumour Necrosis Factor (TNF) receptor, through FasL receptor (Fas) activation or by means of granzyme B containing granule excretion and perforin involvement. These molecules play a role in autoimmune disorders, but also in anti-tumour reaction.

Granzymes are serine proteases that launch cell death in a number of mechanisms. When released to the extracellular space, they promote an inflammatory reaction [9]. The proapoptotic function appears to be dependent on the presence of perforin that is a prerequisite to their entrance into the cell [10]. Granzymes may induce cytochrome c release, directly activate caspases or interfere with cell membrane integrity by cleavage of laminin B [11]. The most significant molecule in this class is granzyme B. The expression of both granzyme B and perforin turns out to play an important role in the reaction against tumour cells. Their concentration is closely related to survival in patients with neoplastic disease.

Perforin is a Ca^{+2}-dependent pore-forming protein with lytic activity. It leads to apoptosis through up-regulation of caspase-3 activity, release of apoptosis inducing factor (AIF), and cytochrome c from the mitochondria [12].

Fas Ligand (FasL) belongs to the TNF superfamily. It is a membrane protein that induces apoptosis by the specific receptor CD95 on a target cell. FasL is mainly expressed by cytotoxic lymphocytes and natural killer cells, but also by regulatory T lymphocytes. Fas activation induces two major mechanisms of cell death, depending on the cell type. It may either cause activation of mitochondria and release of cytochrome C, or induce direct caspase cascade [13]. Fas/FasL interaction is part of a mechanism to prevent autoimmune reaction. It is the pathway to eliminate overactive or abundant lymphocytes [14]. Improper or insufficient expression of FasL has been proven to trigger autoimmune conditions in mice and in humans [15]. Fas is also involved in the interaction between the emerging tumour and the host immune system. On one hand, neoplastic cells escape lymphocyte cytotoxicity by low expression of Fas protein. On the other hand, tumour cells up-regulate FasL to eliminate immune cells that form a tumour counterattack [16]. The expression of FasL has been revealed at the surface of human lung cancer cells [17].

For the complex interactions between cytotoxic immune cells and target cells expressing well-characterised onconeural antibodies, see Figure 1.

Clinical rationale for the study

In the present study, in order to determine the role of humoral and cytotoxic reactions in lung cancer patients, serum

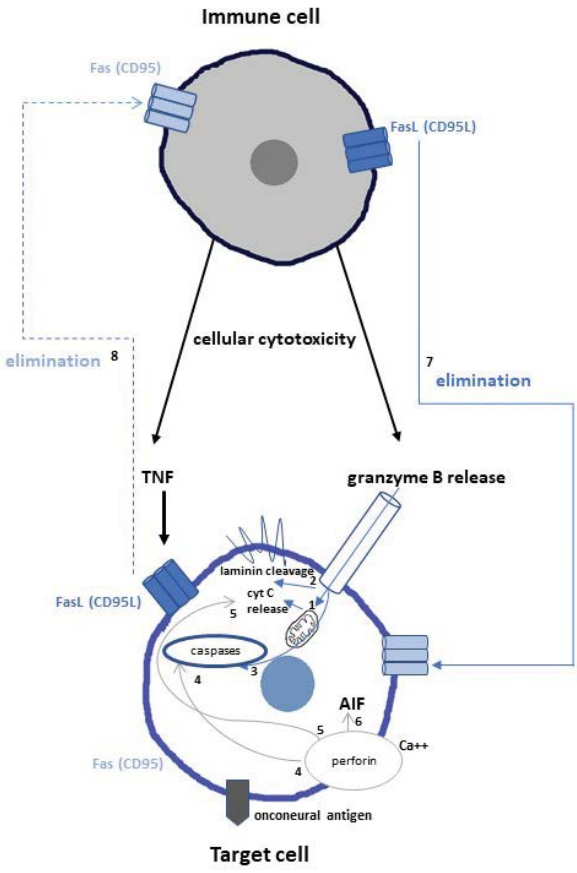

Figure 1. Schematic presentation of the interactions between cytotoxic immune cell and target cell (neoplasm or normal cell expressing onconeural antigen): 1 – granzyme B from immune cell releases cytochrome C from target cell mitochondria; 2 – granzyme B-mediated laminin cleavage; 3 – granzyme B-mediated caspase activation; 4 – perforin-mediated caspase activation; 5 – perforin-mediated cytochrome C release from target cell mitochondria; 6 –perforin-mediated AIF release; 7 – elimination of target cell by immune cell via Fas/FasL interaction; 8 – elimination of immune cell by FasL-expressing tumour cells. AIF – apoptosis inducing factor; cytC – cytochrome C; Ca – calcium; TNF – Tumour Necrosis Factor; FasL – Fas ligand

autoantibodies, as well as the expression of granzyme B, perforin and FasL in peripheral blood mononuclear cells (PBMC), were investigated in the context of PNS. The immunological pathomechanism of paraneoplastic syndrome remains poorly described. A better understanding in this area could contribute to new diagnostic and therapeutic developments.

Material and methods

Fifty-two patients were recruited for the study: 28 subjects with suspected PNS who were hospitalised in the Department of Neurology, Poznan University of Medical Sciences, and 24 subjects with lung cancer who were admitted to the Department of Pulmonology, Allergology and Respiratory Oncology, Poznan University of Medical Sciences. The study protocol was accepted by the Ethical Review Board of Poznan University of Medical Sciences, and each recruited participant gave written informed consent. PNS were diagnosed according to the 2004 Graus criteria [1]. The presence of well-defined onconeural antibodies (anti-Hu, anti-Ri, anti--Yo, anti-Ma/Ta, anti-CV2, anti-amphiphysin) was detected by means of indirect immunofluorescence. If positive, it was confirmed with a Line Blot (Euroimmun, Germany). Indirect immunofluorescence was also used for the detection of other antibodies: anti-myelin, anti-neuroendothelium, anti-myelin associated glycoprotein (anti-MAG) and anti-glutamic acid decarboxylase (anti-GAD). The patterns of positive reactions were evaluated under a fluorescent microscope (EUROStar, Zeiss). Each series of samples was preceded by testing the positive and negative control sera.

PBMCs were isolated from heparinised blood samples by concentration gradient centrifugation (Ficoll Paque Plus, Healthcare) and frozen at -70°C until further analysis. PBMC lysis was carried out with the use of lysis buffer containing a cocktail of proteinase inhibitors (Sigma-Aldrich, USA). In the next step, the expression of cytotoxicity markers: granzyme B (Abcam), perforin (Abcam), FasL (Enzo Life Sciences) was detected in the lysates with the use of ELISA. Protein concentration was estimated by means of the Lowry method [18]. The expression of cytotoxicity markers in PBMCs was expressed in pg/mg protein.

Statistical analysis was performed with the use of licensed MedCalc software version 12.3.0.0. First, the distribution of results was tested using the d'Agostino-Pearson test. The results with Gaussian distribution were expressed as means ± standard deviation (SD) and analysed using the Student's t-test. The results with a non-Gaussian distribution were expressed as median and interquartile range, and analysed using a non-parametric Mann-Whitney test.

Results

Having included all PNS and lung cancer patients, in the final study group there were 31 (60%) lung cancer patients, nine (17%) ovarian cancer, two (4%) prostate cancer, one (2%) with other malignancies, and nine (17%) cases without any identified malignancy.

Of the 31 lung cancer patients, 24 were referred from the Department of Pulmonology, Allergology and Respiratory Oncology, and the other seven were diagnosed in the Department of Neurology where they were admitted for suspected PNS.

Clinically, 20 (64.5%) patients manifested peripheral nervous system involvement (polyneuropathy/neuropathy, myasthenic syndrome, myopathy) and 11 (35.5%) had central nervous system involvement (cerebellar syndrome, motor neuron disease, extrapyramidal syndrome).

Table 1. The expression of FasL in peripheral blood mononuclear cells

Studied group	Studied subgroup	FasL [pg/mg of protein]	p
Lung cancer patients (n = 31)	Total (n = 31)	7.39 0.02–11.87	p = 0.0171*
	PNS (n = 17)	0.11 0.02–12.07	p = 0.9816
	No PNS (n = 14)	8.55 0.02–11.80	
	Well-defined antibodies (n = 8)	0.07 0.03–4.87	p = 0.1043
	Seronegative (n = 15)	11.38 6.25–12.06	
Other cancer patients (n = 12)	Total (n = 12)	0.027 0.01–5.73	p = 0.9955
	PNS (n = 8)	0.05 0.02–8.49	
	No PSN (n = 4)	0.05 0.02–8.11	
	Well-defined antibodies (n = 5)	0.06 0.02–11.60	p = 0.3209
	Seronegative (n = 6)	0.03 0.02–7.03	
All patients (n = 52)	PNS manifestation (n = 31)	0.06 0.02–11.85	p = 0.7052
	Without PNS symptoms (n = 21)	0.06 0.02–9.25	
Antibodies	1. Well-defined onconeural antibodies (n = 15)	0.09 0.02–8.09	1 vs 3: p = 0.7952 2 vs 3: p = 0.9088 1 vs 2: p = 0.5841 (1+2) vs 3: p = 0.8146
	2. Other autoantibodies (n = 15)	0.06 0.02–10.56	
	3. Seronegative (n = 26)	4.11 0.01–11.48	

*Statistically significant difference

In 15 (29%) patients, the presence of well-defined onconeural antibodies (anti-Hu, anti-amphiphysin, anti-Ri, anti--Yo, anti-Ma/Ta) was detected, and in 34 subjects (65%) other autoantibodies (anti-Tr, anti-MAG, anti-myelin) were found. In the lung cancer patients, eight (27%) had well-defined onconeural antibodies (anti-Hu, anti-amphiphysin, anti-Ri, anti-Yo, anti-Ma/Ta) and eight (27%) were seropositive for other autoantibodies (anti-Tr, anti-MAG, anti-myelin).

Coexisting autoantibodies were detected in 17% of lung cancer patients. The coexistence profile included: anti-Hu with anti-Ma/Ta, anti-Hu with anti-amphiphysin, anti-Hu with anti-myelin, and anti-Ri with anti-myelin. In 17% of other neoplasms, the coexistence of onconeural antibodies was detected (anti-Ri with anti-amphiphysin and anti-Ma/Ta with anti-amphiphysin and with anti-Tr).

The expression of FasL in PBMCs was increased in lung cancer patients compared to other groups of patients (Tab. 1).

No differences in granzyme B expression in PBMCs were observed between the studied subgroups of patients (Tab. 2). The Granzyme B to FasL ratio differed (P = 0.0180) between lung cancer patients with peripheral (11,589; 166-58,242) and central PNS (73; 34-112).

The expression of perforin in PBMCs of lung cancer patients with PNS was lower than in asymptomatic subjects (Tab. 3). We observed a trend for down-regulation of perforin in lung cancer patients compared to other neoplasms (Tab. 3).

In multiple regression analysis with gender, the presence of small cell lung cancer, onconeural antibodies and diagnosis of PNS included in the model, gender was an independent factor influencing PBMC expression of granzyme (b = 1,536; p = 0.0126) and perforin (b = 30,925; p = 0.0174).

For the detailed characteristics of each individual patient with PNS in the study cohort, see supplementary Table 4.

Discussion

In the present study, lung cancer has been identified as a systemic malignancy that is associated with both the humoral response directed against neural antigens, as well as with changes of cytotoxicity markers expression on peripheral

Table 2. The expression of Granzyme B in peripheral blood mononuclear cells

Studied group	Studied subgroup	Granzyme B [pg/mg of protein]	p
Lung cancer patients (n = 31)	Total (n = 31)	1,839 1,150–3,213	p = 0.8965
	PNS (n = 17)	1,824 1,265–2,640	p = 0.7297
	No PNS (n = 14)	1,958 1,001–3,740	
	Well-defined antibodies (n = 8)	1,580 930–2,640	p = 0.8430
	Seronegative (n = 15)	1,708 1,177–2,184	
Other cancer patients (n=12)	Total (n = 12)	1,961 1,432–2,576	p = 0.8124
	PNS (n = 8)	1,959 1,284–2,741	
	No PNS (n = 4)	1,895 1,332–2,628	
	Well-defined antibodies (n = 5)	1,936 1,302–2,766	p = 0.8344
	Seronegative (n = 6)	1,961 1,268–2,716	
All patients (n=52)	PNS manifestation (n = 31)	1,895 1,304–2,606	p = 0.8481
	Without PNS symptoms (n = 21)	1,958 1,116–2,922	
Antibodies	1. Well-defined onconeural antibodies (n = 15)	1,936 1,268–2,594	1 vs 2: p = 0.6639 1 vs 3: p = 0.7328
	2. Other autoantibodies (n = 15)	1,942 1,167–3,612	2 vs 3: p = 0.5929 (1+2) vs 3: p = 0.9299
	3. Seronegative (n = 26)	1,839 1,292–2,791	

*Statistically significant difference

blood mononuclear cells. Onconeural antibodies are currently considered a diagnostic tool for the definitive recognition of PNS in general [1], and lung cancer patients in particular [2], but their role in PNS pathogenesis remains unclear. While for many years onconeural antibodies were not considered pathogenic [5], the discovery of clearly pathogenic antibodies directed against surface receptors (i.e. anti-NMDAR) has changed this perspective.

In this study, we observed well-defined onconeural antibodies, and even their coexistence in lung cancer patients. However, the expression of granzyme B, perforin and FasL in PBMCs did not differ between seropositive and seronegative patients. Such an observation suggests an independence of the humoral and the cellular immune response in lung cancer patients. The cytotoxic effects in host-tumour interactions leading to PNS play a particularly important role in the remote effects on the nervous system. Apoptosis and neurodegeneration triggered by mechanisms associated with cytotoxicity may be mediated by granzyme B, perforin and/or FasL. Mononuclear cells infiltrating dentate nucleus in paraneoplastic cerebellar degeneration express granzyme B [7].

Recently, an immunopathological study on autoimmune encephalitis, including cases of paraneoplastic origin, showed a higher CD8/CD3 ratio and a substantial collocation of neurons and T lymphocytes expressing granzyme B [19]. Based on the observed differences between immune reactions against intracellular antigens, Bien et al. suggested the crucial role of cytotoxic reaction mediated by T lymphocytes in cases where response against intracellular antigens was developed, while in autoimmune reaction against surface antigens the involvement of antibodies and complement takes place [19]. Cell specificity analysis revealed the existence of cytotoxic T lymphocytes aggressive towards HuD protein [20], which is an antigen expressed on both small cell lung cancer cells and neurons. One of the most common PNSs is Hu-syndrome that coexists with SLCC

Table 3. The expression of Perforin in peripheral blood mononuclear cells

Studied group	Studied subgroup	Perforin [pg/mg of protein]	p
Lung cancer patients (n = 31)	total (n = 31)	13365 3634–38240	p = 0.0606
	PNS (n = 17)	12633 3968–38949	p = 0.0404*
	no PNS (n = 14)	23480 3639–35426	
	well-defined antibodies (n = 8)	14097 9608–38578	p = 0.9788
	seronegative (n = 15)	11138 3220–37822	
Other cancer patients (n = 12)	total (n = 12)	29663 20336–35881	p = 0.7311
	PNS (n = 8)	27307 16753–35664	
	no PNS (n = 4)	23135 11625–35893	
	well-defined antibodies (n = 5)	24986 6997–35447	p = 0.7490
	seronegative (n = 6)	26587 12633–35881	
All patients (n = 52)	PNS manifestation (n = 31)	22707 7592–33451	p = 0.4669
	without PNS symptoms (n = 21)	24105 11078–37065	
Antibodies	1. well-defined onconeural antibodies (n = 15)	26620 12633–33143	1 *vs* 3: p = 0.7952 2 *vs* 3: p = 0.7892 1 *vs* 2: p = 0.9128 (1+2) *vs* 3: p = 0.7491
	2. other autoantibodies (n = 15)	23480 8925–39325	
	3. seronegative (n = 26)	21736 4754–35012	

*Statistically significant difference

and typically manifests as an encephalomyelitis or sensory neuronopathy associated with anti-Hu antibodies. Tumour infiltrating lymphocytes have also been shown to react specifically with HuD antigen [21]. However, in Hu-syndrome, two distinct functional forms of cytotoxic lymphocytes have been described. It appears that in the acute phase of paraneoplastic syndrome, specific immune cells release type 1 cytokines (tumour necrosis factor-alpha, interleukin-6, interleukin-17), which promote a cell-mediated cytotoxic response. On the other hand, in the chronic phase of the disease, lymphocytes instead produce type 2 cytokines (interleukin-4, interleukin-5, interleukin-13) that abate an anti-tumour cytotoxic reaction. This functional transition was thought to be related to cytokines released by the SCLC [22]. In experimental conditions, paraneoplastic cerebellar degeneration was associated with interplay between tumour necrosis factor-alpha and macrophage chemoattractant protein-1 [23]. Thus, it can be hypothesised that the initially aggressive cell-mediated immune response that triggered paraneoplastic syndrome was distorted by secretions released by the growing tumour.

Our study is in concordance with the above-mentioned observations, because in our cohort of lung cancer patients we have found both, antibodies against intracellular antigens (anti-Hu, anti-Ri, anti-amphiphysin, anti-Yo, anti-Ma/Ta) and up-regulated markers of cytotoxicity in PBMCs (namely FasL). However, in our cohort the spectrum of cytotoxicity markers differs from some other studies. Bernal et al. (2002) did not find Fas and FasL-positive cells in the infiltrates in anti-Hu-associated paraneoplastic encephalomyelitis [24]. Similarly, Tüzün et al. (2009) observed only rare cells with granzyme B, perforin and Fas/Fas ligand expression in ovarian teratoma patients with NMDA-encephalitis [25]. One possible explanation for such discrepancies could be that the patient groups differed in terms of the underlying malignancy, clinical manifestation, and associated antibodies. This may confirm the hypothesis of different pathomechanisms involved in PNS depending on target antigens in autoimmune response.

Table 4. Clinical and immunological characteristics of each individual patient with paraneoplastic neurological syndrome in the study cohort

	Sex	Age	Type of malignancy	Neurological syndrome	PNS (1 - yes, 0 - no)	Onconeural antibody	well characte-rised (1 - yes, 0 - no)	FasL [pg/mg of protein]	Granzyme [pg/mg of protein]	Perforin [pg/mg of protein]
1	F	56	SCLC	Polyneuropathy	1	Anti-Ri, anti-myelin	1	0.115	1,242.580	12,633.078
2	F	46	SCLC	None	0	Anti-myelin	0	0.021	3,627.713	23,480.211
3	F	60	SCLC	Sensory Polyneuropathy	1	None	0	0.023	1,332.100	23,135.136
4	M	65	NSCLC, adenocarcinoma	None	0	Anti-myelin	0	0.021	4,077.149	27,306.679
5	M	64	NSCLC, adenocarcinoma	None	0	Anti-MAG	0	0.010	5,604.870	84,852.121
6	F	55	NSCLC, adenocarcinoma	Sensory Polyneuropathy	1	Anti-MAG	0	11.732	1,941.736	8,186.737
7	F	66	NSCLC, adenocarcinoma	None	0	None	0	13.307	2,861.381	32,612.500
8	M	73	NSCLC, squamous cell lung carcinoma	Sensory Polyneuropathy	1	Anti-Ma/Ta, Anti-Hu	1	0.010	4,053.088	22,706.826
9	M	60	NSCLC, squamous cell lung carcinoma	None	0	Anti-Tr	1	0.046	1,579.724	43,868.208
10	M	68	NSCLC, squamous cell lung carcinoma	Polyneuropathy	1	Anti-myelin	0	0.061	3,564.162	69,232.846
11	M	71	NSCLC	Cerebellar syndrome (PCD)	1	None	0	0.028	4,055.793	53,452.626
12	M	67	NSCLC	None	0	None	0	12.012	4,962.908	100,975.176
13	F	56	NSCLC (adenocarcinoma. bronchiolo--alveolar carcinoma)	None	0	None	0	8.321	1,957.548	24,104.858
14	M	65	SCLC	Polyneuropathy	1	Anti-Hu, anti--amphiphysin	1	13.905	2,628.593	44,220.834
15	F	79	SCLC	None	0	None	0	11.376	832.156	10,895.106
16	F	46	SCLC	None	0	Anti-myelin	0	20.166	1,056.799	11,138.486
17	M	54	NSCLC, large cell lung carcinoma	None	0	Anti-MAG	0	0.021	2,174.901	3,912.751
18	M	71	NSCLC	Cerebellar syndrome (PCD)	1	None	0	11.139	1,853.636	5,807.010
19	F	74	NSCLC, squamous cell lung carcinoma	None	0	None	0	11.732	84.882	1,647.467
20	M	63	Squamous cell lung carcinoma	Polyneuropathy	1	None	0	22.325	1,824.257	1,935.924
21	F	57	Lung adenocarcinoma	MND	1	Anti-MAG	0	13.307	776.313	498.359
22	F	40	Lung adenocarcinoma	None	0	None	0	8.549	293.349	687.356
23	M	61	NSCLC	None	0	None	0	11.480	1,291.789	2,818.571
24	M	65	NSCLC	None	1	Anti-Ri	1	x	x	x
25	F	57	No malignancy identified	Polyneuropathy	1	Anti-Yo	1	16.459	1,936.289	28,916.707
26	M	73	No malignancy identified	Myasthenic syndrome	1	Anti-Ma/Ta, anti-Ri, anti-amphiphysin, anti-myelin	1	5.728	1,276.509	27,372.811

Table 4. cd. Clinical and immunological characteristics of each individual patient with paraneoplastic neurological syndrome in the study cohort

	Sex	Age	Type of malignancy	Neurological syndrome	PNS (1 - yes, 0 - no)	Onconeural antibody	well characterised (1 - yes, 0 - no)	FasL [pg/mg of protein]	Granzyme [pg/mg of protein]	Perforin [pg/mg of protein]
27	M	82	NSCLC, squamous cell lung carcinoma	Polyneuropathy	1	None	0	12.188	1,707.761	70,424.531
28	F	54	Ovarian cancer	Cerebellar syndrome (PCD)	1	Anti-Tr, anti--amphiphysin	1	0.025	x	59,777.031
29	F	59	Ovarian cancer	None	1	Anti-Ri, anti-amphiphysin, anti-Ma/Ta	1	0.016	2,546.217	30,409.217
30	F	60	Ovarian cancer	Polyneuropathy	1	None	0	0.017	2,410.973	22,623.438
31	F	58	No malignancy identified	Polyneuropathy	0	None	0	8.193	2,554.212	20,303.411
32	F	74	Unidentified middle ear carcinoma	Movement disorder	0	Anti-myelin	0	0.021	1,498.024	40,472.876
33	F	53	Ovarian cancer	Cerebellar syndrome (PCD)	1	None	0	0.007	2,690.271	34,374.682
34	F	59	Ovarian cancer	None	0	Ma	1	8.087	1,409.857	5,455.177
35	M	71	No malignancy identified	None	0	Anti-myelin	0	7.026	1,767.929	18,473.667
36	F	56	Ovarian cancer	None	0	None	0	0.014	3,269.178	35,012.063
37	F	56	Ovarian cancer	None	0	None	0	0.006	2,942.212	32,237.117
38	F	72	Uncharacterized lung carcinoma	Polyneuropathy	1	Anti-Hu	1	6.457	571.380	14,097.272
39	F	74	No malignancy identified	Extrapyramidal syndrome	0	None	0	0.005	1,961.048	20,336.313
40	M	76	Prostate cancer	MND	1	None	0	0.035	1,649.618	16,178.975
41	F	52	No malignancy identified	Polyneuropathy	0	None	0	0.046	x	22,308.114
42	F	47	Ovarian cancer	Polyneuropathy	1	Amphiphysin	1	16.459	2,583.096	33,143.388
43	F	62	Ovarian cancer	Cerebellar syndrome	1	Anti-Yo	1	0.024	2,344.540	25,866.552
44	M	49	Lung carcinoma	None	0	None	0	0.007	2,791.262	35,928.829
45	F	51	Lung carcinoma	Myasthenic syndrome	1	Anti-Hu, anti-myelin	1	0.067	825.835	8,600.255
46	F	51	Lung carcinoma	Myasthenic syndrome	1	Anti-Hu, anti-myelin	1	0.023	2,644.582	0.000
47	F	77	No malignancy identified	Neuropathy	0	Anti-myelin	0	0.060	671.414	35,881.237
48	F	54	No malignancy identified	None	0	None	0	0.029	848.222	102,962.118
49	M	86	Prostate cancer	Polyneuropathy	1	None	0	0.013	1,034.246	4,753.848
50	F	54	Carcinoma solidum of the lung	Cerebellar syndrome	1	None	0	0.017	1,640.127	3,354.361
51	F	35	No malignancy identified	Myopathy	0	None	0	0.089	x	41,252.860
52	F	66	NSCLC, squamous cell lung carcinoma	Polyneuropathy	1	None	0	x	x	x

SCLC – small cell lung carcinoma; NSCLC – non-small cell lung carcinoma; PNS – paraneoplastic neurological syndrome; F – female; M – male

Interestingly, we confirmed that gender has an influence on PBMC expression of granzyme B and perforin in lung cancer patients. This observation requires further investigation and confirmation on a larger sample.

We expected to find increased levels of immune cytotoxicity markers in lung cancer patients with PNS, compared to those without neurological involvement. Neuronal destruction observed in the course of paraneoplastic syndromes could be driven by direct cytotoxic effects of immune cells activated in response to the tumour. In this case, the overexpression of immune cell-FasL, which enhances target (nervous system) cell elimination via interaction with Fas, and overexpression of membranolytic proteins (granzyme B and perforin), could reflect the role of cellular response in PNS pathophysiology. We did not manage to confirm this hypothesis. However, we must acknowledge that our study is limited by a relatively small sample size and the marked heterogeneity of our study cohort. It would be worthwhile to assess and compare cytotoxicity markers expression in larger and more focused cohorts, for example between cohorts with different antibody profiles (ant-Hu, anti-amphiphysin etc.) or larger samples of different malignancies.

It should be emphasised that in nine patients who were included in the study cohort, no malignancies were identified. However, according to the 2004 Graus criteria [1], when malignancy is not detected, it is still possible to diagnose a paraneoplastic syndrome. In fact, for definitive PNS, a neurological syndrome (classical or not) with well characterised onconeural antibodies (anti-Hu, Yo, CV2, Ri, Ma2, or amphiphysin) and no cancer, is considered paraneoplastic. For possible PNS, the criteria name two situations: a classical syndrome with no onconeural antibodies, no cancer, but at high risk of having an underlying tumour; or a neurological syndrome (classical or not) with partially characterised onconeural antibodies and no cancer.

In summary, ours is a preliminary study showing that lung cancer patients manifested a broader spectrum of coexisting autoantibodies than other patients with PNS in our cohort, namely patients with other malignancies and without any identified malignancy. FasL expression in PBMC is up--regulated in lung cancer patients. The interplay between granzyme B and FasL may be involved in the development of PNS at the level of the peripheral and central nervous systems in different manners.

Clinical implications and future directions

The novel findings that we report broaden the current knowledge regarding PNS pathomechanism with aspects that have not been previously explored. However, our study is preliminary and needs further research. Firstly, it would be valuable to verify protein expression by other methods, i.e. PCR or flow cytometry. Secondly, measurement of protein levels in particular lymphocytic populations, and not just in total PBMCs, could aid in the interpretation of the results. Importantly, in this study we did not include data with regards to treatment and response to therapy, so we could not analyse the prognostic aspect of our findings.

However, the purpose of this article was to provide an insight into the pathophysiology of PNS and to assess the potential diagnostic value of the proposed markers. For future studies, it would be interesting to investigate the prognostic value of the proposed markers as well.

Conflict of interest statement: *The authors declare no conflict of interest.*

Funding: *Not applicable (no external funding was provided for the study).*

References

1. Graus F, Delattre JY, Antoine JC, et al. Recommended diagnostic criteria for paraneoplastic neurological syndromes. J Neurol Neurosurg Psychiatry. 2004; 75(8): 1135–1140, doi: 10.1136/jnnp.2003.034447, indexed in Pubmed: 15258215.
2. Stefens-Stawna P, Piorunek T, Gabryel-Batura H, et al. Neurological paraneoplastic syndromes in lung cancer patients. Adv Exp Med Biol. 2013; 756: 333–339, doi: 10.1007/978-94-007-4549-0_40, indexed in Pubmed: 22836651.
3. Albert ML, Darnell RB. Paraneoplastic neurological degenerations: keys to tumour immunity. Nat Rev Cancer. 2004; 4(1): 36–44, doi: 10.1038/nrc1255, indexed in Pubmed: 14708025.
4. Darnell RB, DeAngelis LM. Regression of small-cell lung carcinoma in patients with paraneoplastic neuronal antibodies. Lancet. 1993; 341(8836): 21–22, indexed in Pubmed: 8093269.
5. Tanaka M, Tanaka K, Onodera O, et al. Trial to establish an animal model of paraneoplastic cerebellar degeneration with anti-Yo antibody. Clinical Neurology and Neurosurgery. 1995; 97(1): 95–100, doi: 10.1016/0303-8467(95)00005-5.
6. Blumenthal DT, Salzman KL, Digre KB, et al. Early pathologic findings and long-term improvement in anti-Ma2-associated encephalitis. Neurology. 2006; 67(1): 146–149, doi: 10.1212/01.wnl.0000223647.83708.20, indexed in Pubmed: 16832096.
7. Aye MM, Kasai T, Tashiro Y, et al. CD8 positive T-cell infiltration in the dentate nucleus of paraneoplastic cerebellar degeneration. J Neuroimmunol. 2009; 208(1-2): 136–140, doi: 10.1016/j.jneuroim.2009.01.017, indexed in Pubmed: 19217169.
8. Psimaras D, Carpentier AF, Rossi C, et al. PNS Euronetwork. Cerebrospinal fluid study in paraneoplastic syndromes. J Neurol Neurosurg Psychiatry. 2010; 81(1): 42–45, doi: 10.1136/jnnp.2008.159483, indexed in Pubmed: 19324868.
9. Metkar SS, Menaa C, Pardo J, et al. Human and mouse granzyme A induce a proinflammatory cytokine response. Immunity. 2008; 29(5): 720–733, doi: 10.1016/j.immuni.2008.08.014, indexed in Pubmed: 18951048.
10. Bolitho P, Voskoboinik I, Trapani JA, et al. Apoptosis induced by the lymphocyte effector molecule perforin. Curr Opin Immunol. 2007; 19(3): 339–347, doi: 10.1016/j.coi.2007.04.007, indexed in Pubmed: 17442557.
11. Cullen SP, Brunet M, Martin SJ. Granzymes in cancer and immunity. Cell Death Differ. 2010; 17(4): 616–623, doi: 10.1038/cdd.2009.206, indexed in Pubmed: 20075940.

12. Wang LF, Wang F, Li JT, et al. Ectopically expressed perforin-1 is proapoptotic in tumor cell lines by increasing caspase-3 activity and the nuclear translocation of cytochrome C. PLoS One. 2012; 7(7): e40639, doi: 10.1371/journal.pone.0040639, indexed in Pubmed: 22829880.
13. Scaffidi C, Fulda S, Srinivasan A, et al. Two CD95 (APO-1/Fas) signaling pathways. EMBO J. 1998; 17(6): 1675–1687, doi: 10.1093/emboj/17.6.1675, indexed in Pubmed: 9501089.
14. Maher S, Toomey D, Condron C, et al. Activation-induced cell death: the controversial role of Fas and Fas ligand in immune privilege and tumour counterattack. Immunol Cell Biol. 2002; 80(2): 131–137, doi: 10.1046/j.1440-1711.2002.01068.x, indexed in Pubmed: 11940113.
15. Rieux-Laucat F, Le Deist F, Hivroz C, et al. Mutations in Fas associated with human lymphoproliferative syndrome and autoimmunity. Science. 1995; 268(5215): 1347–1349, indexed in Pubmed: 7539157.
16. Wada A, Tada Y, Kawamura K, et al. The effects of FasL on inflammation and tumor survival are dependent on its expression levels. Cancer Gene Ther. 2007; 14(3): 262–267, doi: 10.1038/sj.cgt.7701008, indexed in Pubmed: 17053813.
17. Niehans GA, Brunner T, Frizelle SP, et al. Human lung carcinomas express Fas ligand. Cancer Res. 1997; 57(6): 1007–1012, indexed in Pubmed: 9067260.
18. LOWRY OH, ROSEBROUGH NJ, FARR AL, et al. Protein measurement with the Folin phenol reagent. J Biol Chem. 1951; 193(1): 265–275, indexed in Pubmed: 14907713.
19. Bien CG, Vincent A, Barnett MH, et al. Immunopathology of autoantibody-associated encephalitides: clues for pathogenesis. Brain. 2012; 135(Pt 5): 1622–1638, doi: 10.1093/brain/aws082, indexed in Pubmed: 22539258.
20. Tanaka M, Maruyama Y, Sugie M, et al. Cytotoxic T cell activity against peptides of Hu protein in anti-Hu syndrome. J Neurol Sci. 2002; 201(1-2): 9–12, indexed in Pubmed: 12163187.
21. Szabo A, Dalmau J, Manley G, et al. HuD, a paraneoplastic encephalomyelitis antigen, contains RNA-binding domains and is homologous to Elav and Sex-lethal. Cell. 1991; 67(2): 325–333, indexed in Pubmed: 1655278.
22. Roberts WK, Deluca IJ, Thomas A, et al. Patients with lung cancer and paraneoplastic Hu syndrome harbor HuD-specific type 2 CD8+ T cells. J Clin Invest. 2009; 119(7): 2042–2051, doi: 10.1172/JCI36131, indexed in Pubmed: 19509467.
23. Michalak S, Wender M, Michałowska-Wender G. Cachexia--induced cerebellar degeneration: involvement of serum TNF and MCP-1 in the course of experimental neoplastic disease. Acta Neurobiol Exp (Wars). 2006; 66(2): 113–122, indexed in Pubmed: 16886721.
24. Bernal F, Graus F, Pifarré A, et al. Immunohistochemical analysis of anti-Hu-associated paraneoplastic encephalomyelitis. Acta Neuropathol. 2002; 103(5): 509–515, doi: 10.1007/s00401-001-0498-0, indexed in Pubmed: 11935268.
25. Tüzün E, Zhou L, Baehring JM, et al. Evidence for antibody-mediated pathogenesis in anti-NMDAR encephalitis associated with ovarian teratoma. Acta Neuropathol. 2009; 118(6): 737–743, doi: 10.1007/s00401-009-0582-4, indexed in Pubmed: 19680671.

ORIGINAL ARTICLE

Neurologia i Neurochirurgia Polska
Polish Journal of Neurology and Neurosurgery
2019, Volume 53, no. 3, pages: 227–237
DOI: 10.5603/PJNNS.a2019.0024

ISSN 0028–3843

Multiparametric MRI in differentiating solitary brain metastasis from high-grade glioma: diagnostic value of the combined use of diffusion-weighted imaging, dynamic susceptibility contrast imaging, and magnetic resonance spectroscopy parameters

Kerim Aslan[1], Hediye Pinar Gunbey[2], Leman Tomak[3], Lutfi Incesu[1]

[1]Department of Radiology, Ondokuz Mayis University Faculty of Medicine, Samsun, Turkey
[2]Department of Radiology, Health Sciences University Kartal Lütfi Kırdar Training and Research Hospital, Istanbul, Turkey
[3]Department of Biostatistics, Ondokuz Mayis University Faculty of Medicine, Samsun, Turkey

This study was presented at the 26th Scientific Congress of the Turkish Neuroradiology Society, 17-19 February, 2017 in Istanbul, Turkey.

Abstract

Objective. The purpose of this study was to determine whether the combined use of diffusion weighted imaging (DWI), magnetic resonance spectroscopy (MRS), and dynamic susceptibility contrast imaging (DSCI) parameters could provide a more accurate diagnosis in the differentiation of high-grade glioma (HGG) from solitary brain metastasis (SBM) in the enhancing tumour and in the peritumoural region.

Materials and methods. Fifty-six patients who received DWI, DSCI, and MRS before surgery were assessed. In differentiating SBM from HGG, the cutoff values of the DWI-apparent diffusion coefficient (ADCmin, ADCmax, and ADCmean), DSCI-relative cerebral blood volume (rCBV), and MRS-Cho/Cr, Cho/NAA, and NAA/Cr parameters for the peritumoural region were determined with ROC. The combined ROC curve was used for the different combinations of the peritumoural region DWI, DSCI, and MRS parameters in differentiating between the two tumours, and the best model combination was formed.

All procedures performed in studies involving human participants were in accordance with the ethical standards of the institutional research committee and with the 1964 Helsinki Declaration and its later amendments. This study was approved by the Institutional Review Board at our institutes.

Results. In the enhancing tumour, all the parameters except NAA/Cr ($P = 0.024$) exhibited no statistical difference in differentiating between these two groups ($P > 0.05$). AUC values for ADCmin, ADCmax, ADCmean, rADCmin, rADCmax, rADCmean, rCBV, Cho/Cr, Cho/NAA, and NAA/Cr parameters in the peritumoural region in differentiating SBM from HGG were 0.860, 0.822, 0.848, 0.822, 0.801, 0.822, 0.906, 0.851, 0.903, and 0.784, respectively. In differentiating HGG from SBM, the best model consisted of the combination of peritumoural ADCmin, rCBV, and Cho/NAA parameters. AUC values were 0.970.

Conclusions. The combination of peritumoural region ADCmin, rCBV, and Cho/NAA parameters can help in differentiating SBM from HGG, with a diagnostic accuracy of 97%.

Key words: Solitary brain metastasis, high-grade glioma, diffusion-weighted imaging, dynamic susceptibility contrast imaging, magnetic resonance spectroscopy

(*Neurol Neurochir Pol 2019; 53 (3): 227–237*)

Address for correspondence: Kerim Aslan, Ondokuz Mayis University Faculty of Medicine, Department of Radiology, Kurupelit/Samsun, Turkey; e-mail: mdkerim@hotmail.com, tel.: +90362 3121919- 2541, fax: +903624576041

Introduction

High-grade glial (HGG) tumours and brain metastases are the most frequently diagnosed brain tumours in adults. In the diagnosis of brain metastasis, primary malignancy history, multiple lesions, and the combined localisation of grey–white substance are helpful. However, in patients with primary malignancy, HGG can occur and can sometimes be multiple. In almost 30% of extracranial malignancies, the first manifestation of the disease can be solitary brain metastasis (SBM) [1, 2]. As SBM and HGG usually have similar signal intensities and contrasting patterns in conventional magnetic resonance imaging (MRI), MRI can be inadequate in differentiating between these two tumours [3, 4]. Treatment planning, follow up, and prognosis are different between SBM and HGG. In patients with malignancy, an enhancing brain lesion may not only be treated by surgical resection but also by radiotherapy since such a lesion may often be judged to be a metastasis without a histopathological assessment. In such cases, image-based differentiation could play an important role in the treatment choice. Therefore, reliable imaging is important in differentiating between these two tumours.

Whereas HGG has infiltrative neoplastic cells in the peritumoural oedema, the peritumoural region of SBM is characterised by vasogenic oedema depending on the increase in capillary permeability. Therefore, determining these changes in the peritumoural region is crucial in differentiating HGG from SBM. Apart from conventional MRI, advanced MR imaging modalities such as diffusion-weighted MRI (DWI), MR spectroscopy (MRS), and dynamic susceptibility perfusion MRI (DSCI) are used to identify these changes in the peritumoural region by providing quantitative measurements. Apparent diffusion coefficient (ADC) obtained from DWI provides information on the cellularity of the tissue by measuring independently from the direction of the total magnitude of water diffusion in the tissue. Some studies have shown that low ADC values are associated with high cellularity in the peritumoural region in HGG compared to SBM [5–14] Suh et al. [15] reported that DWI and diffusion tensor imaging (DTI) demonstrated a moderate diagnostic performance for the differentiation of high-grade glioma from solitary brain metastasis. Choline (Cho) metabolite in MRS reflects cellular density and the rate of cellular membrane turnover. Studies on MRS have shown increases in Cho/creatine (Cr) and Cho/N-acetyl aspartate (NAA) in the peritumoural region infiltration in HGG tumours, and reported that these increases could be used in differentiating them from metastases [16–20]. The relative cerebral blood volume (rCBV) obtained from DSCI provides a quantitative assessment of neovascularisation based on the tumour infiltration in the peritumoural region. Some studies have indicated that the high rCBV values associated with neovascularisation in the peritumoural region in HGG could be useful in differentiating between these two tumours [21–25]. Suh et al. [26] reported that perfusion MRI shows high diagnostic performance in differentiating glioma from brain metastasis.

Some studies have used advanced MR modalities in differentiating SBM from HGG [27–31]. However, none of these works examined the difference between SBM and HGG by using a combination of these modalities. Recently, researchers have examined the uses of different combinations of advanced MRI techniques in differentiating between these two tumours. Some of these studies have shown that the combinations of diffusion and perfusion parameter measurements could be helpful in differentiating between these two tumours [32–35]. Tsolaki et al. [36] combined MRS and perfusion techniques with machine learning methods in differentiating between glioblastomas and solitary metastases, and reported that they provided additional diagnostic information in definitive diagnosis. Mouthuy et al. [37] showed that multimodal MRI parameters (perfusion–rCBV, texture parameter contrast, and sum average) could be useful in differentiating between SBM and HGG. Tsougos et al. [38] reported that the MRS and DSCI measurements of the peritumoural region could help differentiate between glioblastomas and metastases, whereas diffusion parameters could not statistically differentiate between the two lesions.

The purpose of this study was to determine whether the combined use of the DWI [minimum (ADCmin), mean (ADCmean), and maximum (ADCmax) ADC and minimum (rADCmin), mean (rADCmean), and maximum (rADCmax) ADC ratio], MRS (Cho/Cr, Cho/NAA, and NAA/Cr) and DSCI (rCBV) parameters could provide a more accurate diagnosis in differentiating SBM from HGG in the enhancing tumour and in the peritumoural region. Our purpose was also to reveal the diagnostic accuracy of both parameters in differentiating between these two tumours.

Materials and methods

Patients

This study was approved by the local ethics committee of our institution (OMÜ KAEK 2017/153). Preoperative MRI and clinical records of 86 consecutive patients who were referred to our hospital between March 2012 and December 2016 and who were diagnosed with brain metastasis and HGG histopathological were examined retrospectively. Several patients were excluded: two patients who had pre-resection stereotactic biopsy, two patients who had been treated, 11 patients who did not have a solitary lesion (HGG, n = 2 and BM, n = 9), four patients who did not have a peritumoural oedema in the lesion, and five patients who did not receive DWI, DSCI, and MRS. Patients with a lesion size smaller than 2 cm were also excluded from the study (n = 6). So eventually, 56 patients who did not receive pre-resection stereotactic biopsy and treatment, who had a solitary enhancing brain tumour and peritumoural oedema, and who received conventional

brain MRI, DWI, MRS, and DSCI were included in the study. The final diagnosis included 39 HGG (19 men, 20 women; mean age: 61.2 ± 10.5 years; range: 37–81 years) and 17 SBM (nine men, eight women; mean age: 61.0 ± 13.8 years; range: 29–83 years).

In 39 patients, the tumours were classified as HGG, including 11 with World Health Organisation (WHO) grade III (eight anaplastic astrocytoma and three anaplastic oligodendrogliomas) and 28 with WHO grade IV (glioblastomas) according to the WHO criteria. Metastatic brain tumours included lung carcinoma (n = 9), breast carcinoma (n = 3), melanoma (n = 1), renal carcinoma (n = 1), colon carcinoma (n = 1), ovarian carcinoma (n =1), and carcinoma of unknown origin (n = 1).

MR image acquisition

MRI imaging was performed using a 1.5-T scanner (Gyroscan Intera, Philips Healthcare, Best, the Netherlands) with an eight-channel head coil. Conventional MR imaging sequences, DWI, DSCI, and multivoxel MRS imaging were performed on all patients. Conventional MRI protocols included pre-contrast axial T1-weighted sequence (repetition time [TR]/echo time [TE]: 450/15 ms; slice thickness: 5 mm; field of view [FOV]: 230 mm; matrix: 256 × 163; number of excitations [NEX]: 2; intersection gap: 1 mm), axial T2-weighted sequence (TR/TE: 4,443/100 ms; section thickness: 5 mm; FOV: 230 mm; matrix: 384 × 240; NEX: 3; intersection gap: 1 mm), coronal fluid attenuation inversion recovery (TR/TE/TI: 8,000/140/2,800 ms; section thickness: 5 mm; FOV: 230 mm; matrix: 224 × 148; NEX: 2; intersection gap: 0.4 mm), sagittal T2-weighted sequence (TR/TE: 4,027/100 ms; section thickness: 5 mm; FOV: 230 mm; matrix: 236 × 205; NEX: 2; intersection gap: 1 mm).

DWI was performed with a single-shot spin-echo EPI (TR/TE: 3,376/74 ms; section thickness: 5 mm; FOV: 230 mm; matrix: 128 × 128; NEX: 2; intersection gap: 1 mm; b values: 0 and 1,000 s/mm^2).

DSCI was conducted using a single-shot spin-echo EPI sequence (TR/TE: 1,524/40 ms; section thickness: 5 mm; FOV: 230 mm; matrix: 128 × 128; NEX: 2; no gap; voxel size: 2.0 mm x 2.0 mm x 5.0 mm). All of the patients were given intravenous gadobutrol (0.05 mmol/kg, 1.0 mmol/mL, Gadovist; Bayer Schering Pharma, Berlin, Germany) in a preloading dose to decrease pre-dynamic imaging contrast agent leakage. DSCI was performed during the first pass of the standard dose (0.1 mmol/kg) bolus of an intravenous contrast agent (gadobutrol). The injection rate was 5 mL/s for all patients and was followed by a 20mL flush of saline at the same rate given through a power injector. Following the contrast injection, a post-contrast 3D T1-weighted sequence was performed (TR/TE: 500/4 ms; NEX: 1; slice thickness: 1 mm; no gap; in-plane resolution: 1 mm; FOV: 240 mm; voxel size: 1.0 mm x 1.0 mm x 1.0 mm).

MRS was conducted after contrast injection in all patients. For MRS imaging, a 3D multivoxel PRESS sequence was performed (automatic shimming and Gaussian water suppression; TR/TE: 988/144 ms; section thickness: 5 mm; FOV: 180 x 160 mm; matrix: 180 x 160; NEX: 2). The volume of interest (VOI) was chosen from the tumour, peritumoural region, and contralateral normal-appearing white matter, avoiding the scalp, skull base, and the sinuses. Saturation slabs were placed outside the VOI to suppress lipid signals from the scalp. VOI position was determined by examining the MR images in three plans (sagittal, coronal, and transverse). The size of the VOI differed according to the sizes of the lesions, and the most frequent was 80 x 80 mm. The voxel size was 10 × 10 × 10–15 mm.

Image analysis

All conventional MRI, DWI, DSCI, and MRS datasets were transferred to an independent workstation (IntelliSpace, software version v6.0.4.03700, Philips). Two neuroradiologists (K.A. and H.P.G., both with six years of experience) were unaware of the clinical and pathological results of the patients, and were completely independent of each other in the measurement of the DWI (ADCmin, ADCmax, ADCmean, rADCmin, rADCmax, and rADCmean), DSCI (rCBV), and MRS (Cho/Cr, Cho/NAA, and NAA/Cr) parameters with the regions of interest (ROIs).

ADC maps were acquired from DWI. ROIs were drawn manually in round or oval shapes in solid portions by avoiding the cystic, necrotic and calcified areas of lesions from ADC maps. These areas were identified in T2-weighted and contrast-enhanced T1W images. The peritumoural region was defined as the 1 cm T2 and FLAIR hyperintense area outside the contrasted area. Circular ROIs, which were drawn at workstations manually to lesions from T2-weighted images, were placed automatically to lesions on ADC maps with the same localisation and size. The peritumoural and tumoural ADC ratios were calculated by dividing the average ADCmin, ADCmax, ADCmean values of the peritumoural area and contrasted solid tumour by the average normal white matter ADCmin, ADCmax, and ADCmean values.

The arterial input function was selected automatically, and the CBV maps were calculated using the block-circulant singular value decomposition technique for DSCI [39]. CBV maps were formed for analysis at the workstation from DSCI perfusion datasets. The CBV maps were then coregistered to contrast-enhanced 3D T1-weighted images for the enhancing tumour and T2-weighted images for the peritumoural region. For the CBV measurements, ROIs were manually drawn by avoiding cerebral blood vessels, calcifications, haemorrhage, and cerebrospinal fluid-filled sulci areas. ROIs were placed carefully on each selected section of the CBV maps, including the areas of the enhancing tumour and the peritumoural region, with the highest CBV determined by visual inspection. The CBV values for the enhancing tumour and the peritumoural region were calculated. The peritumoural and enhancing tumour rCBV was determined by dividing the

average CBV values of the peritumoural area and enhancing tumour by the average CBV values of the lesion level of the contralateral normal area.

The 3D multivoxel PRESS spectroscopic data analysis and the calculation of the metabolite ratios were conducted at the workstation. The post-processing steps, including the frequency shift, baseline correction phase correction, and peak fitting/analysis, were performed automatically. The spectra were automatically analysed for the relative signal intensities (areas under the fitted peaks in the time domain) of metabolites. The maximum values of Cho/Cr and Cho/NAA ratios and the minimum NAA/Cr ratios were obtained from the spectral maps of three localisations (enhancing tumour, peritumoural region, and normal appearing white matter). Cystic or necrotic, calcific, and haemorrhagic areas of the tumour were avoided when choosing the voxel. To minimise the partial volume effect, the voxel was chosen without including the neighbouring peritumoural region as much as possible for the enhancing tumour and for the peritumoural region without including the T2 and FLAIR hyperintensity outside the peritumoural area and the enhancing tumour.

Statistical analysis

Statistical analyses were performed using the Statistical Package for the Social Sciences (IBM SPSS Statistics version 21; IBM, Armonk, NY, USA). Data were presented as the mean (SD), median (min–max), or frequency (%). To identify the differences between SBM and HGG in the enhancing tumour and the peritumoural region, we used Student's t-test for normally distributed data (age, ADCmin, ADCmax, ADCmean, rADCmin, rADCmax, rADCmean, rCBV, Cho/Cr, Cho/NAA, and NAA/Cr). The frequencies were compared using the continuity correction $\chi 2$. AUC was evaluated as the measure of a diagnostic test's discriminatory power. For the differentiation between SBM and HGG in the peritumoural region, the optimum cutoff values of the DWI (ADCmin, ADCmax, ADCmean, rADCmin, rADCmax, and rADCmean), DSCI (rCBV), and MRS (Cho/Cr, Cho/NAA, and NAA/Cr) parameters were determined using the ROC curve. The combined ROC curves were used for the combination of the peritumoural region DWI, DSCI, and MRS parameters in differentiating between the two tumours. The sensitivity, specificity, positive predictive value (PPV), and negative predictive value (NPV) were also identified. The AUC was calculated for the ROC curve of each individual classifier and for the combined ROC curves. The best model combination was then formed. The inter-observer agreement between two readers was assessed using weighted Cohen κ statistics. A κ value of 0.4 or lower indicates poor agreement; 0.41–0.60, moderate agreement; 0.61–0.80, good agreement; and 0.81–1.0, excellent agreement. A P value < 0.05 was considered significant.

Results

Figures 1 and 2 present the samples of our multiparametric MRI in patients with HGG and SBM, respectively.

The ADCmin, ADCmax, ADCmean, rADCmin, rADCmax, and rADCmean values and the NAA/Cr rates of HGG in the peritumoural region were significantly lower than those of SBM ($P < 0.001$, $P < 0.001$, $P < 0.001$, $P < 0.001$, $P < 0.001$, $P < 0.001$, and $P = 0.009$, respectively), and the rCBV, Cho/Cr, and Cho/NAA rates were significantly higher ($P < 0.001$). However, in the enhancing tumour, all the parameters except NAA/Cr ($P = 0.024$) exhibited no statistical differences in differentiating between these two groups ($P > 0.05$). The quantitative values, which include the mean ± SD and median (min-max) of all the parameters (ADCmin, ADCmax, ADCmean, rADCmin, rADCmax, rADCmean, rCBV, Cho/Cr, Cho/NAA, and NAA/Cr) in the enhancing tumour and the peritumoural region, the statistical analyses, and the κ coefficient values are summarised in Table 1 (enhancing tumour) and Table 2 (peritumoural region).

Table 3 presents the cutoff, sensitivity, specificity, PPV, NPV, and AUC values for each parameter in the peritumoural region in differentiating SBM from HGG. Figures 3A, 3B, and 3C illustrate the ROC curve analysis results for all the parameters. Of all the parameters, rCBV had the highest individual distinctive power, with an AUC of 0.906.

Table 4 shows the sensitivity, specificity, PPV, NPV, and AUC values of the different combinations of DWI, DSCI, and MRS parameters used in differentiating SBM from HGG. Figure 4 illustrates the ROC curve analysis results for the combinations of the DWI, DSCI, and MRS parameters. In differentiating between these two tumours, any one of the model combinations (Fig. 4) was superior to using any individual DWI, DSCI, and MRS parameter (Fig. 3A, B). The best model in differentiating SBM from HGG was the combination of ADCmin, rCBV, and Cho/NAA parameters, and the sensitivity, specificity, PPD, NPD, and AUC values were 94.1%, 100%, 100%, 97.4%, and 0.970, respectively.

Discussion

Our study showed that the individual use of any of the peritumoural DWI, DSCI, and MRS parameters can help differentiate SBM from HGG. HGG was distinguished from SBM in the peritumoural region using the ROC analysis. Any model combination was found to be superior to any individual DWI, DSCI, and MRS parameter, and the best model was the combination of the peritumoural ADCmin, rCBV and Cho/NAA parameters, with an AUC of 0.970. Our results indicate that peritumoural DWI, DSCI, and MRS parameter combinations can better explain the following hypothesis: HGG is spread by infiltration into the peritumoural area, whereas peritumoural oedema is mainly composed of vasogenic oedema in metastases.

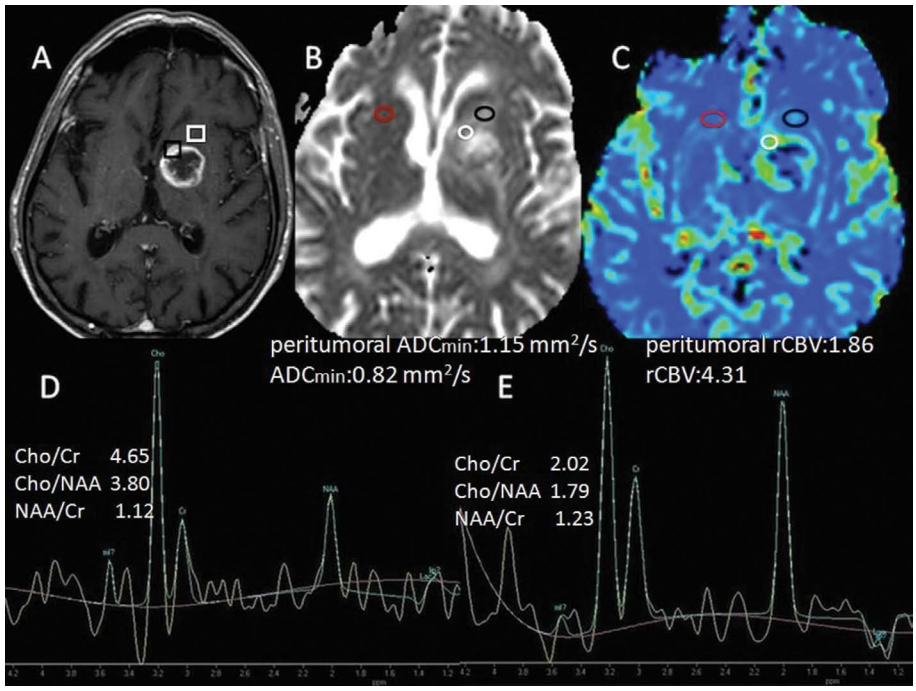

Figure 1. A 67 year-old male patient with pathologically confirmed glioblastoma. **A.** Contrast-enhanced T1-weighted image shows an irregular ring-like enhancement and a necrosis centralised mass in the left basal ganglion. Regions of interest localised in the enhancing tumour (white), peritumoural oedema (black), and contralateral white matter (red) are seen on the ADC map (B) and DSCI–CBV map (C). **B.** The ADC map shows low ADC values in the enhancing tumour and the peritumoural region, reflecting infiltrative oedema. The ADCmin, ADCmax, and ADCmean values for the enhancing tumour and the peritumoural region on the ADC map are 0.82, 1.07, and 0.96 × 10^{-3} mm^2/s and 1.15, 1.33, and 1.22 × 10^{-3} mm^2/s, respectively. **C.** The DSCI–CBV map shows increased rCBV (4.31 and 1.86, respectively) in the enhancing tumour and the peritumoural region, indicating infiltration. **D.** MRS (TE 144 ms) shows increased Cho/Cr (4.65 and 2.02, respectively) and Cho/NAA (3.80 and 1.79, respectively) and decreased NAA/Cr (1.12 and 1.23, respectively) in the enhancing tumour and the peritumoural region, indicating infiltration

The enhancing areas of both HGG and SBM are heterogeneous because of necrosis, haemorrhage, and vascular proliferation, and the normal parenchymal microstructure can be impaired. On the other hand, the peritumoural region is homogeneous because of the absence of necrosis and haemorrhage, and microstructural structure is relatively maintained [35, 40, 41]. In parallel with this, our results showed that in the enhancing tumour, all the parameters except NAA/Cr ($P = 0.024$) were not statistically different in differentiating HGG from SBM ($P > 0.05$).

DWI

The present study showed that the ADCmin, ADCmax, ADCmean, rADCmin, rADCmax, and rADCmean values of HGG in the peritumoural region are statistically low (for all ADC parameters, $P < 0.001$) compared to those of SBM, and these results are consistent with those of other studies [5-14]. Studies have reported that the peritumoural ADCmin values were superior to the ADCmax and ADCmean values in differentiating SBM from HGG [5, 13]. Similarly, our study found that the peritumoural ADCmin value (AUC:0.860) had greater diagnostic accuracy than the ADCmax (AUC:0.822), ADCmean (AUC:0.848), rADCmin (AUC:0.822), rADCmax (AUC:0.801), and rADCmean (AUC:0.822) values in differentiating SBM from HGG. In differentiating between these two tumours, sensitivity was 82.4%, specificity was 89.7%, PPV was 77.8%, and NPV was 92.1% when the peritumoural ADCmin cutoff value was 1.32. Only a few studies have reported that the peritumoural ADC values were not statistically different between HGG and SBM [10, 38].

Tumour ADC (min, max, and mean) and rADC (min, max, and mean) did not show a statistical difference between HGG and SBM in our study ($P > 0.05$). These results were in accordance with the results of previous studies reporting that tumour ADC values are not useful in differentiating SBM from HGG [5–9, 11, 12]. However, some studies have shown that tumoural ADC values could help to differentiate SBM from HGG [10, 14, 28, 33, 34]. The inconsistencies among studies that included ADC values in the differentiation between these two tumours could be secondary to the differences in the underlying tumour histology and different degrees of tumour heterogeneity in the contrasted area caused by necrosis, calcification, and haemorrhage. The results of this study support the hypothesis that peritumoural ADC values

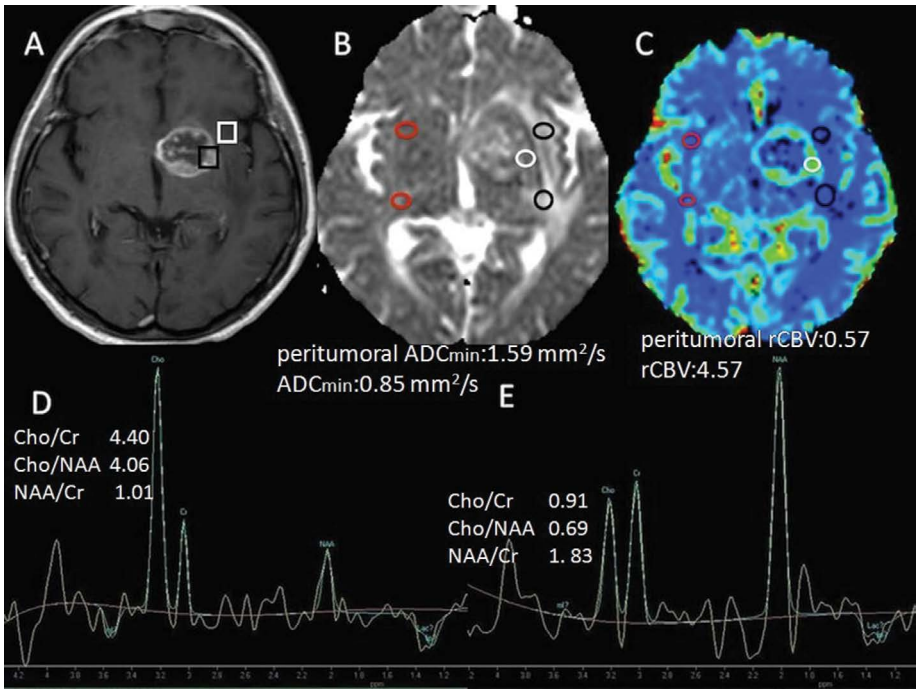

Figure 2. A 67 year-old male patient with pathologically confirmed pulmonary adenocarcinoma metastasis. **A.** Contrast-enhanced T1-weighted image shows an irregular ring-like enhancement and a necrosis centralised mass in the left basal ganglion. Regions of interest localised in the enhancing tumour (white), peritumoural oedema (black), and contralateral white matter (red) are seen on the ADC map (B) and the DSCI–CBV map (C). **B.** The ADC map shows low ADC values in the enhancing tumour but high ADC values in the peritumoural region, thus indicating vasogenic oedema. The ADCmin, ADCmax, and ADCmean values for the enhancing tumour and the peritumoural region on the ADC map are 0.85, 1.04, and 0.93 × 10^{-3} mm^2/s and 1.59, 1.76, and 1.64 × 10^{-3} mm^2/s, respectively. **C.** The DSCI–CBV map shows increased rCBV in the enhancing tumour but decreased rCBV in the peritumoural region, thus reflecting vasogenic oedema (4.57 and 0.57, respectively). **D.** MRS (TE 144 ms) shows increased Cho/Cr (4.40) and Cho/NAA (4.06) in the enhancing tumour and decreased Cho/Cr (0.91) and Cho/NAA (0.69) in the peritumoural region, thus reflecting vasogenic oedema, and decreased NAA/Cr (1.01 and 1.83, respectively) in both

Table 1. DWI, MRS, DSCI parameter values for the enhancing tumour in SBM and HGG

Parameter	Solitary Brain Metastasis		High-grade Glioma		p value	κ
	Mean ± SD	Median (min-max)	Mean ± SD	Median (min-max)		
ADCmin	0.83 ± 0.20	0.81 (0.56–1.31)	0.85 ± 0.15	0.82 (0.59–1.39)	> 0.05	0.856
ADCmax	1.08 ± 0.21	1.00 (0.82–1.62)	1.09 ± 0.16	1.05 (0.88–1.69)	> 0.05	0.911
ADCmean	0.95 ± 0.20	0.92 (0.70–1.42)	0.97 ± 0.15	0.94 (0.70–1.40)	> 0.05	0.814
rADCmin	1.16 ± 0.28	1.12 (0.78–1.81)	1.18 ± 0.21	1.13 (0.81–1.92)	> 0.05	0.713
rADCmax	1.37 ± 0.26	1.27 (1.04– 2.06)	1.38 ± 0.21	1.34 (1.11–2.15)	> 0.05	0.798
rADCmean	1.21 ± 0.26	1.17 (0.89–1.80)	1.24 ± 0.19	1.24 (0.89–1.78)	> 0.05	0.756
rCBV	3.68 ± 1.40	3.24 (1.88–7.41)	3.63 ± 1.40	3.29 (1.65–8.07)	> 0.05	0.895
Cho/Cr	4.42 ± 2.44	3.67 (1.57–11.26)	3.55 ± 1.71	3.12 (1.23–9.68)	> 0.05	0.969
Cho/NAA	3.15 ± 1.89	2.97 (0.77–8.11)	3.49 ± 1.77	3.03 (1.46–10.12)	> 0.05	0.971
NAA/Cr	1.48 ± 0.51	1.54 (0.44–2.51)	1.08 ± 0.49	1.01 (0.27–2.08)	= 0.024	0.922

*Except for the *p*-values, and κ coefficient (κ); minimum, maximum, and mean apparent diffusion coefficient (ADCmin, ADCmax, and ADCmean), cerebral blood volume (rCBV), Choline/creatine (Cho/Cr), Choline/N-acetyl aspartate (Cho/NAA), and N-acetyl aspartate/creatine (NAA/Cr)

Table 2. DWI, MRS, DSCI parameter values for the peritumoural region in SBM and HGG*

Parameter	Solitary Brain Metastasis		High-grade Glioma		p value	κ
	Mean ± SD	Median (min-max)	Mean ± SD	Median (min-max)		
ADCmin	1.47 ± 0.16	1.45 (1.17–1.78)	1.12 ± 0.18	1.11 (0.70–1.51)	< 0.001	0.926
ADCmax	1.61 ± 0.17	1.59 (1.27–1.90)	1.31 ± 0.22	1.30 (0.82–1.88)	< 0.001	0.872
ADCmean	1.52 ± 0.16	1.51 (1.19–1.81)	1.20 ± 0.21	1.19 (0.74–1.69)	< 0.001	0.894
rADCmin	1.85 ± 0.22	1.85 (1.44–2.26)	1.43 ± 0.25	1.41 (0.87–1.91)	< 0.001	0.764
rADCmax	2.05 ± 0.22	2.02 (1.62–2.42)	1.67 ± 0.28	1.65 (1.05–2.38)	< 0.001	0.685
rADCmean	1.93 ± 0.20	1.91 (1.51–2.30)	1.52 ± 0.28	1.51 (0.94–2.15)	< 0.001	0.712
rCBV	0.39 ± 0.18	0.39 (0.05–0.74)	1.14 ± 0.46	1.13 (0.47–2.53)	< 0.001	0.822
Cho/Cr	1.05 ± 0.21	1.05 (0.66–1.44)	1.79 ± 0.26	1.72 (0.88–2.68)	< 0.001	0.952
Cho/NAA	0.72 ± 0.21	0.69 (0.46–1.22)	1.72 ± 0.22	1.70 (1.46–2.54)	< 0.001	0.965
NAA/Cr	1.69 ± 0.51	1.67 (0.87–2.81)	1.26 ± 0.41	1.21 (0.63–2.47)	= 0.009	0.928

*Except for the *p*-values, and κ coefficient (κ); minimum, maximum, and mean apparent diffusion coefficient (ADCmin, ADCmax, and ADCmean), cerebral blood volume (rCBV), Choline/creatine (Cho/Cr), Choline/N-acetyl aspartate (Cho/NAA), and N-acetyl aspartate/creatine (NAA/Cr)

Table 3. Cutoff, sensitivity, specificity, PPV, NPV, and AUC values in differentiating between SBM and HGG in the peritumoural region with ROC

Parameter	Cutoff	Sensitivity	Specificity	PPV	NPV	AUC
ADCmin	1.32	82.4%	89.7%	77.8%	92.1%	0.860
ADCmax	1.48	82.4%	82.1%	66.7%	91.4%	0.822
ADCmean	1.44	82.4%	87.2%	73.7%	91.9%	0.848
rADCmin	1.67	82.4%	82.1%	66.7%	91.4%	0.822
rADCmax	1.86	82.4%	76.9%	60.8%	90.9%	0.801
rADCmean	1.79	82.4%	82.1%	66.7%	91.4%	0.822
rCBV	0.61	94.1%	87.2%	76.2%	97.1%	0.906
Cho/Cr	1.29	88.2%	82.1%	68.2%	94.1%	0.851
Cho/NAA	0.99	88.2%	92.3%	83.3%	94.7%	0.903
NAA/Cr	1.33	%82.4	74.4%	58.3%	90.6%	0.784

Area under the curve (AUC), minimum, maximum, and mean apparent diffusion coefficient (ADCmin, ADCmax, and ADCmean), cerebral blood volume (rCBV), Choline/creatine (Cho/Cr), Choline/N-acetyl aspartate (Cho/NAA), N-acetyl aspartate/creatine (NAA/Cr), positive predictive value (PPV), and negative predictive value (NPV)

Table 4. Sensitivity, specificity, PPV, NPV, and AUC values by using the combination of DWI, MRS, and DSCI parameters in differentiating between SBM and HGG in the peritumoural region with ROC

Models	AUC	Sensitivity	Specificity	PPV	NPV
ADCmin+ rCBV	0.932	94.1%	92.1%	84.2%	97.2%
ADCmin+ Cho/NAA	0.941	88.2%	100%	100%	95.0%
rCBV+ Cho/NAA	0.941	88.2%	100%	100%	95.0%
ADCmin+ rCBV +Cho/NAA	0.970	94.1%	100%	100%	97.4%

Area under the curve (AUC), minimum apparent diffusion coefficient (ADCmin), cerebral blood volume (rCBV), Choline/N-acetyl aspartate (Cho/NAA), positive predictive value (PPV), and negative predictive value (NPV)

can determine neoplastic cell infiltration in the peritumoural oedema in HGG.

CBV

In this study, rCBV was higher in the peritumoural region in HGG than that in SBM (peritumoural rCBV was 1.14 and 0.39 for HGG and SBM, respectively, P < 0.001). This result is similar to those in previous studies [21–25, 32]. In addition, no significant difference was found in the tumour rCBV values between HGG and SBM (tumoural rCBV was 3.63 and 3.68 for HGG and SBM, respectively, P = 0.151). This result is consistent with those in previous studies reporting that tumour rCBV values are not useful in differentiating SBM from HGG [21–25, 32, 33]. When the peritumoural rCBV cutoff

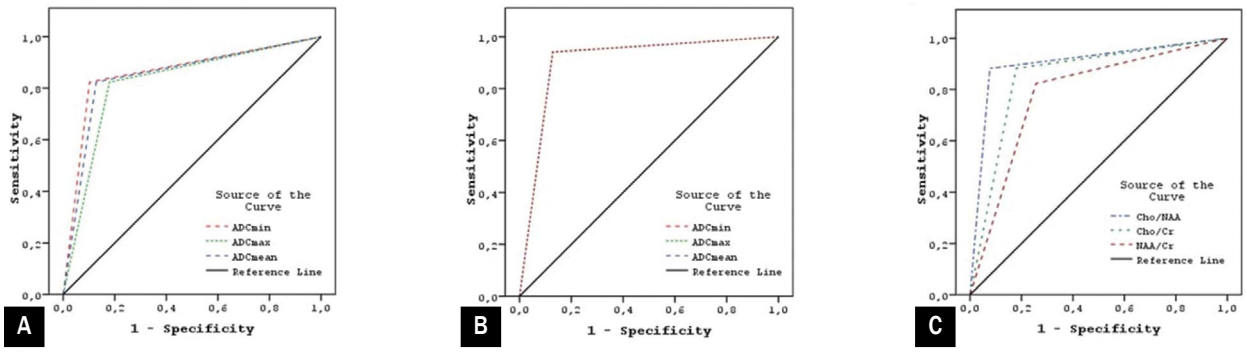

Figure 3. ROC analysis with AUC for each MR parameter when differentiating between SBM and HGG [AUC for DWI–ADCmin, ADCmax and ADCmean (**A**), DSCI–rCBV (**B**) and MRS–Cho/Cr, Cho/NAA, and NAA/Cr (**C**)]

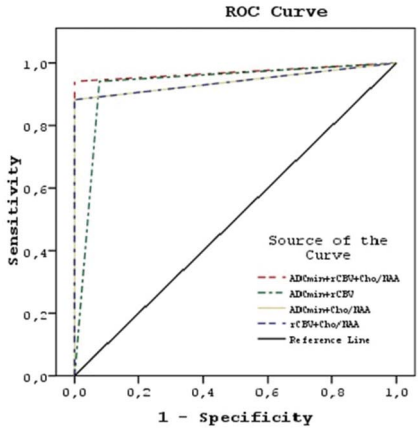

Figure 4. AUCs of different combinations of DWI, DSCI and MRS parameters in the peritumoural region with the ROC curve in differentiating SBM from HGG. The best model in differentiating between these two tumours was formed with the combination of ADCmin, rCBV, and Cho/NAA parameters

value was set to 0.61 in differentiating between these two tumours, sensitivity was 94.1%, specificity was 87.2%, PPV was 76.2%, and NPV was 97.1%. In differentiating between these two lesions, the highest individual power among all the parameters was rCBV, with an AUC of 0.906. Therefore, rCBV seems to be the best individual parameter to determine peritumoural invasion.

The rCBV rates, which are the biological indicator of angiogenesis obtained from peritumoural areas, showed pure vasogenic oedema in SBM despite exhibiting neoangiogenesis in HGG. Therefore, perfusion analysis of the peritumoural areas with DSCI can be considered reliable in differentiating between the two tumours.

MRS

The significant increase in peritumoural Cho/Cr [17, 18, 27, 28, 38] and Cho/NAA [18, 38, 42] rates of HGG compared to those of SBM ($P < 0.001$ for both) and the significant decrease in NAA/Cr [17, 37] rates ($P = 0.009$) in our study were similar to those in previous works. However, some studies have reported no significant differences in the peritumoural NAA/Cr rates between these two tumours [27, 28]. These results show the decrease in NAA based on neuron loss, which is a clear effect of peritumoural invasion in HGG, and the increase in total choline and Cho/NAA rates. These changes are not observed in the peritumoural regions of SBM [43, 44].

In the present study, a significant increase was reported in the NAA/Cr rates in the enhancing tumour in SBM compared to that in HGG ($P = 0.024$). The reason for this increase is probably the Cr deficiency in metastasis reported in previous studies [16] and the negative correlation between tumour infiltration degree and total tumour NAA [45]. This result is inconsistent with those of Law et al. [27] and Tsougos et al. [38], but is consistent with that of Server et al. [18]

No significant difference was found in the enhancing tumour Cho/Cr rates between HGG and SBM ($P = 0.216$), consistent with previous studies [28, 38, 42]. However, some studies have shown that the enhancing tumour Cho/Cr rates were lower in HGG than in SBM, and that this could be due to necrosis [18, 27]. In the present study, no significant difference was found in the enhancing tumour Cho/NAA rates between HGG and SBM ($P = 0.358$). This result agrees with those of previous studies [17, 38, 42]. The sensitivity and specificity values of peritumoural Cho/Cr, Cho/NAA, and NAA/Cr rates in differentiating HGG from SBM were 88.2% and 82.1%; 88.2% and 92.3%; and 82.4% and 74.4%, respectively. The highest individual power in all MRS parameters in differentiating between these two lesions was peritumoural Cho/NAA with an AUC of 0.903. This result is consistent was those of other studies [18, 38]. It also supports the finding in other studies that the Cho/NAA rate is associated with the proliferation of tumour cells [46, 47] and that choline exhibits cell density [48].

ROC analysis

We hypothesised that in differentiating HGG from SBM, advanced MRI techniques such as DWI, DSCI, and MRS, which can explain increased cellularity, density, and neoangiogenesis based on infiltration in the peritumoural region, could be closely associated with complicated and non-linear methods. Therefore, a combination of these MRI techniques could result in greater diagnostic accuracy. As each advanced MRI parameter can give limited information about the peritumoural region characteristic of the tumour (cellularity, density, and neo-angiogenesis), it can be insufficient in differentiating these two tumours.

A combination of multiple parameters can provide great diagnostic accuracy to differentiate between these two tumours. Recently, some researchers have examined the advantages of different combinations of advanced MRI techniques in differentiating SBM from HGG. Svalos et al. [32] combined diffusion (ADC and FA) and perfusion (rCBV) techniques with classification methods in differentiating glioblastomas and metastases from atypical meningiomas, and they reported that this combination provided additional diagnostic information in definitive diagnosis. Wang et al. [33] showed that DTI metrics and rCBV measurements could help in differentiating glioblastomas, brain metastases, and PCLs. In another study conducted with DTI, Wang et al. [34] reported that fractional anisotropy and mean diffusivity classification models could increase diagnostic performance in the contrasted lesion of tumour in differentiating glioblastomas from brain metastases. Bauer et al. [35] showed that the combination of MR diffusion and perfusion parameters was superior to the use of any individual parameter in differentiating SBM from glioblastoma multiforme. To the best of our knowledge, in the differentiation between HGG and SBM, quantitative MR parameter combinations with combined ROC curve analysis provided by DWI, DSCI, and MRS were not used in any of the previous studies. Our study showed that in differentiating HGG from SBM, any of the model combinations in the peritumoural region (Figure 4) had a higher diagnostic accuracy than the individual use of any of the DWI, DSCI, and MRS parameters (Figures 3A, B, C). With ROC analysis, our study showed that the best model that could differentiate HGG from SBM is the combination of peritumoural ADCmin, rCBV, and Cho/NAA parameters; the sensitivity, specificity, PPD, NPD, and AUC values were 94.1%, 100%, 100%, 97.4%, and 0.970, respectively. The combination of quantitative information provided by peritumoural DWI, DSCI, and MRS with ROC analysis methods can better explain the underlying pathophysiology (unlike vasogenic oedema, infiltrative oedema has high cellularity, density, and neo-angiogenesis) in the peritumoural region used in the differentiation of these two tumours. Also, additional diagnostic information provided by each parameter can be combined for improved diagnostic performance. Therefore, this hypothesis is confirmed by the combination of parameters with ROC curve analysis in the peritumoural area.

Limitations

Our study has some limitations. Firstly, as this work is a retrospective study, the ROIs placed in the enhancing tumour and in the peritumoural region did not match with the tissue places sampled for histological analysis. Further prospective studies that directly associate ROIs with histological observations are important, so that the DWI, DSCI, and MRS parameters can be more accurately interpreted. Secondly, this study has a small sample size. A large sample is required to confirm the results of our study. Thirdly, the signals of metabolites could have been influenced by partial volume effects in some cases because of the effects of tumour heterogeneity. Lastly, we did not use absolute metabolite assessment methods.

Conclusion

This study showed that the individual use of any of the peritumoral DWI, DSCI, and MRS parameters could be useful in differentiating between HGG and SBM. In differentiating HGG from SBM in the peritumoural region with ROC analysis, any of the model combinations was superior to any individual DWI, DSCI, and MRS parameter, and the best model found was the combination of peritumoural ADCmin, rCBV, and Cho/NAA, with 97% diagnostic accuracy. Therefore, the combination of peritumoural DWI, DSCI, and MRS parameters can provide more accurate diagnostic information in differentiating SBM from HGG.

Funding. *This publication was prepared without any external source of funding.*
Conflict of interest. *None declared.*
Acknowledgement and financial support. *None declared.*

References

1. Elmariah SB, Huse J, Mason B, et al. Multicentric glioblastoma multiforme in a patient with BRCA-1 invasive breast cancer. Breast J. 2006; 12(5): 470–474, doi: 10.1111/j.1075-122X.2006.00307.x, indexed in Pubmed: 16958968.
2. Single Brain Metastasis. Curr Treat Options Neurol. 2001; 3(1): 89–99, indexed in Pubmed: 11123862.
3. Campos S, Davey P, Hird A, et al. Brain metastasis from an unknown primary, or primary brain tumour? A diagnostic dilemma. Curr Oncol. 2009; 16(1): 62–66, indexed in Pubmed: 19229374.
4. Oh J, Cha S, Aiken AH, et al. Quantitative apparent diffusion coefficients and T2 relaxation times in characterizing contrast enhancing brain tumors and regions of peritumoral edema. J Magn Reson Imaging. 2005; 21(6): 701–708, doi: 10.1002/jmri.20335, indexed in Pubmed: 15906339.
5. Lee EJa, terBrugge K, Mikulis D, et al. Diagnostic value of peritumoral minimum apparent diffusion coefficient for differentiation of glioblastoma multiforme from solitary metastatic lesions. AJR Am J Roentgenol. 2011; 196(1): 71–76, doi: 10.2214/AJR.10.4752, indexed in Pubmed: 21178049.

6. Byrnes TJD, Barrick TR, Bell BA, et al. Diffusion tensor imaging discriminates between glioblastoma and cerebral metastases in vivo. NMR Biomed. 2011; 24(1): 54–60, doi: 10.1002/nbm.1555, indexed in Pubmed: 20665905.
7. Lu S, Ahn D, Johnson G, et al. Peritumoral diffusion tensor imaging of high-grade gliomas and metastatic brain tumors. AJNR Am J Neuroradiol. 2003; 24(5): 937–941, indexed in Pubmed: 12748097.
8. Pavlisa G, Rados M, Pavlisa G, et al. The differences of water diffusion between brain tissue infiltrated by tumor and peritumoral vasogenic edema. Clin Imaging. 2009; 33(2): 96–101, doi: 10.1016/j.clinimag.2008.06.035, indexed in Pubmed: 19237051.
9. Lemercier P, Paz Maya S, Patrie JT, et al. Gradient of apparent diffusion coefficient values in peritumoral edema helps in differentiation of glioblastoma from solitary metastatic lesions. AJR Am J Roentgenol. 2014; 203(1): 163–169, doi: 10.2214/AJR.13.11186, indexed in Pubmed: 24951211.
10. Server A, Kulle B, Maehlen J, et al. Quantitative apparent diffusion coefficients in the characterization of brain tumors and associated peritumoral edema. Acta Radiol. 2009; 50(6): 682–689, doi: 10.1080/02841850902933123, indexed in Pubmed: 19449234.
11. Huang J, Luo J, Peng J, et al. Cerebral schistosomiasis: diffusion-weighted imaging helps to differentiate from brain glioma and metastasis. Acta Radiol. 2017; 58(11): 1371–1377, doi: 10.1177/0284185116687173, indexed in Pubmed: 28090792.
12. Tan Y, Wang XC, Zhang H, et al. Differentiation of high-grade-astrocytomas from solitary-brain-metastases: Comparing diffusion kurtosis imaging and diffusion tensor imaging. Eur J Radiol. 2015; 84(12): 2618–2624, doi: 10.1016/j.ejrad.2015.10.007, indexed in Pubmed: 26482747.
13. Han C, Huang S, Guo J, et al. Use of a high b-value for diffusion weighted imaging of peritumoral regions to differentiate high-grade gliomas and solitary metastases. J Magn Reson Imaging. 2015; 42(1): 80–86, doi: 10.1002/jmri.24747, indexed in Pubmed: 25223489.
14. Caravan I, Ciortea CA, Contis A, et al. Diagnostic value of apparent diffusion coefficient in differentiating between high-grade gliomas and brain metastases. Acta Radiol. 2018; 59(5): 599–605, doi: 10.1177/0284185117727787, indexed in Pubmed: 28835111.
15. Suh CH, Kim HS, Jung SC, et al. Diffusion-Weighted Imaging and Diffusion Tensor Imaging for Differentiating High-Grade Glioma from Solitary Brain Metastasis: A Systematic Review and Meta-Analysis. AJNR Am J Neuroradiol. 2018; 39(7): 1208–1214, doi: 10.3174/ajnr.A5650, indexed in Pubmed: 29724766.
16. Ishimaru H, Morikawa M, Iwanaga S, et al. Differentiation between high-grade glioma and metastatic brain tumor using single-voxel proton MR spectroscopy. Eur Radiol. 2001; 11(9): 1784–1791, doi: 10.1007/s003300000814, indexed in Pubmed: 11511902.
17. Fan G, Sun B, Wu Z, et al. In vivo single-voxel proton MR spectroscopy in the differentiation of high-grade gliomas and solitary metastases. Clin Radiol. 2004; 59(1): 77–85, indexed in Pubmed: 14697379.
18. Server A, Josefsen R, Kulle B, et al. Proton magnetic resonance spectroscopy in the distinction of high-grade cerebral gliomas from single metastatic brain tumors. Acta Radiol. 2010; 51(3): 316–325, doi: 10.3109/02841850903482901, indexed in Pubmed: 20092374.
19. Crisi G, Orsingher L, Filice S. Lipid and macromolecules quantitation in differentiating glioblastoma from solitary metastasis: a short-echo time single-voxel magnetic resonance spectroscopy study at 3 T. J Comput Assist Tomogr. 2013; 37(2): 265–271, doi: 10.1097/RCT.0b013e318282d2ba, indexed in Pubmed: 23493217.
20. Wang Q, Zhang J, Xu W, et al. Role of magnetic resonance spectroscopy to differentiate high-grade gliomas from metastases. Tumour Biol. 2017; 39(6): 1010428317710030, doi: 10.1177/1010428317710030, indexed in Pubmed: 28631566.
21. Lehmann P, Saliou G, de Marco G, et al. Cerebral peritumoral oedema study: does a single dynamic MR sequence assessing perfusion and permeability can help to differentiate glioblastoma from metastasis? Eur J Radiol. 2012; 81(3): 522–527, doi: 10.1016/j.ejrad.2011.01.076, indexed in Pubmed: 21334839.
22. Server A, Orheim TE, Graff BA, et al. Diagnostic examination performance by using microvascular leakage, cerebral blood volume, and blood flow derived from 3-T dynamic susceptibility-weighted contrast-enhanced perfusion MR imaging in the differentiation of glioblastoma multiforme and brain metastasis. Neuroradiology. 2011; 53(5): 319–330, doi: 10.1007/s00234-010-0740-3, indexed in Pubmed: 20625709.
23. Blasel S, Jurcoane A, Franz K, et al. Elevated peritumoural rCBV values as a mean to differentiate metastases from high-grade gliomas. Acta Neurochir (Wien). 2010; 152(11): 1893–1899, doi: 10.1007/s00701-010-0774-7, indexed in Pubmed: 20799046.
24. Hakyemez B, Erdogan C, Gokalp G, et al. Solitary metastases and high-grade gliomas: radiological differentiation by morphometric analysis and perfusion-weighted MRI. Clin Radiol. 2010; 65(1): 15–20, doi: 10.1016/j.crad.2009.09.005, indexed in Pubmed: 20103416.
25. Halshtok Neiman O, Sadetzki S, Chetrit A, et al. Perfusion-weighted imaging of peritumoral edema can aid in the differential diagnosis of glioblastoma mulltiforme versus brain metastasis. Isr Med Assoc J. 2013; 15(2): 103–105, indexed in Pubmed: 23516772.
26. Suh CH, Kim HoS, Jung SC, et al. Perfusion MRI as a diagnostic biomarker for differentiating glioma from brain metastasis: a systematic review and meta-analysis. Eur Radiol. 2018; 28(9): 3819–3831, doi: 10.1007/s00330-018-5335-0, indexed in Pubmed: 29619517.
27. Law M, Cha S, Knopp EA, et al. High-grade gliomas and solitary metastases: differentiation by using perfusion and proton spectroscopic MR imaging. Radiology. 2002; 222(3): 715–721, doi: 10.1148/radiol.2223010558, indexed in Pubmed: 11867790.
28. Chiang IC, Kuo YT, Lu CY, et al. Distinction between high-grade gliomas and solitary metastases using peritumoral 3-T magnetic resonance spectroscopy, diffusion, and perfusion imagings. Neuroradiology. 2004; 46(8): 619–627, doi: 10.1007/s00234-004-1246-7, indexed in Pubmed: 15243726.
29. Fayed N, Modrego PJ. The contribution of magnetic resonance spectroscopy and echoplanar perfusion-weighted MRI in the initial assessment of brain tumours. J Neurooncol. 2005; 72(3): 261–265, doi: 10.1007/s11060-004-2180-6, indexed in Pubmed: 15937650.
30. Rollin N, Guyotat J, Streichenberger N, et al. Clinical relevance of diffusion and perfusion magnetic resonance imaging in assessing intra-axial brain tumors. Neuroradiology. 2006; 48(3): 150–159, doi: 10.1007/s00234-005-0030-7, indexed in Pubmed: 16470375.
31. Sparacia G, Gadde JA, Iaia A, et al. Usefulness of quantitative peritumoural perfusion and proton spectroscopic magnetic resonance imaging evaluation in differentiating brain gliomas from solitary brain metastases. Neuroradiol J. 2016; 29(3): 160–167, doi: 10.1177/1971400916638358, indexed in Pubmed: 26988081.
32. Svolos P, Tsolaki E, Kapsalaki E, et al. Investigating brain tumor differentiation with diffusion and perfusion metrics at 3T MRI using pattern recognition techniques. Magn Reson Imaging. 2013; 31(9): 1567–1577, doi: 10.1016/j.mri.2013.06.010, indexed in Pubmed: 23906533.

33. Wang S, Kim S, Chawla S, et al. Differentiation between glioblastomas, solitary brain metastases, and primary cerebral lymphomas using diffusion tensor and dynamic susceptibility contrast-enhanced MR imaging. AJNR Am J Neuroradiol. 2011; 32(3): 507–514, doi: 10.3174/ajnr.A2333, indexed in Pubmed: 21330399.
34. Wang S, Kim SJ, Poptani H, et al. Diagnostic utility of diffusion tensor imaging in differentiating glioblastomas from brain metastases. AJNR Am J Neuroradiol. 2014; 35(5): 928–934, doi: 10.3174/ajnr.A3871, indexed in Pubmed: 24503556.
35. Bauer AH, Erly W, Moser FG, et al. Differentiation of solitary brain metastasis from glioblastoma multiforme: a predictive multiparametric approach using combined MR diffusion and perfusion. Neuroradiology. 2015; 57(7): 697–703, doi: 10.1007/s00234-015-1524-6, indexed in Pubmed: 25845813.
36. Tsolaki E, Svolos P, Kousi E, et al. Automated differentiation of glioblastomas from intracranial metastases using 3T MR spectroscopic and perfusion data. Int J Comput Assist Radiol Surg. 2013; 8(5): 751–761, doi: 10.1007/s11548-012-0808-0, indexed in Pubmed: 23334798.
37. Mouthuy N, Cosnard G, Abarca-Quinones J, et al. Multiparametric magnetic resonance imaging to differentiate high-grade gliomas and brain metastases. J Neuroradiol. 2012; 39(5): 301–307, doi: 10.1016/j.neurad.2011.11.002, indexed in Pubmed: 22197404.
38. Tsougos I, Svolos P, Kousi E, et al. Differentiation of glioblastoma multiforme from metastatic brain tumor using proton magnetic resonance spectroscopy, diffusion and perfusion metrics at 3 T. Cancer Imaging. 2012; 12: 423–436, doi: 10.1102/1470-7330.2012.0038, indexed in Pubmed: 23108208.
39. Wu O, Østergaard L, Weisskoff RM, et al. Tracer arrival timing-insensitive technique for estimating flow in MR perfusion-weighted imaging using singular value decomposition with a block-circulant deconvolution matrix. Magn Reson Med. 2003; 50(1): 164–174, doi: 10.1002/mrm.10522, indexed in Pubmed: 12815691.
40. Rees JH, Smirniotopoulos JG, Jones RV, et al. Glioblastoma multiforme: radiologic-pathologic correlation. Radiographics. 1996; 16(6): 1413–38; quiz 1462, doi: 10.1148/radiographics.16.6.8946545, indexed in Pubmed: 8946545.
41. Long DM. Capillary ultrastructure in human metastatic brain tumors. J Neurosurg. 1979; 51(1): 53–58, doi: 10.3171/jns.1979.51.1.0053, indexed in Pubmed: 448419.
42. Weber MA, Zoubaa S, Schlieter M, et al. Diagnostic performance of spectroscopic and perfusion MRI for distinction of brain tumors. Neurology. 2006; 66(12): 1899–1906, doi: 10.1212/01.wnl.0000219767.49705.9c, indexed in Pubmed: 16801657.
43. Croteau D, Scarpace L, Hearshen D, et al. Correlation between magnetic resonance spectroscopy imaging and image-guided biopsies: semiquantitative and qualitative histopathological analyses of patients with untreated glioma. Neurosurgery. 2001; 49(4): 823–829, doi: 10.1097/00006123-200110000-00008, indexed in Pubmed: 11564242.
44. Wijnen JP, Idema AJS, Stawicki M, et al. Quantitative short echo time 1H MRSI of the peripheral edematous region of human brain tumors in the differentiation between glioblastoma, metastasis, and meningioma. J Magn Reson Imaging. 2012; 36(5): 1072–1082, doi: 10.1002/jmri.23737, indexed in Pubmed: 22745032.
45. Stadlbauer A, Gruber S, Nimsky C, et al. Preoperative grading of gliomas by using metabolite quantification with high-spatial-resolution proton MR spectroscopic imaging. Radiology. 2006; 238(3): 958–969, doi: 10.1148/radiol.2382041896, indexed in Pubmed: 16424238.
46. Guo J, Yao C, Chen H, et al. The relationship between Cho/NAA and glioma metabolism: implementation for margin delineation of cerebral gliomas. Acta Neurochir (Wien). 2012; 154(8): 1361–70; discussion 1370, doi: 10.1007/s00701-012-1418-x, indexed in Pubmed: 22729482.
47. Price SJ, Young AMH, Scotton WJ, et al. Multimodal MRI can identify perfusion and metabolic changes in the invasive margin of glioblastomas. J Magn Reson Imaging. 2016; 43(2): 487–494, doi: 10.1002/jmri.24996, indexed in Pubmed: 26140696.
48. Nafe R, Herminghaus S, Raab P, et al. Preoperative proton-MR spectroscopy of gliomas--correlation with quantitative nuclear morphology in surgical specimen. J Neurooncol. 2003; 63(3): 233–245, indexed in Pubmed: 12892229.